Anomalous Chiral Plasmas in the Hydrodynamic Regime

by

Denys Rybalka

A Dissertation Presented in Partial Fulfillment
of the Requirements for the Degree
Doctor of Philosophy

Approved March 2019 by the
Graduate Supervisory Committee:

Igor Shovkovy, Chair
Cecilia Lunardini
Francis Timmes
Tanmay Vachaspati

ARIZONA STATE UNIVERSITY

May 2019

ABSTRACT

Chiral symmetry and its anomalous and spontaneous breaking play an important role in particle physics, where it explains the origin of pion and hadron mass hierarchy among other things. Despite its microscopic origin chirality may also lead to observable effects in macroscopic physical systems – relativistic plasmas made of chiral (spin-$\frac{1}{2}$) particles. Such plasmas are called *chiral*. The effects include non-dissipative currents in external fields that could be present even in quasi-equilibrium, such as the chiral magnetic (CME) and separation (CSE) effects, as well as a number of inherently chiral collective modes called the chiral magnetic (CMW) and vortical (CVW) waves. Applications of chiral plasmas are truly interdisciplinary, ranging from hot plasma filling the early Universe, to dense matter in neutron stars, to electronic band structures in Dirac and Weyl semimetals, to quark-gluon plasma produced in heavy-ion collisions.

The main focus of this dissertation is a search for traces of chiral physics in the spectrum of collective modes in chiral plasmas. I start from relativistic chiral kinetic theory and derive first- and second-order chiral hydrodynamics. Then I establish key features of an equilibrium state that describes many physical chiral systems and use it to find the full spectrum of collective modes in high-temperature and high-density cases. Finally, I consider in detail the fate of the two inherently chiral waves, namely the CMW and the CVW, and determine their detection prospects.

The main results of this dissertation are the formulation of a fully covariant dissipative chiral hydrodynamics and the calculation of the spectrum of collective modes in chiral plasmas. It is found that the dissipative effects and dynamical electromagnetism play an important role in most cases. In particular, it is found that both the CMW and the CVW are heavily damped by the usual Ohmic dissipation in charged plasmas and the diffusion effects in neutral plasmas. These findings prompt a search

for new physical observables in heavy-ion collisions, as well as a revision of potential applications of chiral theories in cosmology and solid-state physics.

ACKNOWLEDGMENTS

This dissertation would have been impossible without the guidance, help, and tremendous patience of Igor Shovkovy and Eduard Gorbar, who were my scientific advisors and collaborators on the path to the PhD degree. I am enormously grateful to my parents and my family for their support and care. I thank the faculty and my friends in ASU, whom I enjoyed working and socialize with. I am indebted to my school math teacher Vitalii Polonskyi and especially my brother Igor for challenging and inspiring my curiosity. Finally, I thank my wife Olia for her love and dedication in sharing this path with me.

TABLE OF CONTENTS

Page

LIST OF FIGURES vi

CHAPTER

1 INTRODUCTION 1

1.1 Phenomenology of Chiral Theories 4

1.1.1 Anomalous Transport Effects in Chiral Plasmas 6

1.1.2 Anomalous Collective Modes in Chiral Plasmas 9

1.2 Macroscopic Descriptions of Chiral Plasmas 11

1.2.1 Chiral Kinetic Theory 11

1.2.2 Chiral Magnetohydrodynamics 16

2 DERIVATION OF CHIRAL HYDRODYNAMICS 19

2.1 Lorentz Covariant Chiral Kinetic Theory 19

2.2 First-order Chiral Hydrodynamics 23

2.3 Higher-order Chiral Hydrodynamics 31

3 COLLECTIVE MODES IN CHIRAL PLASMAS 38

3.1 Equilibrium State 38

3.2 Linearized Equations of Chiral Hydrodynamics 44

3.2.1 The Linearized Equations at Vanishing Vorticity 46

3.2.2 The Linearized Equations at Nonzero Vorticity 49

3.3 Hydrodynamic Modes in High Temperature Plasma 52

3.3.1 Charged Plasma at $\Omega = 0$ 53

3.3.2 Charged Plasma at $\Omega \neq 0$ 57

3.3.3 Charged Plasma at $\Omega \neq 0$ Without Dynamical Electromagnetic Fields 61

3.3.4 Plasma of Neutral Particles at $\Omega \neq 0$ 63

CHAPTER Page

3.4 Hydrodynamic Modes in Dense Plasma 64
3.4.1 Charged Plasma at $\Omega = 0$ 64
3.4.2 Charged Plasma at $\Omega \neq 0$ 66
3.4.3 Charged Plasma at $\Omega \neq 0$ Without Dynamical Electromagnetic Fields 69
3.4.4 Chiral Plasma of Neutral Particles at $\Omega \neq 0$ 70
3.5 The Chiral Magnetic Wave 70
3.5.1 The Chiral Magnetic Wave in Heavy-ion Collisions 77
3.6 The Chiral Vortical Wave 84
4 CONCLUSIONS 91
REFERENCES 95
APPENDIX
A TABLE INTEGRALS AND THERMODYNAMIC FUNCTIONS IN EQUILIBRIUM 103
B SEARCH FOR THE COLLECTIVE MODES IN THE PRESENCE OF VORTICITY 105
C BESSEL FUNCTIONS 110
D EXPLICIT FORM OF LINEARIZED EQUATIONS 112

LIST OF FIGURES

FIGURE Page

1.1 The Figure Shows the Intuitive Description of the Chiral Magnetic Effect. External Magnetic Field **B** Produces a Net Spin Polarization in Plasma. If Coupled with the Chiral Imbalance μ_5 This Creates a Net Electric Current Called the Chiral Magnetic Effect (CME). The Picture Is Taken from Kharzeev *et al.* (2016). 7

3.1 A Charged Element in a Rotating Plasma and the Local Electromagnetic Fields. Note That the Electric and Lorentz Forces on a Local Element of Plasma Are Equal in Magnitude and Opposite in Direction. 42

3.2 The Comparison of the Approximate Analytical Results (Solid Lines) for the Real (Red Lines and Points) and Imaginary (Blue Lines and Points) Parts of the Energy for the Alfvén Waves with the Corresponding Numerical Results (Points) at $\Omega = 0$ for Three Fixed Values of the Magnetic Field: $\hbar EB/T^2 = 0.5 \times 10^{-3}$ (Top Panel), $\hbar EB/T^2 = 10^{-3}$ (Middle Panel), and $\hbar EB/T^2 = 1.5 \times 10^{-3}$ (Bottom Panel). The Real and Imaginary Parts of the Energy Are Shown in Red and Blue, Respectively. The Other Model Parameters Are $\tau T/\hbar = 10^2$, $\mu/T = 10^{-4}$, and $\hbar K_\perp/T = 10^{-4}$. 56

3.3 The Real Parts of the Energies of the Alfvén Waves with Different Values of the Angular Momentum: $m = 0$ (Top Panel), $m = \pm 3$ (Middle Panel), and $m = \pm 6$ (Bottom Panel). The Other Model Parameters Are $\tau T/\hbar = 10^2$, $\mu/T = 10^{-4}$, $\hbar\Omega/T = 10^{-6}$, $\hbar EB/T^2 = 10^{-3}$, $RT/\hbar = 10^4 \alpha_{0,1} \approx 2.4 \times 10^4$, and $k_\perp = \alpha_{m,1}/R$. 60

3.4 The Positive Branches of the Real Part of Helicon Energies for Several Values of the Angular Momentum, I.e., $m = -4$ (Red Line), $m = -2$ (Orange Line), $m = 0$ (Olive Line), $m = 2$ (Green Line), and $m = 4$ (Blue Line). The Other Model Parameters Are $\hbar EB/\mu^2 \approx 2 \times 10^{-3}$, $\tau\mu/\hbar = 100$, $\hbar\Omega/\mu = 10^{-7}$, and $k_\perp = \alpha_{m,1}/R$. 67

3.5 The Ranges of Angular Momenta m for Which Helicon Modes Can Have Negative Group Velocity. The Colored Bands Correspond to Three Smallest Values of the Transverse Momenta $k_\perp^{(i)}$ with $i = 1, 2, 3$ (from Red to Blue, Respectively). 68

3.6 The Real Parts of the Energies (Left Panels) and the Ratios of the Real to Imaginary Parts of the Energies (Right Panels) of the CMW-type Collective Modes at Three Fixed Values of Temperature. The Three Rows of Panels Show the Results for Three Choices of the Magnetic Field, I.e., $EB = (50\text{ MeV})^2$, $(100\text{ MeV})^2$, and $(200\text{ MeV})^2$, Respectively. In the Gray Shaded Regions, the Wavelengths Lie Outside the Range 2 fm $\lesssim \lambda_k \lesssim$ 12 fm. The Actual Results Are Plotted down to the Wave Vectors as Small as $k \approx 50$ MeV, Which Corresponds to $\lambda_k \lesssim 24$ fm. 82

3.7 The Graphical Representation of the Parameter Space Regions (Shaded) Where One of the Modes Becomes Completely Diffusive. Different Colors (and Line Types) Represent the Results for Three Fixed Values of Temperature. 84

FIGURE Page

3.8 The Two Parameters $v_{1,2}$ That Control the Speed of the Chiral Vortical Wave in the Case of High Temperature (Top Row) and High Density (Bottom Row). The Graph Clearly Shows the Essential Role of μ_5 in Splitting the Speeds of the CVW When It Propagates along or Against the Direction of Vorticity (the Two Coincide for $\mu_5 = 0$). This Is Also in Agreement with the Symmetry Argument That the Chiral Chemical Potential Breaks Parity. 89

B.1 Coefficients a_i and b_i from the Expansions in Eq. (B.1) for the Few Indexes i Around $j = 3$ at $m = 0, 3, 5$. As Can Be Seen from the Graph Both Coefficients Subside Quickly for Large $|i - j|$. 107

Chapter 1

INTRODUCTION

Chirality is a concept in theoretical physics and mathematics that distinguishes an object from its mirror image. In particle physics, chirality is well defined for massless particles (anti-particles) and coincides with (differs by a sign from) their helicity. Recall that the latter is the sign of the projection of the particle's spin onto its momentum. It is also connected to the parity symmetry, which interchanges particles of opposite chiralities. Chirality can also be defined as an approximately conserved quantity for a massive particle moving with ultra-relativistic velocity.

Although chirality is defined at the microscopic level, its effects can be significant also in large material systems called chiral relativistic plasmas, or just chiral plasmas for short. Examples of such plasmas appear in many branches of physics: from hot plasma in the early Universe and degenerate matter in neutron stars, to Dirac and Weyl semimetals, and to quark gluon-plasma in heavy-ion collisions. In the hydrodynamic description chiral plasmas are characterized by an approximately conserved chiral (axial) charge, in addition to the standard exactly conserved quantities in plasmas, namely the electric charge, the energy, the momentum, and the angular momentum. As a result, chiral plasmas in external fields demonstrate a number of anomalous macroscopic quantum phenomena. For example, in the presence of a magnetic field, they exhibit non-dissipative electric and axial currents called the chiral magnetic effect (CME) and the chiral separation effect (CSE), respectively. In turn, the interplay between these effects leads to novel collective excitations unique to chiral plasmas.

Anomalous effects in chiral plasmas were first discovered in a series of papers by

Vilenkin (1978, 1979, 1980a) in the context of astrophysics. Recent resurgence of interest in the field is attributed to the possibility of detecting anomalous collective modes in the multi-particle correlators in heavy-ion collisions, as well as producing novel effects in condensed matter physics and astrophysics. Below we consider some examples in more detail.

In the modern heavy-ion collision experiments, nuclei are accelerated to energies between hundreds of GeV and a few TeV per nucleon pair and smashed together to produce a shower of particles that are then analyzed in designated detectors (Heinz and Snellings (2013); Loizides (2016); Florkowski *et al.* (2018a); Nagle and Zajc (2018)). During the collision the system undergoes a series of transformations, that may produce quasi-equilibrated states of matter, one of which is believed to be a liquid-like soup of strongly interacting quarks and gluons, called the quark-gluon plasma (Gyulassy and McLerran (2005); Adams *et al.* (2005); Adcox *et al.* (2005)). At sufficiently high energies, quarks, being spin-$\frac{1}{2}$ fermions, form a chiral relativistic plasma. Non-central collisions of positively charged ions also produce significant electromagnetic fields and carry a substantial angular momentum (locally characterized by the fluid vorticity). Therefore, the chiral plasma of quarks is subjected to strong external fields, thus making perfect conditions for observing anomalous quantum effects (Miransky and Shovkovy (2015); Kharzeev *et al.* (2016)). It is believed that chiral effects can be useful for probing the fundamental properties of the quark-gluon plasma, including the P- and CP-violation (Kharzeev (2006); Kharzeev *et al.* (2008)), chiral anomaly in QCD, etc.. Recent findings revealed a promising signal in the elliptic flow coefficient v_2, as well as the polarization of Λ-baryons, that could be attributed to the CME and CSE currents generated in the plasma (Kharzeev *et al.* (2016)). There is also an ongoing search for the anomalous collective modes and related observables (Kharzeev and Yee (2011); Jiang *et al.* (2015); Chernodub (2016)).

Chiral systems in the condensed matter setting open the possibility of testing relativistic quantum theories in tabletop experiments. Recently predicted and discovered Dirac and Weyl semimetals possess relativistic-like quasi-particles with a conical-shaped spectrum around several gapless nodes (valleys) (Wang *et al.* (2012, 2013); Xu *et al.* (2015); Lv *et al.* (2015)). Low-lying excitations around these nodes behave exactly like relativistic fermions with their Fermi velocity playing the role of an effective speed of light, and the valley degrees of freedom mimicking different species. These materials can be used to probe the behavior of relativistic chiral plasmas in a controlled setting (Hosur and Qi (2013); Kharzeev (2014); Armitage *et al.* (2018)). For example, in addition to being able to easily adjust plasma temperature and density, it was recently proposed that the chiral imbalance in these systems can be produced by a circularly polarized photocurrent (Kaushik *et al.* (2018)). Moreover, anomalous physics in condensed matter can be used for designing new tools of manipulating various transport properties. It must be mentioned, however, that electrons, forming the chiral plasma in Dirac and Weyl materials, are not completely decoupled from ion lattices in those materials and may scatter on phonons and defects in them. As a result, the outcome of some physics phenomena may be different (or more convoluted) than in truly high-energy systems.

Physics of chiral systems on the largest of scales is studied in cosmology and astrophysics. Chiral effects in a hot plasma produced after the Big Bang can influence the contemporary cosmological observables. For example, it has been suggested that coherent large-scale magnetic fields filling the voids in between the galaxies and galactic clusters can originate from the so-called inverse magnetic cascade (Christensson *et al.* (2001)). In such a cascade the energy is transferred from smaller to larger distance scales by the conversion of the chirality of the early Universe plasma into the helicity of magnetic fields (Tashiro *et al.* (2012); Del Zanna and Bucciantini (2018)).

Alternatively, magnetars, which are rapidly rotating neutron stars with one of the strongest magnetic fields found in the Universe, make ideal candidates for observing anomalous physics. Also, chiral effects in asymmetric supernova explosions can alter neutrino and photon fluxes/polarizations similar to the elliptic flows in heavy-ion collisions (Masada *et al.* (2018); Obergaulinger *et al.* (2018)). These can be observed either directly in observatories or indirectly via the properties of the remnants of the explosion. Lastly, magnetohydrodynamic waves can be detected in solar jets with a much better resolution, and may also contain chiral physics (Zhelyazkov and Chandra (2018)).

Throughout this paper we use the units with the speed of light $c = 1$. We also set $\hbar = 1$ in the introduction for simplicity, but keep it explicitly in the main text as the quantum correction power-counting parameter. We also use the Minkowski metric $g_{\mu\nu} = \mathrm{diag}(1, -1, -1, -1)$ and the Levi-Civita tensor such that $\varepsilon^{0123} = 1$.

This dissertation is based on the original results published in Gorbar *et al.* (2017), Shovkovy *et al.* (2018), and Rybalka *et al.* (2019) by the author.

1.1 Phenomenology of chiral theories

Let us now remind the definition of chirality (Peskin and Schroeder (1995)) from the quantum mechanics. The free spin-$\frac{1}{2}$ fermions are described by the Dirac equation

$$(i\gamma^\mu \partial_\mu - m)\psi = 0. \tag{1.1}$$

The set of four anti-commuting Dirac matrices γ^μ satisfies $\{\gamma^\mu, \gamma^\nu\} = 2g^{\mu\nu}$. It is also supplemented by the fifth matrix $\gamma^5 = i\gamma^0\gamma^1\gamma^2\gamma^3$ that anti-commutes with all the other matrices. A particle's chirality is defined as the eigenvalue of γ^5 and equals either $+1$ or -1. In the massless theory, it is equivalent to the notion of helicity, which is a projection of spin onto the momentum. Indeed, this follows from the massless

Dirac equation, that can be rewritten as:

$$\frac{2\boldsymbol{S}\cdot\mathbf{p}}{|\mathbf{p}|}\psi = \text{sign}(p_0)\gamma^5\psi, \tag{1.2}$$

where $S^i = \frac{i}{4}\varepsilon^{ijk}\gamma^j\gamma^k$ is the spin operator. The same relation implies that massless particles have their spin aligned either along or against the momentum, which correspond to the right-handed and the left-handed particles, respectively.

It is clear that the free-particle states that satisfy the Dirac equation have a definite chirality only in the massless case $m = 0$. Strictly speaking, therefore, chiral forms of matter are only those made of massless fermions. In reality, most of the physical systems mentioned earlier deal with either massless excitations anyway or are subject to high temperatures or densities, so that their characteristic energies E are much larger than their masses m. In such cases, it can be argued that in massive theories the chirality is an approximately conserved quantity with the chirality flipping processes suppressed by some power of m/E. In what follows, for simplicity, we will exclusively concentrate on the massless case.

In particle physics chiral symmetry plays a particularly important role. For example, the pair of u and d quarks possess an approximate $SU(2)_L \times SU(2)_R$ chiral symmetry that interchanges particles of different chirality. This symmetry turns out to be spontaneously broken to a vector-like isospin subgroup $SU(2)_V$. Such breaking leads to the three (in accordance with number of broken generators) Nambu-Goldstone bosons called pions in the low-energy spectrum of QCD. This mechanism of chiral symmetry breaking explains how the masses of protons ($m_p = 938.3$ MeV) and neutrons ($m_n = 939.6$ MeV) are much larger than the current masses of quarks ($\bar{m}_u = 2.2$ MeV, $\bar{m}_d = 4.7$ MeV) (Tanabashi *et al.* (2018)).

Another important feature inherent to chiral theories is the anomalous braking of the singlet axial symmetry $U(1)_A$, under which the field transforms as $\psi \to e^{i\gamma_5\theta}\psi$.

This leads to the anomalous non-conservation of the axial current $j_5^\mu = j_{\rm R}^\mu - j_{\rm L}^\mu$, where $j_{\rm R/L}^\mu$ is the current of right- and left-handed fermions, respectively. In other words the number of left- and right-handed fermions is not a conserved quantity. In 3+1 dimensions the anomaly takes the form (Peskin and Schroeder (1995)):

$$\partial_\mu j_5^\mu = -\frac{e^2}{16\pi^2}\varepsilon^{\mu\nu\alpha\beta}F_{\mu\nu}F_{\alpha\beta} = \frac{e^2}{2\pi^2}(\mathbf{B}\cdot\mathbf{E}), \tag{1.3}$$

where $F_{\mu\nu}$ is the electromagnetic field strength tensor. This non-conservation is a purely quantum effect absent in the classical field theory and thus called an anomaly. Chiral charge can be produced in a system of chiral fermions via co-aligned electric $\mathbf{E}$ and magnetic $\mathbf{B}$ fields. The chiral anomaly can be used to explain the neutral pion π^0 two-photon decay mode ($\pi^0 \to 2\gamma$) via the famous triangular diagram (Adler (1969); Bell and Jackiw (1969)). On a macroscopic scale the chiral, anomaly also leads to several interesting effects even in quasi-equilibrium.

1.1.1 Anomalous transport effects in chiral plasmas

One of the effects typical to the chiral theories is the so-called chiral magnetic effect. It leads to the emergence of a non-dissipative electrical current in a quasi-equilibrium plasma in a background magnetic field. The easiest way to trace the physics behind it is the following somewhat oversimplified argument. Let us imagine a relativistic gas of chiral fermions with chiral imbalance in an external magnetic field. The difference between the number of right-handed and left-handed particles in equilibrium can be modeled by a chiral chemical potential $\mu_5 = \mu_R - \mu_L$. Here we implicitly assume that the spin-flipping processes are weak or, alternatively, we consider the plasma on a time-scale small compared to the mean spin-flipping time. Due to the paramagnetic effect the gas in the background magnetic field obtains a spin polarization proportional to $\mathbf{B}$. However, the momentum of relativistic chiral

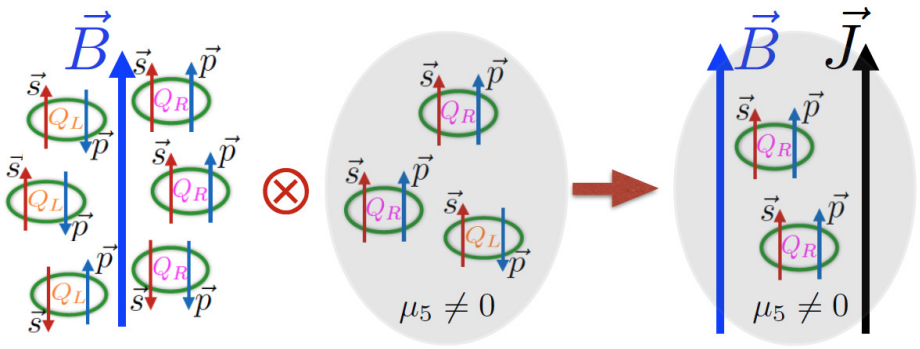

Figure 1.1: The figure shows the intuitive description of the chiral magnetic effect. External magnetic field **B** produces a net spin polarization in plasma. If coupled with the chiral imbalance μ_5 this creates a net electric current called the chiral magnetic effect (CME). The picture is taken from Kharzeev *et al.* (2016).

fermions is locked to the direction of the spin. Therefore, due to this polarization, the right-handed particles are moving preferably along the magnetic field and left-handed particles – in the opposite direction. Due to the difference in the numbers of particles of different chiralities, the system acquires an electric current along the magnetic field $\mathbf{j}_{\rm CME} \propto \mu_5 \mathbf{B}$, see Fig. 1.1. Note, that the electric current is odd, whereas the magnetic field is even under the parity transformation. Such an effect is absent in usual plasmas. Therefore, the CME is an anomalous transport process that is possible only in a chirally imbalanced environment with $\mu_5 \neq 0$.

Of course, the exact coefficient of proportionality in the expression for $\mathbf{j}_{\rm CME}$ has to be determined using more rigorous theoretical arguments. In fact, analysis of various systems ranging from a free fermion gas to infinitely strongly coupled systems has given the same coefficient fixed by the chiral anomaly (Fukushima *et al.* (2008); Kharzeev *et al.* (2013, 2016)). One of the short and beautiful arguments giving the correct expression is the following. Let us consider a CME current $\mathbf{j}_{\rm CME}$ induced by an external magnetic field **B**. To probe such current we turn on a small electric field **E** parallel to the magnetic field. The power generated in the system due to the electric field is given by a textbook formula $\int_V \mathbf{j}_{\rm CME} \cdot \mathbf{E}$. Alternatively, from the viewpoint

of the chiral anomaly, parallel electric and magnetic fields lead to the generation of a chiral charge $\partial Q_5/\partial t = \int_V \frac{e^2}{2\pi^2}(\mathbf{B}\cdot\mathbf{E})$. Using the definition of the chiral chemical potential μ_5, the power needed to produce this imbalance is $\mu_5 \partial Q_5/\partial t$. Matching the powers generated and consumed, we get the coefficient for the chiral magnetic effect completely determined by the chiral anomaly: $\mathbf{j}_{\mathrm{CME}} = \frac{e^2}{2\pi^2}\mu_5\mathbf{B}$. Note, that the nature of this current is qualitatively different from the conventional Ohmic current. The CME current is non-dissipative, which means that by itself it does not produce energy and entropy, can be present even in equilibrium, and is a direct consequence of quantum anomaly.

Similarly to the chiral magnetic effect, an external magnetic field also generates an axial current $\mathbf{j}_5$, called the chiral separation effect (CSE). The intuition behind this effect is the same as behind the CME. The external magnetic field $\mathbf{B}$ produces a net spin polarization, which drives right- and left-handed particles in opposite directions. The number of particles is controlled by the conventional chemical potential μ and so we get $\mathbf{j}_5^{\mathrm{CSE}} \propto \mu\mathbf{B}$. In fact, the coefficient of proportionality is the same as in the CME and is also controlled by the chiral anomaly $\mathbf{j}_5^{\mathrm{CSE}} = \frac{e^2}{2\pi^2}\mu\mathbf{B}$. Note, that in this case the axial current is even under parity in agreement with the discrete symmetry acting on both sides of the equality. In fact, considering the CME and CSE for each chirality separately, it can be seen that they represent different sides of the same coin, which explains the same coefficient of proportionality.

Other external fields can also produce conventional electric (fermion number) and axial currents in a chiral plasma. In the case of an electric field the corresponding effects are called the chiral electric and the chiral electric separation effects, respectively. Unlike the CME and the CSE these effects are dissipative although also related to the quantum nature of the plasma. They are no longer universally defined by the chiral anomaly, but depend on the specifics of physical systems. Another important

source of spin polarization is the global plasma rotation, also called vorticity. In simple terms vorticity is defined as the curl of the plasma velocity field $\omega = \nabla \times \mathbf{u}$. Due to the spin-orbit coupling of particles vorticity produces a net spin polarization, that in its turn induces the conventional and axial transport in chiral plasmas called the chiral vortical and the chiral vortical separation effects, respectively. These effects are expected to be the main manifestations of chiral physics in relativistic gases of neutral fermions (such as a gas of neutrinos in supernova explosions), which do not interact with the electromagnetic fields.

1.1.2 Anomalous collective modes in chiral plasmas

The chiral effects discussed in the previous section demonstrate the effect of quantum mechanics on the equilibrium properties of the plasma. However, their direct experimental verification and application is much more subtle than the theoretical derivations suggest. The axial current generated by the CSE is hard to probe, whereas a much more accessible for detection electrical CME current is generated only in the macroscopic regions with non-zero μ_5, which are hard to produce and are generally short-lived. The most readily available confirmation of the chiral magnetic effect is a negative magneto-resistance in Weyl semimetals (Son and Spivak (2013); Gorbar *et al.* (2014); Huang *et al.* (2015); Li *et al.* (2016)). However, in the realms of high-energy physics and astrophysics, clear observables are still lacking.

It has been predicted by Kharzeev and Yee (2011) (see also Jiang *et al.* (2015); Kharzeev *et al.* (2016); Chernodub (2016)), that the interplay of the chiral effects can lead to novel gapless collective excitation modes in plasma even in the absence of an overall chiral imbalance. The most famous one is called the chiral magnetic wave (CMW), it involves mutual fluctuations of the electric and axial charges. There is an ongoing experimental effort to detect its presence in quadrupole correlations

in heavy-ion collisions at the LHC and RHIC (Burnier *et al.* (2011); Gorbar *et al.* (2011); Zhao (2018)).

The idea behind the CMW can be explained using the charge n and axial charge n_5 conservation equations. Considering a dissipationless chiral plasma in an external magnetic field $\mathbf{B}$, and neglecting all perturbations except δn and δn_5, the two conservation equations:

$$\partial_\mu j^\mu = 0 \tag{1.4}$$

$$\partial_\mu j_5^\mu = 0 \tag{1.5}$$

take the form:

$$k_0 e\delta n + (\mathbf{k}\cdot\delta\mathbf{j}_{\rm CME}) = k_0 e\delta n + \frac{e^2(\mathbf{B}\cdot\mathbf{k})}{2\pi^2\chi_5}\delta n_5 = 0, \tag{1.6}$$

$$k_0 e\delta n_5 + (\mathbf{k}\cdot\delta\mathbf{j}_5^{\rm CSE}) = k_0 e\delta n_5 + \frac{e^2(\mathbf{B}\cdot\mathbf{k})}{2\pi^2\chi}\delta n = 0, \tag{1.7}$$

where we introduced susceptibilities $\chi = \partial n/\partial\mu$ and $\chi_5 = \partial n_5/\partial\mu_5$. It is easy to see that the system above has a wave-like solution with the dispersion $k_0 = \pm(e\mathbf{B}\cdot\mathbf{k})/(2\pi^2\sqrt{\chi\chi_5})$. This is the chiral magnetic wave. From the physical point of view it can be explained as follows. A charge perturbation δn induces a chiral current $\delta j^5_{\rm CSE}$ via the CSE. This current in its turn creates an axial charge imbalance δn_5. The axial charge then induces a charge current $\delta j_{\rm CME}$ via the CME. This current generates $\delta\mu$ and so the process sustains itself in the form of a wave. Using the analogous arguments it can be shown that the vorticity effects also lead to a wave-like mode called the chiral vortical wave.

It is clear, however, that such an analysis is oversimplified, as it does not account for dissipation and dynamical electromagnetism. The role of energy-momentum conservation and other hydrodynamic variables of the plasma should also be carefully addressed in the analysis of such modes. In fact, comprehensive analysis of collective

excitation is the main focus of this dissertation, requiring a fully-consistent hydrodynamical theory of the chiral plasma. The issue of the chiral magnetic wave will be considered in depth in section 3.5, where we will argue that plasma conductivity and diffusion completely overdamp the CMW in most realistic scenarios. So we find that the chiral magnetic wave is, most probably, cannot be detected in heavy-ion collisions.

1.2 Macroscopic descriptions of chiral plasmas

Although quantum field theory can be used to derive various chiral effects, when it comes to the description of chiral forms of matter out of equilibrium its use becomes very difficult. It is therefore essential to derive a chiral theory that can be applicable for large systems and non-equilibrium processes. The two common approaches are the chiral kinetic theory (CKT), dealing with the one-particle distributions, and the chiral magnetohydrodynamics (chiral MHD), dealing with hydrodynamic plasma variables, such as temperature, density and flow velocity. In both frameworks, the complete description should include dynamical electromagnetism. In this section we will discuss common methods used in deriving these two types of theories and their common applications.

1.2.1 Chiral kinetic theory

Let us start from the chiral kinetic theory. There exist two distinct enough approaches: one involves the world-line description and the other utilizes the Wigner function. In this subsection we will use the former approach to illustrate the most interesting properties of the chiral kinetic theory and only touch briefly upon the philosophy behind the latter. We will use the full power of the Wigner function in deriving the relativistic covariant chiral kinetic theory later in section 2.1.

Following Stephanov and Yin (2012) (see also Son and Yamamoto (2012, 2013)),

let us start from the Hamiltonian for a right-handed Weyl fermion: $\hat{H} = \boldsymbol{\sigma}\cdot\mathbf{p}$, where $\boldsymbol{\sigma}$ is a vector of Pauli matrices. It is clear that the two eigenvalues of this Hamiltonian $\pm|\mathbf{p}|$ correspond to a particle and anti-particle states, respectively. The propagation amplitude of the fermion can be written as a path integral over all trajectories $\mathbf{x}(t), \mathbf{p}(t)$ in the phase space:

$$\langle f|e^{i\hat{H}(t_f-t_i)}|i\rangle = \int \mathcal{D}x\ \mathcal{D}p\ \mathcal{P} \exp\left[i\int_{t_i}^{t_f}(\mathbf{p}\cdot\dot{\mathbf{x}} - \boldsymbol{\sigma}\cdot\mathbf{p})dt\right]. \tag{1.8}$$

The path integral is a 2 by 2 matrix in the spin space. It can be diagonalized by dividing it into small time intervals Δt and diagonalizing each point of the trajectory separately using a unitary matrix V_p, such that $V_p^\dagger(\boldsymbol{\sigma}\cdot\mathbf{p})V_p = |\mathbf{p}|\sigma_3$. The path integral then becomes:

$$\begin{aligned} &...V_{p_2}V_{p_2}^\dagger \exp\left[-i\boldsymbol{\sigma}\cdot\mathbf{p}_2\Delta t\right] V_{p_2}V_{p_2}^\dagger V_{p_1}V_{p_1}^\dagger \exp\left[-i\boldsymbol{\sigma}\cdot\mathbf{p}_1\Delta t\right] V_{p_1}V_{p_1}^\dagger... \\ &\quad = ...V_{p_2}\exp\left[-i\sigma_3|\mathbf{p}_2|\Delta t\right] V_{p_2}^\dagger V_{p_1}\exp\left[-i\sigma_3|\mathbf{p}_1|\Delta t\right] V_{p_1}^\dagger... \end{aligned} \tag{1.9}$$

For small Δt the change of momentum $\Delta\mathbf{p} = \mathbf{p}_2 - \mathbf{p}_1$ is also small and so we can write:

$$V_{p_2}^\dagger V_{p_1} \approx \exp\left[-i\hat{\mathbf{a}}_p\cdot\Delta\mathbf{p}\right], \qquad \hat{\mathbf{a}}_p = iV_p^\dagger\boldsymbol{\nabla}_p V_p. \tag{1.10}$$

This additional term is a geometric phase due to the fact that fermions live in the $SU(2)$ spin space. It is also known as the Berry phase, and $\hat{\mathbf{a}}_p$ is the Berry connection. The path integral then becomes:

$$\langle f|e^{i\hat{H}(t_f-t_i)}|i\rangle = V_{p_f}\int \mathcal{D}x\ \mathcal{D}p\ \mathcal{P}\exp\left[i\int_{t_i}^{t_f}(\mathbf{p}\cdot\dot{\mathbf{x}} - |\mathbf{p}|\sigma_3 - \hat{\mathbf{a}}_p\cdot\dot{\mathbf{p}})dt\right]V_{p_i}^\dagger. \tag{1.11}$$

One can argue that, in the classical limit for particles with large momentum $|\mathbf{p}|$, the separation between the eigenstates $2|\mathbf{p}|$ is also large enough to suppress the off-diagonal spin-flipping processes. Therefore, we can take the upper diagonal element as an effective semi-classical action for a right-handed chiral particle, with the effects

of spin encoded in the Berry connection term. It is also possible to minimally couple the particle to an external electromagnetic potential $(\Phi, \mathbf{A})$ and obtain the action:

$$I = \int_{t_i}^{t_f} (\mathbf{p} \cdot \dot{\mathbf{x}} - |\mathbf{p}| - \mathbf{a}_p \cdot \dot{\mathbf{p}} - e\Phi + e\mathbf{A} \cdot \dot{\mathbf{x}}) dt. \tag{1.12}$$

Variating the trajectory one can find the following equations of motion:

$$\dot{\mathbf{x}} = \hat{\mathbf{p}} + \dot{\mathbf{p}} \times \mathbf{b}, \tag{1.13}$$

$$\dot{\mathbf{p}} = e(\mathbf{E} + \dot{\mathbf{x}} \times \mathbf{B}), \tag{1.14}$$

where $\mathbf{b} = \boldsymbol{\nabla}_p \times \mathbf{a}_p = \hat{\mathbf{p}}/(2|\mathbf{p}|^2)$ is called the Berry flux or Berry curvature, and $\hat{\mathbf{p}} = \mathbf{p}/|\mathbf{p}|$. From the structure of the equations it is clear that $\mathbf{b}$ can be viewed as the field of a "magnetic" monopole in the momentum space ('t Hooft (1974)).

Using the equations of motion we finally end up with the chiral kinetic equation for collisionless plasma:

$$\frac{\partial \rho}{\partial t} + \frac{\partial(\rho \dot{\mathbf{x}})}{\partial \mathbf{x}} + \frac{\partial(\rho \dot{\mathbf{p}})}{\partial \mathbf{p}} = 2\pi e^2 \mathbf{E} \cdot \mathbf{B} f \delta^3(\mathbf{p}), \tag{1.15}$$

where $\rho = (1 + e\mathbf{B} \cdot \mathbf{b})f$ is the phase-space particle density, i.e., the usual particle distribution function f modified by the phase-space invariant measure. The term on the right-hand side of the equation stems from the quantum anomaly. Indeed, by integrating over the momentum we get the correct anomalous current non-conservation:

$$\frac{\partial n}{\partial t} + \frac{\partial \mathbf{j}}{\partial \mathbf{x}} = \frac{e^2}{4\pi^2} \mathbf{E} \cdot \mathbf{B}, \qquad \text{(single chirality)} \tag{1.16}$$

where $(n, \mathbf{j}) = \int_p (\rho, \rho \dot{\mathbf{x}})$ and we used $f_{\mathbf{p}=0} = 1$, that follows from the Fermi-Dirac distribution. Note also, that by substituting $\dot{\mathbf{x}}$ into the current definition one can successfully reproduce the CME current. The particle non-conservation is in a strong contrast to the classical kinetic theory, where the particle number conservation is connected with the fact, that world-lines cannot be created or destroyed. In the chiral

kinetic theory, on the other hand, the Berry monopole singularity at $\mathbf{p} = 0$ breaks down the classical description and allows for a creation of new particles (world-lines).

Although the chiral kinetic theory correctly predicts the CME, it gives an incorrect value of the CVE coefficient. What is even more troubling, the Lorentz invariance is broken in the system. It was shown in Chen *et al.* (2014) that CVE and Lorentz symmetry can be restored by the introduction of an additional magnetic coupling term in the classical action. They found that the dispersion of a chiral right-handed particle must be corrected $E_p = |\mathbf{p}| - (e\mathbf{B}\cdot\hat{\mathbf{p}})/(2|\mathbf{p}|)$ (the sign of the correction is opposite for a left-handed particle). The Lorentz invariance then can be rescued by the so-called "side-jump", which can be derived using a beautiful thought experiment presented below.

Let us consider two identical right-handed fermions with energy $|\mathbf{p}|$ colliding elastically in their center-of-mass frame with zero impact parameter. After the collision they move in collinear trajectories with momentums $\mathbf{p}$ and $-\mathbf{p}$. It is clear that both the orbital and spin contributions to the angular momentum vanish before and after the collision in this frame. Let us now consider the same process in a system boosted with infinitesimal velocity β along the direction of one of the incoming particles. The total angular momentum before the collision is still trivially zero and, therefore, must still be zero after it. However, the trajectories of the outgoing particles are no longer collinear and so are their spins. In fact, it is easy to show that the total spin of the outgoing particles equals $\mathbf{S}_{\text{out}} = [\boldsymbol{\beta} - \hat{\mathbf{p}}(\boldsymbol{\beta}\cdot\hat{\mathbf{p}})]/|\mathbf{p}|$. This spin must be counterbalanced by the total orbital momentum of the two outgoing particles. This is only possible if each of them side-jumps from the point of collision by the amount of $(\boldsymbol{\beta}\times\hat{\mathbf{p}})/(2|\mathbf{p}|)$ into opposite directions, so that the total orbital momentum equals $\mathbf{L}_{\text{out}} = \frac{\boldsymbol{\beta}\times\hat{\mathbf{p}}}{|\mathbf{p}|}\times\mathbf{p} = -\mathbf{S}_{\text{out}}$. Therefore, the modified Lorentz invariance has the form: $\delta_\beta t = \boldsymbol{\beta}\cdot\mathbf{x}$, $\delta_\beta\mathbf{x} = \boldsymbol{\beta}t + \frac{\boldsymbol{\beta}\times\hat{\mathbf{p}}}{2|\mathbf{p}|}$.

The chiral kinetic theory discussed above can, in principle, be generalized to a covariant form. There is, however, another way of deriving a fully covariant kinetic theory from the quantum field theory written in a Wigner function formalism, developed in Vasak *et al.* (1987). The free spin-$\frac{1}{2}$ Wigner matrix-function $W_{\alpha\beta}(x,p) \equiv \langle : \int \frac{d^4y}{(2\pi)^4} e^{-ip\cdot y} \bar{\psi}_\beta(x+\frac{1}{2}y)\psi_\alpha(x-\frac{1}{2}y) : \rangle = \langle \psi^\dagger_\beta(x)\delta^4(\hat{p}-p)\psi_\alpha(x)\rangle$ is a quantum analogue of a classical particle distribution function, which represents a number of particles with the four-momentum p at position x. Using the Dirac equation for the wavefunction ψ one can derive the evolution equation for the Wigner function. In the zeroth order in $\hbar$ it is equivalent to the classical kinetic (Boltzmann) equation, whereas higher-order terms give quantum corrections. Using the Keldysh formalism it can be generalized to include non-equilibrium phenomena and collisions. The resulting covariant CKT equation for a spin-$\frac{1}{2}$ fermion with chirality $\lambda = \pm 1$ has the following form (Hidaka *et al.* (2017, 2018)):

$$\mathcal{D}_\mu W^\mu(p,x) = \delta(p^2) p\cdot C + \lambda\hbar e \tilde{F}^{\mu\nu} C_\mu p_\nu \delta'(p^2), \tag{1.17}$$

where $\mathcal{D}^\mu = \partial/\partial x^\mu - eF^{\mu\nu}\partial/\partial p^\nu$ is the phase-space derivative, $F^{\mu\nu}$ and $\tilde{F}^{\mu\nu}$ are the electromagnetic field strength tensor and its dual, C^μ is the collision operator. The Wigner function has the following form:

$$W^\mu(p,x) \equiv p^\mu \delta(p^2) f + \lambda\hbar S^{\mu\nu}\delta(p^2)(D_\nu f - C_\nu) + \lambda\hbar e\tilde{F}^{\mu\nu} p_\nu \delta'(p^2) f + O(\hbar^2), \tag{1.18}$$

where $S^{\mu\nu}$ is the particle spin tensor and $f = f(x,p)$ is the distribution function. The spin tensor is defined so that $S^{\mu\nu} = \epsilon^{0\mu\nu i} s^i$ in the local frame of plasma with average spin $\mathbf{s}$. The first term in the Wigner function gives the classical free-streaming, second one gives spin-orbit coupling and side-jumps due to collisions, whereas the third one gives the magnetic coupling correction to the dispersion. Using this approach with a model distribution function (such as pure Fermi-Dirac distribution or Fermi-Dirac

with a small out-of-equilibrium correction) it is then possible to derive a fully covariant dissipative chiral magnetohydrodynamics.

1.2.2 Chiral magnetohydrodynamics

The chiral kinetic theory provides a natural starting point for deriving the hydrodynamic description of a chiral plasma that includes dissipation. However, hydrodynamics by itself is a very general theory that studies large-scale low-energy phenomena. It is therefore natural, that there are other more direct approaches to the low-energy theory of chiral plasmas, which usually fall into two categories. Approaches in the first category start from the quantum field theory and consider the evolution of some set of hydrodynamically relevant operators. Examples include a density operator approach (Buzzegoli and Becattini (2018)), Zubarev's non-equilibrium statistical operator method (Huang *et al.* (2011)), or even more abstract and general methods (Dubovsky *et al.* (2012); Haehl *et al.* (2018)). Approaches in the other category use thermodynamic and symmetry considerations to write the most general hydrodynamic theory truncated at some order in derivatives (Son and Surówka (2009); Isachenkov and Sadofyev (2011); Monnai (2018)). The advantage of the hydrodynamic approach is that it is universal and may be applicable to a wide range of locally equilibrated system, i.e., when the particles are no longer free-streaming like or weakly interacting. The usual disadvantages are excessive abstractness, inapplicability to thermal and dissipative cases in the first category, or proliferation of coefficients that require additional equations of state in the second category.

Let us illustrate how thermodynamic considerations can constrain a chiral hydrodynamic theory (Son and Surówka (2009)). The usual ingredients of any hydrodynamic theory is a stress-energy (energy-momentum) tensor $T^{\mu\nu}$ and four-current

j^μ:

$$T^{\mu\nu} = (\epsilon + P)u^\mu u^\nu + Pg^{\mu\nu} + \tau^{\mu\nu}, \tag{1.19}$$

$$j^\mu = nu^\mu + \nu^\mu. \tag{1.20}$$

The corresponding conserved quantities satisfy the continuity equations:

$$\partial_\mu T^{\mu\nu} = F^{\nu\lambda} j_\lambda, \tag{1.21}$$

$$\partial_\mu j^\mu = CE^\mu B_\mu, \tag{1.22}$$

where ϵ is the energy density, P is the pressure, n is the charge density, u^μ is the local fluid velocity flow satisfying $u_\mu u^\mu = 1$, parameters $\tau^{\mu\nu}$ and ν^μ incorporate dissipative contributions, and C is the quantum anomaly coefficient, which we left unspecified for now. Here we consider the plasma with particles of only one chirality (either right- or left-handed).

From the thermodynamic considerations we require the identity $\epsilon + P = Ts + \mu n$ and the existence of an entropy current s^μ such that $\partial_\mu s^\mu \geq 0$. Using the conservation equations it is possible to derive the following equality:

$$\partial_\mu \left(su^\mu - \frac{\mu}{T}\nu^\mu \right) = -\frac{1}{T}\partial_\mu u_\nu \tau^{\mu\nu} - \nu^\mu \left(\partial_\mu \frac{\mu}{T} - \frac{E_\mu}{T} \right) - C\frac{\mu}{T}EB. \tag{1.23}$$

In the non-anomalous case, $C = 0$, it is usually interpreted as the entropy production equation. Assuming it keeps the same physical meaning in the presence of anomaly, from the non-negativity condition one finds:

$$\tau^{\mu\nu} = -\eta\Delta^{\mu\alpha}\Delta^{\nu\beta}(\partial_\alpha u_\beta + \partial_\beta u_\alpha) - \left(\zeta - \frac{2}{3}\eta \right) \Delta^{\mu\nu}(\partial_\alpha u^\alpha), \tag{1.24}$$

$$\nu^\mu = -\sigma T \Delta^{\mu\nu}\partial_\nu \left(\frac{\mu}{T} \right) + \sigma E^\mu, \tag{1.25}$$

where $\Delta^{\mu\nu} = g^{\mu\nu} - u^\mu u^\nu$ is a transverse projector and, as usual, η and ζ are bulk and shear viscosities, and σ is conductivity. However, the anomalous term in the

entropy production equation can have either sign and may even dominate the others. Therefore, in order to ensure the entropy production positivity the hydrodynamic equations have to be modified.

The most general modification one can make to the charge and entropy currents is:

$$\nu^\mu = -\sigma T \Delta^{\mu\nu} \partial_\nu \left(\frac{\mu}{T}\right) + \sigma E^\mu + \xi_\omega \omega^\mu + \xi_B B^\mu, \tag{1.26}$$

$$s^\mu = s u^\mu - \frac{\mu}{T} \nu^\mu + D_\omega \omega^\mu + D_B B^\mu. \tag{1.27}$$

Now the entropy production positivity condition $\partial_\mu s^\mu \geq 0$ produces an even more stringent set of constraints, which completely fixes the CVE and CME coefficients:

$$\xi_\omega = C \left(\mu^2 - \frac{2}{3} \frac{n\mu^3}{\epsilon + P}\right), \qquad \xi_B = C \left(\mu - \frac{1}{2} \frac{n\mu^2}{\epsilon + P}\right). \tag{1.28}$$

This example illustrates how using just basic thermodynamic considerations one can derive the chiral magnetic and the chiral vortical effects in chiral hydrodynamic plasma without any microscopical input. In general, however, chiral magnetohydrodynamics requires also the equation of state and the specific knowledge of all dissipative transport coefficients. Moreover, beyond the first order in derivatives and fields, magnetohydrodynamic description will contain many more coefficients, which cannot be uniquely fixed without any additional input.

Chapter 2

DERIVATION OF CHIRAL HYDRODYNAMICS

2.1 Lorentz covariant chiral kinetic theory

In this section we derive a closed system of chiral hydrodynamic equations from the covariant version of the CKT (Hidaka *et al.* (2017, 2018)). The latter was obtained from the quantum-field theoretic formulation of massless QED by applying the Schwinger-Keldysh formalism. In the corresponding description, the lesser/greater propagators are directly connected to the Wigner function. Unlike the early heuristic approaches based on the Wigner function for noninteracting fermions (Gao *et al.* (2012); Chen *et al.* (2013)), the derivation by Hidaka *et al.* (2017, 2018) not only accounts for background electromagnetic fields but also includes the effects of interactions. A similar description might also be possible by using the on-shell effective field theory that was recently proposed by Carignano *et al.* (2018).

When dealing with charged plasmas in the hydrodynamic regime, the electromagnetic fields should be treated as fully dynamical, even in the static and steady-state cases. This implies that the commonly used background field approximation is not reliable in investigations of hydrodynamic modes. Therefore, in our study below, we supplement the equations for the hydrodynamic variables with the coupled Maxwell equations for the electromagnetic fields. As we will demonstrate below, such a self-consistent treatment will be important not only for the correct description of the hydrodynamic modes but also for identifying the global equilibrium state in a magnetized relativistic plasma with nonzero vorticity.

In order to capture dissipative effects, we should start our derivation from the

CKT that takes particle interactions into account. Instead of introducing a complete particle collision integral, however, we will utilize the so-called relaxation-time approximation. From the viewpoint of the resulting hydrodynamic description, which assumes a local thermal equilibrium on sufficiently short distance scales, this should be an adequate approximation. It should be noted, however, that enforcing Lorentz invariance in the relaxation-time approximation is far from trivial (Hidaka and Yang (2018)). Traces of this problem will also show up in our derivation below where we will find that the consistency of hydrodynamic equations (2.18)–(2.20) requires a special choice of the reference frame.

In order to set up the notations, let us start from a short introduction into the formalism used by Hidaka *et al.* (2017, 2018). By definition, the Wigner function of Weyl fermions is given by $W_{\alpha\beta}(p,x) = (2\pi)^3\langle\psi^\dagger_\beta(x)\delta^4(\hat{p}-p)\psi_\alpha(x)\rangle$, where $\alpha,\beta = 1,2$ are the spinor indices, $\hat{p}_\mu \equiv \frac{i}{2}\left(\partial_\mu - \partial^\dagger_\mu\right)$, and $\psi(x)$ is a second quantized Weyl spinor of a given chirality. (For a general overview of the Wigner function formalism, see Vasak *et al.* (1987).) Since the Wigner function is a matrix in the spinor space, it can be conveniently represented in terms of the Pauli matrices, i.e., $W(p,x) = W^\mu(p,x)\sigma_\mu$, where $\sigma^\mu = (1,\vec{\sigma})$. The four-vector $W^\mu(p,x)$ is related to the phase-space density of the number density current of chiral fermions with momentum p at position x. As we will see below, therefore, one can also relate the trace of the Wigner function to the (quasi)classical distribution function of chiral particles.

In general, we will consider chiral plasmas that are made of fermions of both chiralities, denoted by $\lambda = \pm 1$, where the plus (minus) sign corresponds to the right-handed (left-handed) fermions. In the following, we will assume that fermions of each chirality are described by independent Wigner functions or, in other words, that $W(p,x)$ depends on the chirality index λ. For simplicity of the notation, however, such a dependence will not be displayed explicitly, although it will always tacitly be

assumed.

The quasiclassical solution for the Wigner function can be obtained iteratively by using the expansion in powers of $\hbar$ (Hidaka *et al.* (2017, 2018)). The zeroth order result, in particular, is given by $W^{\mu}_{(0)}(p,x) = p^{\mu}\delta(p^2)f(p,x)$, where function $f(p,x)$ satisfies the relativistic Boltzmann equation for an ideal gas in a background electromagnetic field, i.e., $p^{\mu}\mathcal{D}_{\mu}f(p,x) = 0$. Here, the phase space derivative is defined by $\mathcal{D}^{\mu} = \partial/\partial x^{\mu} - eF^{\mu\nu}\partial/\partial p^{\nu}$ and $F^{\mu\nu}$ is the electromagnetic field strength tensor. The function $f(p,x)$ can be interpreted as a particle distribution function.

To the linear order in $\hbar$, the distribution function $f(p,x)$ satisfies the following covariant CKT equation (Hidaka *et al.* (2017, 2018)):

$$\mathcal{D}_{\mu}W^{\mu}(p,x) = \delta(p^2)p\cdot C + \lambda\hbar e\tilde{F}^{\mu\nu}C_{\mu}p_{\nu}\delta'(p^2), \tag{2.1}$$

where $\tilde{F}^{\mu\nu} = \frac{1}{2}\varepsilon^{\mu\nu\alpha\beta}F_{\alpha\beta}$ is the dual of the field strength tensor and $W^{\mu}(p,x)$ is the Wigner function with the corrections up to subleading order. The explicit form of the latter is given in terms of $f(p,x)$ as follows:

$$W^{\mu}(p,x) \equiv p^{\mu}\delta(p^2)f + \lambda\hbar S^{\mu\nu}\delta(p^2)(D_{\nu}f - C_{\nu}) + \lambda\hbar e\tilde{F}^{\mu\nu}p_{\nu}\delta'(p^2)f + O(\hbar^2) \tag{2.2}$$

Here, $S^{\mu\nu} = \frac{1}{2}\varepsilon^{\mu\nu\alpha\beta}p_{\alpha}u_{\beta}/(p\cdot u)$ is a particle spin tensor and C^{μ} is a collision operator which will be defined later. Note that the spin tensor is expressed in terms of a timelike four-vector $u^{\mu}(x)$ that defines the local frame.

It is instructive to review the physical meaning of the individual terms on the right-hand side of Eq. (2.2). The first one, which gives the zeroth order result, describes the classical free particle streaming. The second term captures the spin-orbit interaction and the effects of collisions. It is critical for the chiral vortical effect and the current connected with side jumps (see also Chen *et al.* (2014)). The third term on the right-hand side of Eq. (2.2) describes the interaction of the magnetic moment with the

background field and is responsible for the chiral magnetic effect. We also note that the first two terms enforce the conventional massless dispersion relation for chiral fermions, i.e., $p^2 = 0$, whereas the last one accounts for quantum corrections to the dispersion relation.

As mentioned earlier, we will treat the collisions in the CKT by employing the relaxation-time approximation. In this approximation, the Lorentz covariant collision operator has a particularly simple form $C^\mu = -u^\mu(f - f_{\rm eq})/\tau$, where τ is the relaxation time and $f_{\rm eq}(p, x)$ is the equilibrium distribution function (Hidaka and Yang (2018)). In this case, $S^{\mu\nu}C_\nu \equiv 0$ and, therefore, the side-jump term in the Wigner function vanishes. After taking into account Eq. (2.2), the CKT equation (2.1) takes a rather simple form, i.e.,

$$\mathcal{D}_\mu W^\mu = -\frac{u_\mu(W^\mu - W^\mu_{\rm eq})}{\tau}, \tag{2.3}$$

where $W^\mu_{\rm eq}$ is the Wigner function, associated with the equilibrium state. For the equilibrium distribution function in the local frame of the fluid, we will assume the usual Fermi-Dirac distribution, i.e.,

$$f_{\rm eq}(p, x) = \frac{1}{1 + e^{{\rm sign}(p_0)(\varepsilon_p - \mu_\lambda)/T}}. \tag{2.4}$$

Note that the chirality index λ (not to be confused with a Lorentz index) is shown explicitly in the chemical potential $\mu_\lambda \equiv \mu + \lambda\mu_5$, where μ is the fermion number chemical potential and μ_5 is the chiral chemical potential. By definition, the particle dispersion relation is given by

$$\varepsilon_p = u_\mu p^\mu + \frac{\lambda\hbar}{2}\frac{p\cdot\omega}{p\cdot u}, \tag{2.5}$$

where $\omega^\mu = \frac{1}{2}\varepsilon^{\mu\nu\alpha\beta}u_\nu\partial_\alpha u_\beta$ is the local vorticity (Hidaka *et al.* (2017, 2018)). The vortical term in Eq. (2.5) accounts for the spin-orbit coupling and, as suggested by its dependence on $\hbar$, has a quantum origin. In order to describe both particles (with

$p_0 > 0$) and antiparticles (with $p_0 < 0$), we introduced the energy sign factor, $\mathrm{sign}(p_0)$, in the exponent of the distribution function (2.4).

Note, that any information about the equilibrium plasma polarization is incorporated in the vorticity in the second term of the dispersion (2.5). As we will see later this leads to certain subtleties with the fluid velocity u^μ, in particular, the necessity to use an unconventional no-drag reference frame with a non-trivial relation between the heat-flow and velocity in Eq. (2.20). It has been speculated by Becattini *et al.* (2019), however, that in certain situations the total angular momentum of the plasma can be promoted to an independent thermodynamic and hydrodynamic quantity with a separate contribution to the dispersion. This may disentangle the fluid velocity from the polarization and lead to a more intuitive physical picture.

2.2 First-order chiral hydrodynamics

As is clear from Eqs. (2.4) and (2.5), the local equilibrium state is determined by six independent parameters, i.e., the local temperature $T(x)$, the two local chemical potentials $\mu_\lambda(x)$ (for the two species of fermions with opposite chiralities), and three (out of total four) independent components of the local rest-frame velocity $u^\mu(x)$, constrained by the normalization condition $u^\mu u_\mu = 1$. These parameters fully describe the local thermodynamic state of a chiral plasma. It might be important to emphasize that we will treat the plasma, which is made of two types of particles of opposite chirality, as a one-component fluid. This means that the local equilibrium state is characterized by the same common temperature and fluid velocity independent of the chirality. However, we will allow for the chemical potentials of opposite chirality fermions to be different. The corresponding hydrodynamic regime can be justified when the chirality-changing (anomalous) processes are sufficiently rare, i.e., when the rate of the thermal (kinetic) equilibration is much faster than the rate of the

anomalous processes. From a theoretical viewpoint, this is a particularly interesting regime as it allows for the chiral effects to be realized and observed in quasiclassical systems.

In essence, the hydrodynamic equations are nothing else but the continuity equations for the conserved quantities. In the case of a charged chiral plasma, they are the fermion number and chiral charge currents, as well as the energy-momentum tensor. (Note that here we use the fermion number current j^μ instead of the electric current $j^\mu_{\rm el} \equiv e j^\mu$.) In terms of the chiral Wigner functions, the corresponding quantities are given as follows (Vasak *et al.* (1987)):

$$j^\mu = 2\sum_\lambda \int \frac{d^4p}{(2\pi\hbar)^3} W^\mu, \tag{2.6}$$

$$j^\mu_5 = 2\sum_\lambda \lambda \int \frac{d^4p}{(2\pi\hbar)^3} W^\mu, \tag{2.7}$$

$$T^{\mu\nu} = \sum_\lambda \int \frac{d^4p}{(2\pi\hbar)^3} (W^\mu p^\nu + p^\mu W^\nu). \tag{2.8}$$

It might be instructive to note that these expressions contain an additional dependence on the Planck constant $\hbar$ entering through the phase-space measure. Such a dependence is not connected with the use of the quasiclassical approximation for the Wigner function, but simply accounts for a correct number of microstates in any given macrostate. Interestingly, the same dependence on $\hbar$ in the phase-space measure should appear even in the classical theory, although it usually drops out from many classical observables and thermodynamic relations. In our study of a chiral plasma, however, an explicit dependence on $\hbar$ will remain in most thermodynamic quantities, including the particle and energy densities, the pressure, and transport coefficients. (For explicit expressions of some thermodynamic quantities, see Appendix A.)

Before proceeding further, it is useful to comment on several possible definitions of the local rest frame $u^\mu(x)$ in chiral fluids. In relativistic hydrodynamics, the most

common choices of local frames are the so-called Eckart frame, connected with the conserved charge (e.g., the fermion number or the electric charge) current ($u^\mu \parallel j^\mu$), and the Landau frame, connected with the energy flow ($u^\mu \parallel T^{\mu\nu}u_\nu$). In the case of chiral fluids, however, the preferred choice might be the so-called no-drag frame introduced by Rajagopal and Sadofyev (2015); Stephanov and Yee (2016); Sadofyev and Yin (2016). The local thermal equilibrium in the corresponding frame is described by the usual Fermi-Dirac distribution function. This is also the choice that we assume here.

By making use of the local rest frame of the fluid u^μ, it is convenient to decompose the currents in terms of the longitudinal and transverse components, i.e.,

$$j^\mu = nu^\mu + \nu^\mu, \tag{2.9}$$

$$j_5^\mu = n_5 u^\mu + \nu_5^\mu, \tag{2.10}$$

where $n = j^\mu u_\mu$ and $n_5 = j_5^\mu u_\mu$ are the fermion number and chiral charge densities, respectively. The transverse currents, $\nu^\mu = \Delta^{\mu\nu} j_\nu$ and $\nu_5^\mu = \Delta^{\mu\nu} j_{5,\nu}$, are obtained by removing the longitudinal components of the corresponding four-currents with the help of the projection operator $\Delta^{\mu\nu} \equiv g^{\mu\nu} - u^\mu u^\nu$. Here it might be appropriate to mention in passing that, in the case of chiral fluids, the currents ν^μ and ν_5^μ may contain not only the usual dissipative contributions but also anomalous nondissipative ones that originate from quantum anomalies.

Indeed, let us calculate the currents in the equilibrium by substituting the distribution function from Eq. (2.4) into the definitions (2.6)-(2.7). The result can be found using the integrals from Appendix A:

$$n_{\rm eq} = \frac{\mu(\mu^2 + 3\mu_5^2 + \pi^2 T^2)}{3\pi^2\hbar^3}, \qquad \nu^\mu_{\rm eq} = \sigma_\omega \omega^\mu + \sigma_B B^\mu, \tag{2.11}$$

$$n_{5,\rm eq} = \frac{\mu_5(\mu_5^2 + 3\mu^2 + \pi^2 T^2)}{3\pi^2\hbar^3}, \qquad \nu^\mu_{5,\rm eq} = \sigma^5_\omega \omega^\mu + \sigma^5_B B^\mu, \tag{2.12}$$

where the densities $n_{\rm eq}$ and $n_{5,\rm eq}$ coincide with the ones for an ideal massless non-chiral fluid. The chiral nondissipative contributions to the currents $\nu^\mu_{\rm eq}$ and $\nu^\mu_{5,\rm eq}$ include the celebrated chiral magnetic effect (Fukushima *et al.* (2008); Vilenkin (1980a); Metlitski and Zhitnitsky (2005)) and chiral vortical effect (Vilenkin (1978, 1979, 1980b); Erdmenger *et al.* (2009); Banerjee *et al.* (2011); Son and Surówka (2009); Isachenkov and Sadofyev (2011); Neiman and Oz (2011); Landsteiner *et al.* (2011)). The corresponding anomalous transport coefficients are given by

$$\sigma_\omega = \frac{\mu\mu_5}{\pi^2\hbar^2}, \qquad \sigma_B = e\frac{\mu_5}{2\pi^2\hbar^2}, \tag{2.13}$$

$$\sigma^5_\omega = \frac{3(\mu^2+\mu_5^2)+\pi^2T^2}{6\pi^2\hbar^2}, \qquad \sigma^5_B = e\frac{\mu}{2\pi^2\hbar^2}. \tag{2.14}$$

The analogous decomposition for the energy-momentum tensor reads

$$T^{\mu\nu} = \epsilon u^\mu u^\nu - \Delta^{\mu\nu}P + (h^\mu u^\nu + u^\mu h^\nu) + \pi^{\mu\nu}, \tag{2.15}$$

where $\epsilon = T^{\mu\nu}u_\mu u_\nu$ is the energy density, $P = \Delta_{\mu\nu}T^{\mu\nu}/3$ is the pressure, $h^\mu = \Delta^{\mu\alpha}T^{\alpha\beta}u_\beta$ is the energy flow (or, equivalently, the momentum density vector), and $\pi^{\mu\nu} = \Delta^{\mu\nu}_{\alpha\beta}T^{\alpha\beta}$ is the dissipative part of the energy-momentum tensor, which is defined in terms of the traceless four-index projection operator $\Delta^{\mu\nu}_{\alpha\beta} = \frac{1}{2}\Delta^\mu_\alpha\Delta^\nu_\beta + \frac{1}{2}\Delta^\mu_\beta\Delta^\nu_\alpha - \frac{1}{3}\Delta^{\mu\nu}\Delta_{\alpha\beta}$.

We note that, by making use of the definition of the energy-momentum tensor (2.8) and the Wigner function (2.2), one can derive the well-known equation of state for an ideal gas of massless fermions: $P = \Delta_{\mu\nu}T^{\mu\nu}/3 = \epsilon/3$. In such an approximation, the speed of sound is $c_s = 1/\sqrt{3}$. In a more realistic case of interacting massless fermions, the value of c_s^2 is expected to be somewhat smaller than 1/3, but usually not much. Indeed, even in a strongly interacting quark-gluon plasma, the value of c_s^2 is found to be about 0.25 to 0.3 for almost all temperatures above the deconfinement transition (Bazavov *et al.* (2014)). Moreover, c_s^2 increases with temperature and reaches within 10% of the ideal gas value already at $T \simeq 350$ MeV.

In our study here, we address the qualitative features of collective modes and the role of dynamical electromagnetism in the chiral hydrodynamics framework. Since a specific value of the sound velocity in this context is not of much importance, it will be sufficient for us to use the simplest equation of state of an ideal massless gas. It will also be clear that none of our qualitative results will change if a more complicated equation of state is used.

Analogously to the currents one can find the energy-momentum tensor in the equilibrium by substituting the distribution function from Eq. (2.4) into the definition (2.8). The resulting parameters are:

$$\epsilon_{\rm eq} = \frac{\mu^4 + 6\mu^2\mu_5^2 + \mu_5^4}{4\pi^2\hbar^3} + \frac{T^2(\mu^2+\mu_5^2)}{2\hbar^3} + \frac{7\pi^2T^4}{60\hbar^3}, \qquad h^\mu_{\rm eq} = \xi_\omega\omega^\mu + \xi_B B^\mu, \tag{2.16}$$

where the energy density is again coincide with the one for the ideal non-chiral massless fluid and $P_{\rm eq} = \epsilon_{\rm eq}/3$. The equilibrium heat current $h^\mu_{\rm eq}$ is again nondissipative with contributions from the energy counterparts of the chiral magnetic and vortical effects. These are controlled by the coefficients:

$$\xi_\omega = \frac{\mu_5\,(\mu_5^2 + 3\mu^2 + \pi^2T^2)}{3\pi^2\hbar^2}, \qquad \xi_B = e\frac{\mu\mu_5}{2\pi^2\hbar^2}. \tag{2.17}$$

By calculating the divergences of the current densities, defined in Eqs. (2.6) and (2.7) in terms of the Wigner function, and the energy-momentum tensor in Eq. (2.8) and then taking also the CKT equation (2.3) into account, we obtain the following relations:

$$\partial_\mu j^\mu = -\frac{1}{\tau}(n - n_{\rm eq}), \tag{2.18}$$

$$\partial_\mu j_5^\mu + \frac{e^2}{8\pi^2\hbar^2}F^{\mu\nu}\tilde{F}_{\mu\nu} = -\frac{1}{\tau}(n_5 - n_{5,\rm eq}), \tag{2.19}$$

$$\begin{aligned}\partial_\nu T^{\mu\nu} - eF^{\mu\nu}j_\nu &= -\frac{u^\mu}{\tau}\left(\epsilon - \epsilon_{\rm eq} + \frac{\hbar}{2}\omega_\nu(\nu_5^\nu - \nu_{5,\rm eq}^\nu)\right) \\ &\quad -\frac{1}{\tau}\left(h^\mu - h^\mu_{\rm eq} - \frac{\hbar}{4}\varepsilon^{\mu\alpha\beta\gamma}u_\alpha\dot{u}_\beta(\nu_{5,\gamma} - \nu_{5,\gamma}^{\rm eq})\right),\end{aligned} \tag{2.20}$$

where $\dot{u}_\beta = u^\alpha \partial_\alpha u_\beta$. Of course, the correct forms of the corresponding continuity equations in the chiral plasma should have the vanishing right-hand sides. This is clearly not the case for Eqs. (2.18)–(2.20) derived from the CKT in the relaxation-time approximation. In fact, this is a well-known artifact of such an approximation (Anderson and Witting (1974)). The root of the problem lies in the equilibrium distribution function, which is used in the definition, but was not fully specified yet. The conservation laws are enforced by imposing the following self-consistency conditions (Anderson and Witting (1974)):

$$n = n_{\rm eq}, \tag{2.21}$$

$$n_5 = n_{5,\rm eq}, \tag{2.22}$$

$$\epsilon + \frac{\hbar}{2}\omega_\mu \nu_5^\mu = \epsilon_{\rm eq} + \frac{\hbar}{2}\omega_\mu \nu_{5,\rm eq}^\mu, \tag{2.23}$$

$$h^\mu - \frac{\hbar}{4}\varepsilon^{\mu\alpha\beta\gamma} u_\alpha \dot{u}_\beta \nu_{5,\gamma} = h^\mu_{\rm eq} - \frac{\hbar}{4}\varepsilon^{\mu\alpha\beta\gamma} u_\alpha \dot{u}_\beta \nu_{5,{\rm eq},\gamma}. \tag{2.24}$$

These can be viewed as the defining relations for the local equilibrium parameters T, μ_λ, and u^μ in terms of the local values of the fermion number density n, the chiral charge density n_5, the energy density ϵ, and the momentum density h^μ. Alternatively, the above conditions specify the local fermion number density, the chiral charge density, the energy density, and the momentum density, respectively, in terms of the local equilibrium values of T, μ_λ, and u^μ.

Before proceeding further with the derivation, it is instructive to mention that the second term in Eq. (2.19) describes the chiral anomaly, which explicitly breaks the conservation of the chiral charge. In principle, Eq. (2.19) may also contain a similar anomalous contribution from the non-Abelian gauge fields. In fact, it is known that non-Abelian topological configurations could play an important role in heavy-ion collisions. For example, they may produce metastable $\mathcal{P}$- and $\mathcal{CP}$-odd domains with a nonzero chiral imbalance that could be detected via the chiral magnetic ef-

fect (Kharzeev (2006); Kharzeev *et al.* (2008)). Additionally, the non-Abelian gauge configurations with parallel chromoelectric and chromomagnetic fields could play an important role in the early ("glasma") stage of heavy-ion collisions (Lappi and McLerran (2006)). In the hydrodynamic description used here, however, we do not include such effects explicitly. In the long-wavelength limit, they are captured effectively by inclusion of a nonzero chiral chemical potential.

The dissipative components of the currents and the energy-momentum tensor, i.e., ν^μ, ν_5^μ, and $\pi^{\mu\nu}$, can be calculated in the first order of gradients by using the gradient-expansion solution to the CKT equation (2.3), i.e.,

$$f = f_{\rm eq} - \frac{\tau}{p\cdot u} p\cdot\mathcal{D} f_{\rm eq} + O(\tau^2\mathcal{D}^2). \tag{2.25}$$

By substituting this distribution function into the definitions in Eqs. (2.6)–(2.8), calculating the integrals over the momenta using the formulas in Appendix A, and then extracting the longitudinal and transverse components, we derive the following results up to terms $O(\hbar^2, \hbar\tau\mathcal{D}, \tau^2\mathcal{D}^2)$:

$$\nu^\mu = \nu^\mu_{\rm eq} + \frac{\tau}{3}\nabla^\mu n - \tau\dot{u}^\mu n + \frac{1}{e}\sigma_E E^\mu, \tag{2.26}$$

$$\nu_5^\mu = \nu^\mu_{5,\rm eq} + \frac{\tau}{3}\nabla^\mu n_5 - \tau\dot{u}^\mu n_5 + \frac{1}{e}\sigma_E^5 E^\mu, \tag{2.27}$$

$$\pi^{\mu\nu} = \frac{8\tau\epsilon}{15}\Delta^{\mu\nu}_{\alpha\beta}(\partial^\alpha u^\beta), \tag{2.28}$$

where $\nu^\mu_{\rm eq}$ and $\nu^\mu_{5,\rm eq}$ are the anomalous nondissipative contributions present even in the equilibrium. Their explicit form is given in Eqs. (2.13)-(2.14). Note that, by definition, $\nabla^\mu \equiv \Delta^{\mu\nu}\partial_\nu = \partial^\mu - u^\mu u^\nu\partial_\nu$ and σ_E is the conventional (positive definite) electrical conductivity that appears in Omh's law, i.e., $j^\mu_{\rm el} \equiv e\nu^\mu = \sigma_E E^\mu$. Also, the electric and magnetic fields in the local fluid frame are given by $E^\mu = F^{\mu\nu}u_\nu$ and $B^\mu = \tilde{F}^{\mu\nu}u_\nu$, respectively.

In the relaxation-time approximation used here, the expressions for the two types

of dissipative conductivities in Eqs. (2.26) and (2.27) are given by

$$\sigma_E = \tau e^2 \frac{3(\mu^2+\mu_5^2)+\pi^2 T^2}{9\pi^2\hbar^3}, \tag{2.29}$$

$$\sigma_E^5 = \tau e^2 \frac{2\mu\mu_5}{3\pi^2\hbar^3}. \tag{2.30}$$

Furthermore, after taking into account the self-consistency conditions (2.21)–(2.24), we arrive at the following first-order hydrodynamic equations:

$$\dot{n} + n\partial_\mu u^\mu + \partial_\mu \nu^\mu = 0, \tag{2.31}$$

$$\dot{n}_5 + n_5\partial_\mu u^\mu + \partial_\mu \nu_5^\mu = -\frac{e^2}{2\pi^2\hbar^2} E^\mu B_\mu, \tag{2.32}$$

$$\dot{\epsilon} + (\epsilon+P)\partial_\mu u^\mu + \partial_\mu h^\mu + u_\mu \dot{h}^\mu - \pi^{\mu\nu}\partial_\mu u_\nu = -eE^\mu \nu_\mu, \tag{2.33}$$

$$(\epsilon+P)\dot{u}^\mu - \nabla^\mu P + h^\alpha \partial_\alpha u^\mu + h^\mu(\partial_\alpha u^\alpha) + \Delta^\mu_\alpha \dot{h}^\alpha + \Delta^\mu_\alpha \partial_\beta \pi^{\alpha\beta} = \varepsilon^{\mu\nu\alpha\beta}\nu_\nu u_\alpha e B_\beta + eE^\mu n. \tag{2.34}$$

Here and later in the text we will denote a comoving derivative with a dot over a symbol, i.e., $\dot{X} \equiv u_\mu \partial^\mu X$. Finally, by recalling that the electromagnetic fields should be treated as fully dynamical in charged plasmas, the above set of equations should be supplemented by the Maxwell equations, i.e.,

$$\partial_\nu F^{\nu\mu} = enu^\mu + e\nu^\mu - en_{\rm bg}u^\mu_{\rm bg}, \tag{2.35}$$

as well as the Bianchi identity, $\partial_\nu \tilde{F}^{\nu\mu} = 0$. Note that Eq. (2.35) captures both the Gauss and the Ampere laws. In writing down the corresponding equations, we assumed that, in general, the total electric current density may include a nonzero contribution from a static nonchiral background, $\rho^\mu_{\rm bg} = en_{\rm bg}u^\mu_{\rm bg}$. Such a contribution could play an important role, for example, in cases when a nonzero electric charge of the chiral plasma is compensated by a neutralizing background charge of heavy (possibly nonrelativistic) particles.

By taking into account the constraint for the flow velocity four-vector, $u^\mu u_\mu = 1$, it should be clear that not all of hydrodynamic equations (2.31)–(2.34) are truly

independent. Also, by noting that $u^\mu E_\mu = u^\mu B_\mu = 0$, we find that two out of the total eight equations (including the Bianchi identity) for the electromagnetic field strength tensor are redundant. In fact, as one can check, there are a total of 12 independent equations for 12 variables (i.e., six hydrodynamic variables and six components of the electromagnetic field) that govern the hydrodynamic evolution of charged chiral plasma.

2.3 Higher-order chiral hydrodynamics

The set of conservation equations (2.31)-(2.34) found in the previous section governing a chiral plasma contains eleven independent dissipative parameters ν^μ, ν_5^μ, and $\pi^{\mu\nu}$, which have to be specified separately. In the first order in gradients this can be done using the kinetic equation rewritten as Eq. (2.25); the result is given by Eqs. (2.26)-(2.28). However, if one tries to extend the same procedure to the second and higher orders, the resulting system generally turns out to be non-causal and singular (Hiscock and Lindblom (1983); Denicol *et al.* (2008); Pu *et al.* (2010)). This problem was recognized a long time ago and is usually solved by promoting the mentioned above dissipative parameters to independent degrees of freedom - a method proposed by Israel (1976) and Israel and Stewart (1979). In order to close the system the evolution equations for these new degrees of freedom are then have to be truncated using some approximation scheme. The most common schemes used are a 14-moment approximation (Denicol *et al.* (2012)), which truncates the system by neglecting higher-order in momentum correlation functions, and the Chapman-Enskog method (Chapman and Cowling (1970)), which uses an iterative solution to the kinetic equation. In this section we will follow the latter scheme in an approach similar to that by Jaiswal (2013b), by first deriving the second-order chiral hydrodynamics and then using it to come up with a system encapsulating effectively infinitely many

orders. Note, however, that our analysis deals with a neutral chiral plasma, the case of charged chiral plasma will be addressed in the future projects.

Let us start by rewriting the kinetic equation (2.3) in the following form:

$$\delta(p^2)\left[\dot{f}+\frac{f}{\tau}\right]=\delta(p^2)\left[\frac{f_{\rm eq}}{\tau}-\frac{p\cdot\nabla f}{p\cdot u}-\frac{\lambda\hbar}{p\cdot u}(\partial_\sigma S^{\sigma\rho})\partial_\rho f\right]+O(\hbar)^2. \tag{2.36}$$

Using the definitions for the dissipative functions, $\nu^\mu=\Delta^\mu_\nu j^\nu$, $\nu_5^\mu=\Delta^\mu_\nu j_5^\nu$, and $\pi^{\mu\nu}=\Delta^{\mu\nu}_{\alpha\beta}T^{\alpha\beta}$, we can express their comoving derivatives to the linear order in $\hbar$ in the following form:

$$\begin{aligned}
\dot{\nu}^{\langle\mu\rangle}&=-\dot{u}^\mu n+\Delta^\mu_\nu\sum_\lambda\int p^\nu\dot{f}\\
&\quad+\hbar\Delta^\mu_\nu\sum_\lambda\lambda\int\Big[S^{\nu\alpha}\partial_\alpha\dot{f}-S^{\nu\alpha}(\partial_\alpha u^\beta)\partial_\beta f+\dot{S}^{\nu\alpha}\partial_\alpha f\Big], &(2.37)\\
\dot{\nu}_5^{\langle\mu\rangle}&=-\dot{u}^\mu n_5+\Delta^\mu_\nu\sum_\lambda\lambda\int p^\nu\dot{f}\\
&\quad+\hbar\Delta^\mu_\nu\sum_\lambda\int\Big[S^{\nu\alpha}\partial_\alpha\dot{f}-S^{\nu\alpha}(\partial_\alpha u^\beta)\partial_\beta f+\dot{S}^{\nu\alpha}\partial_\alpha f\Big], &(2.38)\\
\dot{\pi}^{\langle\mu\nu\rangle}&=-2\Delta^{\mu\nu}_{\alpha\beta}h^\alpha\dot{u}^\beta+\Delta^{\mu\nu}_{\alpha\beta}\sum_\lambda\int p^\alpha p^\beta\dot{f}\\
&\quad+\hbar\Delta^{\mu\nu}_{\alpha\beta}\sum_\lambda\lambda\int\Big[p^\alpha S^{\beta\gamma}\partial_\gamma\dot{f}-p^\alpha S^{\beta\gamma}(\partial_\gamma u^\delta)\partial_\delta f+p^\alpha\dot{S}^{\beta\gamma}\partial_\gamma f\Big], &(2.39)
\end{aligned}$$

where, by definition, the quantities with the Lorentz indices in angle brackets are the projections of the corresponding quantities onto the subspace orthogonal to the four-velocity, i.e., $\dot{\nu}^{\langle\mu\rangle}\equiv\Delta^\mu_\alpha\dot{\nu}^\alpha$ and $\dot{\pi}^{\langle\mu\nu\rangle}\equiv\Delta^{\mu\nu}_{\alpha\beta}\dot{\pi}^{\alpha\beta}$. We also introduced a short-hand notation:

$$\int X\equiv\int\frac{d^4p}{(2\pi\hbar)^3}2\,\delta(p^2)X. \tag{2.40}$$

The use of projectors here is needed in order to force the dissipative current densities and the shear stress tensor to remain consistent with their generic definitions. This can be also viewed as a necessary condition for a self-consistent truncation of the evolution equations.

By making use of the kinetic equation (2.36), the relations for the comoving derivatives, Eqs. (2.41)–(2.43), can be equivalently rewritten as follows:

$$\dot{\nu}^{\langle\mu\rangle} + \frac{\nu^\mu}{\tau} = -\dot{u}^\mu n + \Delta^\mu_\nu \sum_\lambda \int p^\nu \left(\frac{f_{\rm eq}}{\tau} - \frac{p\cdot\nabla f}{p\cdot u} - \frac{\lambda\hbar}{p\cdot u}(\partial_\sigma S^{\sigma\rho})\partial_\rho f \right) + \hbar\Delta^\mu_\nu \sum_\lambda \lambda \int \left[S^{\nu\alpha}\partial_\alpha \left(\frac{f_{\rm eq}}{\tau} - \frac{p\cdot\nabla f}{p\cdot u} \right) - S^{\nu\alpha}(\partial_\alpha u^\beta)\partial_\beta f + \dot{S}^{\nu\alpha}\partial_\alpha f \right], \tag{2.41}$$

$$\dot{\nu}_5^{\langle\mu\rangle} + \frac{\nu_5^\mu}{\tau} = -\dot{u}^\mu n_5 + \Delta^\mu_\nu \sum_\lambda \lambda \int p^\nu \left(\frac{f_{\rm eq}}{\tau} - \frac{p\cdot\nabla f}{p\cdot u} - \frac{\lambda\hbar}{p\cdot u}(\partial_\sigma S^{\sigma\rho})\partial_\rho f \right) + \hbar\Delta^\mu_\nu \sum_\lambda \int \left[S^{\nu\alpha}\partial_\alpha \left(\frac{f_{\rm eq}}{\tau} - \frac{p\cdot\nabla f}{p\cdot u} \right) - S^{\nu\alpha}(\partial_\alpha u^\beta)\partial_\beta f + \dot{S}^{\nu\alpha}\partial_\alpha f \right], \tag{2.42}$$

$$\dot{\pi}^{\langle\mu\nu\rangle} + \frac{\pi^{\mu\nu}}{\tau} = -2\Delta^{\mu\nu}_{\alpha\beta} h^\alpha \dot{u}^\beta + \Delta^{\mu\nu}_{\alpha\beta} \sum_\lambda \int p^\alpha p^\beta \left(\frac{f_{\rm eq}}{\tau} - \frac{p\cdot\nabla f}{p\cdot u} - \frac{\lambda\hbar}{p\cdot u}(\partial_\sigma S^{\sigma\rho})\partial_\rho f \right) + \hbar\Delta^{\mu\nu}_{\alpha\beta} \sum_\lambda \lambda \int \left[p^\alpha S^{\beta\gamma}\partial_\gamma \left(\frac{f_{\rm eq}}{\tau} - \frac{p\cdot\nabla f}{p\cdot u} \right) - p^\alpha S^{\beta\gamma}(\partial_\gamma u^\delta)\partial_\delta f + p^\alpha \dot{S}^{\beta\gamma}\partial_\gamma f \right], \tag{2.43}$$

These equations for dissipative functions contain the distribution function f. In order to obtain a closed set of equations, the right-hand sides of the equations above should be reexpressed in terms of the hydrodynamic variables and dissipative functions. To achieve this, we replace the distribution function with its iterative solution from the kinetic equation Eq. (2.3) in the form:

$$f \simeq f_{\rm eq} - \frac{\tau}{p\cdot u} p\cdot\partial f_{\rm eq} + O(\partial^2), \tag{2.44}$$

where only one order is sufficient for the second-order hydrodynamics. We then further approximate the equilibrium distribution function by its expansion to the linear order in $\hbar$ using Eq. (2.4):

$$f_{\rm eq} \simeq f_0 + \frac{\lambda\hbar}{2}\frac{p^\mu\omega_\mu}{p\cdot u} f_0' + O(\hbar^2), \tag{2.45}$$

where f_0 is the equilibrium function at a vanishing vorticity and $f_0' \equiv \partial f_0/\partial\varepsilon_{p,0} = -\partial f_0/\partial\mu_\lambda$. Now, by using the moments of the equilibrium distribution function from

Appendix A, we rewrite the evolution equations for the dissipative functions in the following form:

$$\begin{aligned}\dot{\nu}^{\langle\mu\rangle}+\frac{\nu^{\mu}}{\tau}=&-\dot{u}^{\mu}n+\sum_{\lambda}\Bigg[\frac{1}{3}\nabla^{\mu}I_3+\lambda\frac{\hbar}{\tau}\omega^{\mu}I_2\\&-\frac{2\tau}{5}\nabla^{\mu}(\partial\cdot u)I_3-\frac{7\tau}{15}(\partial\cdot u)\nabla^{\mu}I_3+\tau\dot{u}^{\mu}(\partial\cdot u)I_3+\frac{4\tau}{5}\dot{u}^{\rho}(\partial_{\rho}u^{\mu})I_3-\frac{\tau}{3}\nabla^{\mu}\dot{I}_3\\&-\frac{7\tau}{15}(\nabla_{\rho}u^{\mu})\nabla^{\rho}I_3-\frac{2\tau}{5}(\nabla^{\mu}u_{\rho})\dot{u}^{\rho}I_3-\frac{2\tau}{15}(\nabla^{\mu}u^{\rho})\partial_{\rho}I_3-\frac{\tau}{5}\Delta^{\mu}_{\nu}(\partial\cdot\partial u^{\nu})I_3+\frac{\tau}{5}\Delta^{\mu}_{\nu}\ddot{u}^{\nu}I_3\\&-\lambda\frac{14\hbar}{15}\omega^{\mu}(\partial\cdot u)I_2-\lambda\frac{14\hbar}{15}\omega^{\nu}(\partial_{\nu}u^{\mu})I_2+\lambda\frac{\hbar}{15}\omega^{\nu}(\nabla^{\mu}u_{\nu})I_2-\lambda\frac{2\hbar}{3}\omega^{\mu}\dot{I}_2\\&+\lambda\frac{\hbar}{6}\varepsilon^{\mu\nu\alpha\beta}u_{\alpha}\dot{u}_{\beta}\partial_{\nu}I_2-\lambda\frac{\hbar}{3}\varepsilon^{\mu\nu\alpha\beta}u_{\beta}(\partial_{\nu}u^{\rho})(\partial_{\rho}u_{\alpha})I_2\Bigg],\end{aligned}\tag{2.46}$$

$$\begin{aligned}\dot{\nu}_5^{\langle\mu\rangle}+\frac{\nu_5^{\mu}}{\tau}=&-\dot{u}^{\mu}n_5+\sum_{\lambda}\lambda\Bigg[\frac{1}{3}\nabla^{\mu}I_3+\lambda\frac{\hbar}{\tau}\omega^{\mu}I_2\\&-\frac{2\tau}{5}\nabla^{\mu}(\partial\cdot u)I_3-\frac{7\tau}{15}(\partial\cdot u)\nabla^{\mu}I_3+\tau\dot{u}^{\mu}(\partial\cdot u)I_3+\frac{4\tau}{5}\dot{u}^{\rho}(\partial_{\rho}u^{\mu})I_3-\frac{\tau}{3}\nabla^{\mu}\dot{I}_3\\&-\frac{7\tau}{15}(\nabla_{\rho}u^{\mu})\nabla^{\rho}I_3-\frac{2\tau}{5}(\nabla^{\mu}u_{\rho})\dot{u}^{\rho}I_3-\frac{2\tau}{15}(\nabla^{\mu}u^{\rho})\partial_{\rho}I_3-\frac{\tau}{5}\Delta^{\mu}_{\nu}(\partial\cdot\partial u^{\nu})I_3+\frac{\tau}{5}\Delta^{\mu}_{\nu}\ddot{u}^{\nu}I_3\\&-\lambda\frac{14\hbar}{15}\omega^{\mu}(\partial\cdot u)I_2-\lambda\frac{14\hbar}{15}\omega^{\nu}(\partial_{\nu}u^{\mu})I_2+\lambda\frac{\hbar}{15}\omega^{\nu}(\nabla^{\mu}u_{\nu})I_2-\lambda\frac{2\hbar}{3}\omega^{\mu}\dot{I}_2\\&+\lambda\frac{\hbar}{6}\varepsilon^{\mu\nu\alpha\beta}u_{\alpha}\dot{u}_{\beta}\partial_{\nu}I_2-\lambda\frac{\hbar}{3}\varepsilon^{\mu\nu\alpha\beta}u_{\beta}(\partial_{\nu}u^{\rho})(\partial_{\rho}u_{\alpha})I_2\Bigg],\end{aligned}\tag{2.47}$$

$$\begin{aligned}\dot{\pi}^{\langle\mu\nu\rangle}+\frac{\pi^{\mu\nu}}{\tau}=&-2\Delta^{\mu\nu}_{\alpha\beta}h^{\alpha}\dot{u}^{\beta}+\Delta^{\mu\nu}_{\alpha\beta}\sum_{\lambda}\Bigg[\frac{8}{15}(\partial^{\alpha}u^{\beta})I_4\\&-\frac{32\tau}{35}(\partial^{\alpha}u^{\beta})(\partial\cdot u)I_4-\frac{8\tau}{15}\partial^{\alpha}(\dot{u}^{\beta}I_4)-\frac{16\tau}{35}(\nabla_{\rho}u^{\alpha})(\nabla^{\rho}u^{\beta})I_4-\frac{8\tau}{21}(\partial^{\alpha}u^{\rho})(\partial^{\rho}u^{\beta})I_4\\&+\frac{2\tau}{15}\partial^{\alpha}\partial^{\beta}I_4-\frac{2\tau}{3}(\partial^{\alpha}u^{\beta})\dot{I}_4+\frac{8\tau}{105}(\partial^{\alpha}u_{\rho})(\partial^{\beta}u^{\rho})I_4\\&+\lambda\frac{\hbar}{5}(\partial^{\alpha}\omega^{\beta})I_3+\lambda\frac{7\hbar}{15}\omega^{\alpha}\partial^{\beta}I_3+\lambda\frac{\hbar}{5}\dot{u}^{\alpha}\omega^{\beta}I_3+\lambda\frac{\hbar}{10}\varepsilon^{\beta\sigma\rho\delta}u_{\delta}\partial_{\sigma}(I_3\nabla^{\alpha}u_{\rho})\\&+\lambda\frac{\hbar}{10}\varepsilon^{\beta\sigma\rho\delta}u_{\delta}(\partial_{\sigma}u^{\alpha})\partial_{\rho}I_3+\lambda\frac{\hbar}{5}\dot{u}^{\alpha}\varepsilon^{\beta\sigma\rho\delta}u_{\rho}(\partial_{\sigma}u_{\delta})I_3+\lambda\frac{\hbar}{5}\varepsilon^{\beta\sigma\rho\delta}u_{\sigma}\dot{u}_{\rho}(\partial_{\delta}u^{\alpha})I_3\Bigg].\end{aligned}\tag{2.48}$$

As is easy to check, these equations for dissipative functions are sufficient to close the whole system of equations of the second-order dissipative hydrodynamics. Indeed, we have Eqs. (2.31)–(2.34) for hydrodynamic variables n, n_5, ϵ, and h^μ. Note also that the thermodynamic pressure is defined by the corresponding constitutive equation, $P = \epsilon/3$. The corresponding equations are supplemented by Eqs. (2.46)–(2.48) for functions ν^μ, ν_5^μ, and $\pi^{\mu\nu}$. According to Eqs. (A.8)–(A.10) in Appendix A, quantities I_2, I_3, and I_4 on the right-hand side of Eqs. (2.46)–(2.48) are expressed through the local equilibrium chemical potentials μ, μ_5 and temperature T, which in turn could be expressed through the local values of n, n_5, and ϵ, respectively; see the constraints in Eqs. (2.21)–(2.23).

The right-hand side of the equations for dissipative functions can be further simplified by making use of the following first-order relations:

$$\nu^\mu = \sum_\lambda \left[\lambda\hbar\omega^\mu I_2 + \frac{\tau}{3}\nabla^\mu I_3 - \tau\dot{u}^\mu I_3\right] + O(\partial^2), \tag{2.49}$$

$$\nu_5^\mu = \sum_\lambda \lambda\left[\lambda\hbar\omega^\mu I_2 + \frac{\tau}{3}\nabla^\mu I_3 - \tau\dot{u}^\mu I_3\right] + O(\partial^2), \tag{2.50}$$

$$\pi^{\mu\nu} = \sum_\lambda \frac{8\tau}{15}\Delta^{\mu\nu}_{\alpha\beta}(\partial^\alpha u^\beta) I_4 + O(\partial^2), \tag{2.51}$$

which follow from Eqs. (2.46)–(2.48). (Let us note in passing that the above first-order relations define the diffusion constant and the shear viscosity in terms of the relaxation time: $D = \tau/3$ and $\zeta = 8\tau\epsilon/15$, respectively.) Indeed, by making use of these equations as well as the continuity equations in the leading order in derivatives, we can reexpress most of the terms with an explicit dependence on the relaxation time in Eqs. (2.46)–(2.48) in terms of the hydrodynamic functions themselves. After doing this, the final set of equations for dissipative functions takes a simpler form,

i.e.,

$$\dot{\nu}^{\langle\mu\rangle} + \frac{\nu^\mu - \nu^\mu_{\rm eq}}{\tau} = -\dot{u}^\mu n + \frac{1}{3}\nabla^\mu n - \frac{n}{\epsilon+P}\Delta^{\mu\nu}\partial^\rho\pi_{\rho\nu} - \nu_\rho\omega^{\rho\mu} - (\partial\cdot u)\nu^\mu \\ - \frac{9}{5}(\partial^{\langle\mu}u^{\rho\rangle})\nu_\rho + \frac{14}{15}(\nabla^{\langle\mu}u^{\rho\rangle})\nu_{{\rm eq},\rho} - \frac{2}{9}(\partial\cdot u)\nu^\mu_{\rm eq} \\ - \frac{2\hbar}{3}\omega^\mu\sum_\lambda \lambda\dot{I}_2 + \sum_\lambda \lambda\frac{\hbar}{6}\varepsilon^{\mu\nu\alpha\beta}\left[u_\alpha\dot{u}_\beta\partial_\nu I_2 - 2u_\beta(\partial_\nu u^\rho)(\partial_\rho u_\alpha)I_2\right], \tag{2.52}$$

$$\dot{\nu}_5^{\langle\mu\rangle} + \frac{\nu_5^\mu - \nu^\mu_{5,{\rm eq}}}{\tau} = -\dot{u}^\mu n_5 + \frac{1}{3}\nabla^\mu n_5 - \frac{n_5}{\epsilon+P}\Delta^{\mu\nu}\partial^\rho\pi_{\rho\nu} - \nu_{5,\rho}\omega^{\rho\mu} - (\partial\cdot u)\nu_5^\mu \\ - \frac{9}{5}(\partial^{\langle\mu}u^{\rho\rangle})\nu_{5,\rho} + \frac{14}{15}(\nabla^{\langle\mu}u^{\rho\rangle})\nu_{5,{\rm eq},\rho} - \frac{2}{9}(\partial\cdot u)\nu^\mu_{5,{\rm eq}} \\ - \frac{2\hbar}{3}\omega^\mu\sum_\lambda \dot{I}_2 + \sum_\lambda \frac{\hbar}{6}\varepsilon^{\mu\nu\alpha\beta}\left[u_\alpha\dot{u}_\beta\partial_\nu I_2 - 2u_\beta(\partial_\nu u^\rho)(\partial_\rho u_\alpha)I_2\right], \tag{2.53}$$

$$\dot{\pi}^{\langle\mu\nu\rangle} + \frac{\pi^{\mu\nu}}{\tau} = -2h^{\langle\mu}\dot{u}^{\nu\rangle} + 2\pi_\rho^{\langle\mu}\omega^{\nu\rangle\rho} - \frac{10}{7}\pi_\rho^{\langle\mu}\sigma^{\nu\rangle\rho} - \frac{4}{3}\pi^{\mu\nu}\partial_\alpha u^\alpha \\ + \frac{8}{15}(\partial^{\langle\mu}u^{\nu\rangle})\epsilon + \frac{\hbar}{5}\left((\partial^{\langle\mu}\omega^{\nu\rangle})n_5 + \frac{7}{3}\omega^{\langle\mu}\partial^{\nu\rangle}n_5 - \dot{u}^{\langle\mu}\omega^{\nu\rangle}n_5\right) \\ + \frac{\hbar}{5}\Delta^{\mu\nu}_{\alpha\beta}\varepsilon^{\beta\sigma\rho\delta}\left[\frac{1}{2}u_\delta\partial_\sigma(n_5\nabla^\alpha u_\rho) + \frac{1}{2}u_\delta(\partial_\sigma u^\alpha)\partial_\rho n_5 + u_\sigma\dot{u}_\rho(\partial_\delta u^\alpha)n_5\right], \tag{2.54}$$

where $\sigma^{\mu\nu} = \partial^{\langle\alpha}u^{\beta\rangle} = \Delta^{\mu\nu}_{\alpha\beta}(\partial^\alpha u^\beta)$, $\omega^{\mu\nu} = (\nabla^\mu u^\nu - \nabla^\nu u^\mu)/2$, and $A^{\langle\mu\nu\rangle} \equiv \Delta^{\mu\nu}_{\alpha\beta}A^{\alpha\beta}$. In the derivation, we used the following relation:

$$\frac{1}{\epsilon+P}\Delta^{\mu\nu}\partial^\rho\pi_{\rho\nu} = \frac{\tau}{5}\Delta^{\mu\nu}(\partial^2 u_\nu) - \frac{\tau}{5}\Delta^{\mu\nu}\ddot{u}_\nu + \frac{\tau}{15}\nabla^\mu(\partial\cdot u) \\ - \frac{3\tau}{5}\dot{u}^\mu(\partial\cdot u) + \frac{3\tau}{5}\dot{u}^\rho(\partial_\rho u^\mu) + \frac{4\tau}{5}\dot{u}^\rho(\nabla^\mu u_\rho) + O(\partial^3), \tag{2.55}$$

which follows from Eq. (2.51) as well as the first-order continuity equations.

The set of second-order equations (2.52), (2.53), and (2.54) for dissipative functions in a chiral plasma is the main result of this section. This is a generalization of

the previous results by Anderson and Witting (1974); Denicol *et al.* (2010); Jaiswal (2013a,b); Jaiswal *et al.* (2015), which were obtained for massless plasmas without a chiral asymmetry (i.e., $n_5 = 0$ and $\nu_5^\mu = 0$) and without $\hbar$ corrections due to the spin. In the current study, in contrast, we treated the fermion chiralities as two components of a relativistic fluid. The (approximate) conservation of the axial charge in the chiral plasma gives rise to an additional continuity equation; see Eq. (2.53). Moreover, the quantum effects of the chiral plasma are captured by the linear in $\hbar$ corrections in the second-order theory.

Let us note here that by using Eqs. (2.49)–(2.51) to simplify the right hand sides of Eqs. (2.46)–(2.48) we also effectively included higher-order terms (although not all of them) into the system. Such an inclusion provides a "cheap" improvement to the second-order hydrodynamics bringing it closer to higher-order approximations without additional work (Jaiswal (2013a)). The same procedure can also be applied to derive the third- and higher-order chiral hydrodynamics.

Chapter 3

COLLECTIVE MODES IN CHIRAL PLASMAS

3.1 Equilibrium state

Before addressing the properties of collective modes in a magnetized chiral plasma with nonzero vorticity, we should determine the unperturbed (equilibrium) state of the corresponding system. In this section, we discuss how such a state is defined and what its main properties are. We will assume that the chiral charge density $n_{5,\mathrm{eq}}$ vanishes in equilibrium (i.e., $\mu_5 = 0$). In the corresponding state, as one can see from Eq. (2.30), the chiral electric separation effect is absent, i.e., $\sigma_E^5 = 0$, and several anomalous transport coefficients are trivial, i.e., $\sigma_\omega = \sigma_B = \xi_\omega = \xi_B = 0$, as is clear from Eqs. (2.13), (2.14) and (2.17).

Here it might be appropriate to mention that, despite the absence of an average chiral imbalance in equilibrium, it is still appropriate to call the corresponding plasma "chiral." Indeed, local fluctuations of the chirality imbalance can be generically induced by the anomalous processes triggered, for example, by collective modes. Also, from a technical viewpoint, the use of *chiral* hydrodynamics in the description implies that the additional (anomalous) chiral charge continuity relation is included in the complete set of equations. The corresponding extra degree of freedom can affect the dynamics and modify the properties of collective modes. We might also add that, from a conceptual viewpoint, there is no qualitative difference between a long-range hydrodynamic fluctuation and a nonzero local average of the chiral imbalance. Formally, this is due to the fact that the hydrodynamic description assumes local equilibrium even in the regions with slowly oscillating chiral imbalances induced

by collective modes.

In order to address the effects of vorticity on hydrodynamic modes, we assume that the background vorticity is approximately uniform on distance scales larger than the wavelengths of the modes. Otherwise, of course, the vortical effects would average to zero. In our study below, we model an isolated macroscopic region with approximately uniform vorticity by a uniformly rotating plasma. Without loss of generality, we assume that the plasma is confined to a cylindrical region of radius R and is uniformly rotating with angular velocity Ω about the z axis. In this study, we will concentrate primarily on the case with $\Omega R \ll 1$. Note, however, that many considerations, at least qualitatively, will remain valid even when $\Omega R \lesssim 1$. For simplicity, we also assume that the magnetic field $\mathbf{B}$ points along the same z axis. While this is clearly not the most general configuration, it is expected to be relevant for applications in heavy-ion collisions and the early universe, because the vorticity and magnetic field often tend to be aligned.

For the uniformly rotating plasma, the local fluid velocity in the hydrodynamic equilibrium $\bar{u}^\nu$, satisfying $\bar{u}^\nu \bar{u}_\nu = 1$, is given by (Florkowski *et al.* (2018b)):

$$\bar{u}^\nu = \gamma \begin{pmatrix} 1 \\ -\Omega y \\ \Omega x \\ 0 \end{pmatrix}, \tag{3.1}$$

where $\gamma = 1/\sqrt{1-\Omega^2 r^2}$ and $r \equiv |\mathbf{r}_\perp| = \sqrt{x^2+y^2}$. Here and below, the notations with bars, such as $\bar{u}^\nu$, represent fields in hydrodynamic equilibrium. It should be noted that $\partial_\mu \bar{u}^\mu = 0$ and $\Delta^{\mu\nu}_{\alpha\beta}(\partial^\alpha \bar{u}^\beta) = 0$. At the same time, the radial component of the acceleration is nonzero, $\dot{\bar{u}}^\mu = -\gamma^2 \Omega^2 \mathbf{r}_\perp$, as expected for a circular motion. The latter may suggest, however, that some dissipative processes are unavoidable in a rotating plasma (even if negligible to the linear order in Ω). Indeed, as one can see from

Eqs. (2.26) and (2.27), a nonzero $\dot{\bar{u}}^\mu$ could potentially trigger dissipative currents. As we will see below, this is not necessarily the case because the hydrodynamic equilibrium state is radially nonuniform.

As is easy to check, the flow velocity in Eq. (3.1) is characterized by a nonzero vorticity, i.e.,

$$\bar{\omega}^\mu = \frac{1}{2}\varepsilon^{\mu\nu\alpha\beta}\bar{u}_\nu\partial_\alpha\bar{u}_\beta = \gamma^2\Omega\delta^\mu_3. \tag{3.2}$$

It should be mentioned here that, unless stated differently, all explicit expressions for Lorentz vectors and tensors in the component form will be given from the viewpoint of the laboratory frame. In order to obtain these quantities in the comoving frame, one would need to perform the corresponding Lorentz transformation $\bar{u}'^\mu = \Lambda^\mu{}_\nu\bar{u}^\nu$ and $\bar{F}'^{\mu\nu} = \Lambda^\mu{}_\kappa\Lambda^\nu{}_\lambda\bar{F}^{\kappa\lambda}$, where

$$\Lambda^\mu{}_\nu = \begin{pmatrix} \gamma & \gamma\Omega y & -\gamma\Omega x & 0 \\ \gamma\Omega y & \frac{x^2+\gamma y^2}{r^2} & \frac{xy(1-\gamma)}{r^2} & 0 \\ -\gamma\Omega x & \frac{xy(1-\gamma)}{r^2} & \frac{\gamma x^2+y^2}{r^2} & 0 \\ 0 & 0 & 0 & 1 \end{pmatrix}. \tag{3.3}$$

For example, for the fluid flow velocity, we obtain $\bar{u}'^\mu = (1,0,0,0)$, as expected in the local comoving frame.

In the presence of a magnetic field, the definition of an equilibrium state of a charged rotating plasma is far from trivial. For example, a naive assumption that, in the lab frame, there is only a nonzero magnetic field pointing in the z direction is not self-consistent. Indeed, for such a configuration, there would be nonzero electric fields present in the comoving frame. Since such electric fields would drive nonvanishing dissipative currents [see Eqs. (2.26) and (2.27)], it would imply that the thermodynamic equilibrium is not reached in the local frame of the fluid.

In order to construct the global equilibrium state of the magnetized rotating plasma, therefore, we require that the electric fields vanish in the local fluid frame,

i.e., $\bar{E}^\mu \equiv \bar{F}^{\mu\nu}\bar{u}_\nu = 0$. As for the magnetic field in the same local frame $\bar{B}^\mu \equiv \tilde{F}^{\mu\nu}\bar{u}_\nu$, we assume only that it points in the z direction, i.e., $\bar{B}^\mu = B\delta^\mu_3$, and its magnitude may have a nontrivial dependence on the cylindrical radius coordinate, i.e., $B \equiv B(r)$. Then, the corresponding electromagnetic field stress tensor in the lab frame takes the following form:

$$\bar{F}^{\mu\nu} = \varepsilon^{\mu\nu\alpha\beta}\bar{u}_\alpha\bar{B}_\beta + \bar{E}^\mu\bar{u}^\nu - \bar{u}^\mu\bar{E}^\nu = \begin{pmatrix} 0 & \gamma B\Omega x & \gamma B\Omega y & 0 \\ -\gamma B\Omega x & 0 & -\gamma B & 0 \\ -\gamma B\Omega y & \gamma B & 0 & 0 \\ 0 & 0 & 0 & 0 \end{pmatrix}. \tag{3.4}$$

As we see, this includes not only a magnetic field in the z direction, $\mathbf{B}_{\rm lab} = \gamma B\hat{\mathbf{z}}$, but also an electric field in the radial direction, i.e., $\mathbf{E}_{\rm lab} = -\gamma B\Omega\mathbf{r}_\perp$. Alternatively, this can be viewed as the consequence of Ohm's law for an ideal plasma, $\mathbf{E}_{\rm lab} = -\mathbf{v}\times\mathbf{B}_{\rm lab}$. Note that such a configuration in the lab frame is possible because the electric force on a local element of the charged fluid is exactly compensated by the Lorentz force, see Fig. 3.1. In order to be consistent with Ampere's law, as we will argue below, the magnetic field B should additionally have a very specific dependence on the radial coordinate.

For the configuration in Eq. (3.4), the Bianchi identity is satisfied identically, while the Maxwell equations take the following explicit form:

$$-\delta^\mu_0\Omega\left[2\gamma B + r\partial_r(\gamma B)\right] + \left(\delta^\mu_1\frac{y}{r} - \delta^\mu_2\frac{x}{r}\right)\partial_r(\gamma B) = en_{\rm eq}\bar{u}^\mu - en_{\rm bg}u^\mu_{\rm bg}. \tag{3.5}$$

Here we took into account that $e\nu^\mu_{\rm eq} = 0$, which is indeed the case when $\mu_5 = 0$. Let us note in passing that major modifications would be needed in the analysis if one allows for a nonzero μ_5. Indeed, in order to enforce the hydrodynamic equilibrium and the absence of dissipative currents at $\mu_5 \neq 0$, additional nonzero components of the electromagnetic field would be required.

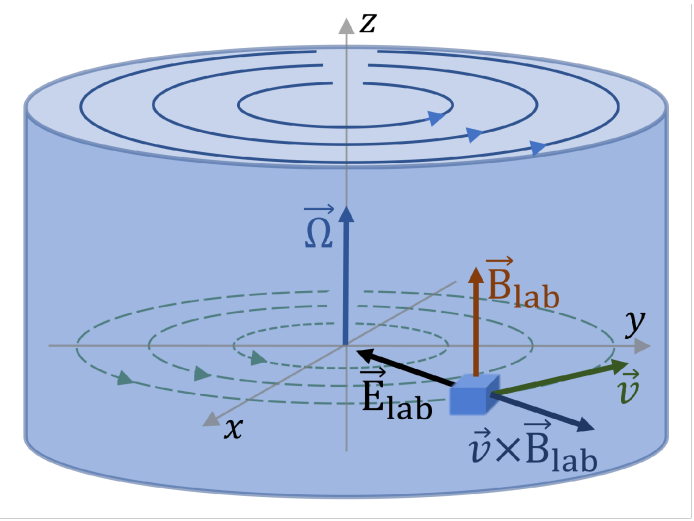

Figure 3.1: A charged element in a rotating plasma and the local electromagnetic fields. Note that the electric and Lorentz forces on a local element of plasma are equal in magnitude and opposite in direction.

We assume that the background charge is at rest in the lab frame, i.e., $u^\mu_{\rm bg,1} = (1,0,0,0)$. (It might also be interesting to consider a comoving background with $u^\mu_{\rm bg,2} = \bar{u}^\mu$, but we will not investigate such a possibility in this paper.) As is easy to check, the Maxwell equations require that the magnetic field and the charge density of the plasma have the following dependence on the radial coordinate:

$$B(r) = \gamma\left(B_0 - \frac{1}{2}en_{\rm bg}\Omega r^2\right) \simeq B_0 - \frac{1}{2}en_{\rm bg}\Omega r^2 + O\left(B_0 r^2\Omega^2\right), \qquad (3.6)$$

$$en_{\rm eq}(r) = \gamma^3\left(en_{\rm bg} - 2B_0\Omega\right) \simeq en_{\rm bg} - 2B_0\Omega + O\left(en_{\rm bg}r^2\Omega^2\right), \qquad (3.7)$$

where B_0 is the value of the magnetic field on the rotation axis (i.e., at $r = 0$). An interesting feature of this solution is that $\frac{1}{3}\nabla^\mu n_{\rm eq}(r) - \dot{\bar{u}}^\mu n_{\rm eq}(r) = 0$ to all orders in Ω. This means, in particular, that the dissipative part of the fermion number (electric) current in Eq. (2.26) vanishes exactly. This is quite amazing considering that the solution was obtained by solving the Maxwell equations (3.5) without any explicit considerations of dissipative effects.

We should remark that, in the absence of a background charge (i.e., $n_{\rm bg} = 0$), the solutions in Eqs. (3.6) and (3.7) appear to agree with the vortexlike solutions

found by Florkowski *et al.* (2018b). The dependence of the plasma density on the γ factor in Eq. (3.7) is also consistent with the findings of Becattini and Tinti (2010), stating that the local chemical potentials and temperature should be linear in γ: $\bar{\mu}(r) = \gamma\mu_0$, $\bar{\mu}_5(r) = \gamma\mu_{5,0}$, and $\bar{T}(r) = \gamma T_0$, where μ_0, $\mu_{5,0}$, and T_0 are the values of the corresponding parameters on the rotation axis. Indeed, in the case of a charged plasma made of massless particles, such a linear dependence automatically leads to the scaling law in Eq. (3.7). (It is not clear, though, whether similar arguments can be generalized for a plasma made of massive particles.)

As we see from the solutions in Eqs. (3.6) and (3.7), the Maxwell equations require that the local charge density is nonzero in a rotating plasma (e.g., to the leading order in vorticity, $en_{\rm eq} - en_{\rm bg} \simeq -2B_0\Omega$). From a physics viewpoint, one might interpret this as a charge separation induced by the uniform rotation. A nonzero electric charge in the bulk is achieved by pushing the compensating charge of the opposite sign out to the cylindrical boundary of the system. Interestingly, the sign of the induced charge in the bulk is determined by the relative orientation of the magnetic field and vorticity and, thus, it can easily be flipped, for example, by changing the direction of the magnetic field.

It should be noted that a charge separation in the rotating plasma is consistent with the fact that there is a nonzero electric field in the radial direction, $\mathbf{E}_{\rm lab} = -\gamma B\Omega\mathbf{r}_\perp$. As mentioned earlier, the electric force of such a field on a moving element of the charged plasma is exactly compensated by the Lorentz force from the magnetic field, $\mathbf{B}_{\rm lab} = \gamma B\hat{\mathbf{z}}$; see Fig. 3.1. Additionally, in agreement with Ampere's law, the circular currents of the plasma result in a total magnetic field that depends on the radial coordinate, see Eq. (3.6). In the presence of a background charge, moreover, the nontrivial dependence of the field on the radial coordinate appears already at the linear order in Ω, i.e., $B(r) \simeq B_0 - \frac{1}{2}en_{\rm bg}\Omega r^2$.

3.2 Linearized equations of chiral hydrodynamics

In order to set the stage for a systematic study of hydrodynamic collective modes in a rotating chiral plasma, here we will discuss how to derive the linearized equations for small perturbations of the hydrodynamic quantities around their equilibrium values. In the derivation, it is beneficial to take into account the symmetry of the unperturbed state with respect to time translations, translations in the spatial z direction, as well as the rotational symmetry about the z axis. (Recall that both the background magnetic field and the vorticity are parallel to the z axis.)

By taking into account the cylindrical symmetry in the problem, it is convenient to write down the general wavelike perturbations of (pseudo)scalar and (pseudo)vector quantities in the following form:

$$\delta s(x) = e^{-ik_0 t + ik_z z + im\theta} \delta s(r), \tag{3.8}$$

$$\delta v^3(x) = e^{-ik_0 t + ik_z z + im\theta} \delta v^3(r), \tag{3.9}$$

$$\delta v_\pm(x) = e^{-ik_0 t + ik_z z + i(m\pm 1)\theta} \delta v_\pm(r), \tag{3.10}$$

where s is a placeholder for all scalar and pseudoscalar parameters (i.e., μ, μ_5, or T). Similarly, the generic notations v^3 and $v_\pm$ stand for the longitudinal (i.e., u^3, B^3, or E^3) and transverse (i.e., $u_\pm$, $B_\pm$, or $E_\pm$) components of the vector quantities. Note that the plus and minus components are defined as follows: $v_\pm = \frac{1}{2}\left(v^1 \pm i v^2\right)$. Such a separation of the longitudinal and transverse components, as well as their dependence on the cylindrical radius $r = \sqrt{x^2 + y^2}$ and the polar angle $\theta = \arctan(y/x)$, follow from the requirement that the corresponding perturbations are the eigenstates of the angular momentum operator $\hat{J}_z$ with the eigenvalues $m \in \mathbb{Z}$. [Note that $\hat{J}_z = -i\partial_\theta$ for scalar and pseudoscalar fields and $\hat{J}_z = -i\partial_\theta + S_z$ with $(S_z)^i{}_j = -i\varepsilon^{ij3}$ for the vector fields.] In agreement with the remaining translational symmetry, the only well-defined components of the wave vector are the timelike and longitudinal ones, i.e., k_0

and k_z, respectively.

By taking into account the constraints for the flow velocity and the electromagnetic field (i.e., $u^\mu u_\mu = 1$ and $B^\mu u_\mu = E^\mu u_\mu = 0$, respectively) it is clear that only three out of the total four components in each four-vector are independent. Without loss of generality, we assume that the spatial components are the independent ones. Then, as is easy to check, the deviations of the zeroth components from their equilibrium values are not independent. They are given by

$$\begin{aligned}
\delta u^0 &= \Omega \left[x\delta u^2(x) - y\delta u^1(x) \right] \\
&= i\Omega r \left[e^{i\theta}\delta u_-(x) - e^{-i\theta}\delta u_+(x) \right], \qquad (3.11) \\
\delta E^0 &= \Omega \left[x\delta E^2(x) - y\delta E^1(x) \right] \\
&= i\Omega r \left[e^{i\theta}\delta E_-(x) - e^{-i\theta}\delta E_+(x) \right], \qquad (3.12) \\
\delta B^0 &= \Omega \left[x\delta B^2(x) - y\delta B^1(x) \right] + B\delta u^3(x) \\
&= i\Omega r \left[e^{i\theta}\delta B_-(x) - e^{-i\theta}\delta B_+(x) \right] + B\delta u^3(x). \qquad (3.13)
\end{aligned}$$

It should be noted, that the general form of the perturbation to the electromagnetic field strength tensor in the lab frame can be conveniently written in terms of the perturbations of the electric and magnetic fields as follows:

$$\delta F^{\mu\nu} = \varepsilon^{\mu\nu\alpha\beta} \left(\delta u_\alpha \bar{B}_\beta + \bar{u}_\alpha \delta B_\beta \right) + \delta E^\mu \bar{u}^\nu - \bar{u}^\mu \delta E^\nu, \qquad (3.14)$$

$$\delta \tilde{F}^{\mu\nu} = \varepsilon^{\mu\nu\alpha\beta} \delta E_\alpha \bar{u}_\beta + \delta B^\mu \bar{u}^\nu - \bar{u}^\mu \delta B^\nu + \bar{B}^\mu \delta u^\nu - \delta u^\mu \bar{B}^\nu, \qquad (3.15)$$

where we took into account that the electric field is absent in the unperturbed state. By making use of these relations and assuming that all perturbations are small, it is straightforward to obtain a linearized system of hydrodynamic equations from Eqs. (2.31)–(2.35). The corresponding linearized equations are presented in Appendix D. Note that no explicit dependence on t, z, and θ coordinates is present

in those equations because the common exponent $e^{-ik_0t+ik_zz+im\theta}$, containing such a dependence, was factored out.

In order to solve the hydrodynamic equations for collective modes, we should also specify the boundary conditions for the fields. For simplicity, we will assume that the perturbations of the scalar, pseudoscalar and longitudinal vector perturbations vanish at the boundary, i.e., $\delta s(R) = 0$ and $\delta v^3(R) = 0$, where R is the cylindrical radius of the system. [Note, however, that $\delta v_\pm(R) = 0$ cannot be enforced at the same time.] It should be clear, however, that the dispersion relations for most of the bulk modes will not be very sensitive to the choice of the boundary conditions, unless their transverse wave vectors are very small, $k_\perp \simeq 1/R$ (the exact definition of $k_\perp$ will be specified later).

3.2.1 The linearized equations at vanishing vorticity

Before discussing any solutions in the most general case with a nonzero vorticity and magnetic field, let us first consider a simple setup without rotation, $\Omega = 0$, but with the effects of dynamical electromagnetism fully accounted for. As will be clear, in our analysis, we also include all effects associated with the dynamical vorticity induced by collective modes themselves.

The linearized system of the hydrodynamic equations takes the following explicit

form:

$$u^\mu\partial_\mu\delta n + n\partial_\mu\delta u^\mu + B^\mu\partial_\mu\delta\sigma_B + \frac{\tau}{3}\nabla_\mu\nabla^\mu\delta n - \tau n u^\nu\partial_\mu\partial_\nu\delta u^\mu + \frac{1}{e}\sigma_E\partial_\mu\delta E^\mu = 0, \quad (3.16)$$

$$u^\mu\partial_\mu\delta n_5 + \sigma_B^5\partial_\mu\delta B^\mu + B^\mu\partial_\mu\delta\sigma_B^5 + \frac{\tau}{3}\nabla_\mu\nabla^\mu\delta n_5 + \frac{e^2}{2\pi^2\hbar^2}(B\cdot\delta E) = 0, \quad (3.17)$$

$$u^\mu\partial_\mu\delta\epsilon + (\epsilon+P)\partial_\mu\delta u^\mu + B^\mu\partial_\mu\delta\xi_B = 0, \quad (3.18)$$

$$(\epsilon+P)u^\nu\partial_\nu\delta u^\mu - \nabla^\mu\delta P + B^\mu u^\nu\partial_\nu\delta\xi_B + \frac{8\tau\epsilon}{15}\Delta^{\mu\nu}_{\alpha\beta}(\partial_\nu\partial^\alpha\delta u^\beta)$$
$$-en\delta E^\mu - \varepsilon^{\mu\nu\alpha\beta}\left(\frac{\tau}{3}\nabla_\nu\delta n - \tau n u^\phi\partial_\phi\delta u_\nu + \frac{1}{e}\sigma_E\delta E_\nu\right)u_\alpha eB_\beta = 0, \quad (3.19)$$

which should also be supplemented by the Maxwell equations

$$\varepsilon^{\mu\nu\alpha\beta}u_\nu\partial_\alpha\delta E_\beta + u^\nu\partial_\nu\delta B^\mu + B^\mu\partial_\nu\delta u^\nu - B^\nu\partial_\nu\delta u^\mu - u^\mu\partial_\nu\delta B^\nu = 0, \quad (3.20)$$

$$\varepsilon^{\mu\nu\alpha\beta}(u_\nu\partial_\alpha\delta B_\beta - B_\nu\partial_\alpha\delta u_\beta) + u^\mu\partial_\nu\delta E^\nu - u^\nu\partial_\nu\delta E^\mu - en\delta u^\mu - eu^\mu\delta n$$
$$-e\delta\sigma_B B^\mu - \frac{e\tau}{3}\nabla^\mu\delta n + e\tau n u^\phi\partial_\phi\delta u^\mu - \sigma_E\delta E^\mu = 0. \quad (3.21)$$

The variations of the fermion number density, as well as other functions (e.g., $\delta\epsilon$ and $\delta\sigma_B$) are assumed to be of the most general form, i.e., $\delta n = \frac{\partial n}{\partial\mu}\delta\mu(x) + \frac{\partial n}{\partial\mu_5}\delta\mu_5(x) + \frac{\partial n}{\partial T}\delta T(x)$. They are space and time dependent, although such a dependence may not always be shown explicitly, e.g., $\delta n \equiv \delta n(x)$ and $\delta n_5 \equiv \delta n_5(x)$.

In the case of vanishing vorticity, the independent wavelike solutions of the hydrodynamic equations can be conveniently expressed in terms of the cylindrical harmonics. The corresponding solutions for the local perturbations are given by Eqs. (3.8)–(3.10), with radial parts of the functions given by

$$\delta s(r) = \delta s\, J_m(k_\perp r), \quad \text{for} \quad s = \mu, \mu_5, T, \quad (3.22)$$

$$\delta v^3(r) = \delta v^3\, J_m(k_\perp r), \quad \text{for} \quad v^3 = u^3, B^3, E^3, \quad (3.23)$$

$$\delta v_\pm(r) = \delta v_\pm\, J_{m\pm1}(k_\perp r), \quad \text{for} \quad v_\pm = u_\pm, B_\pm, E_\pm. \quad (3.24)$$

Here $J_m(k_\perp r)$ is the Bessel function of the first kind and parameter $k_\perp$ is an analogue of the transverse wave vector for a system with cylindrical symmetry.

The linearized system (3.16)–(3.21) has the general structure $\hat{M}\delta\vec{f} = 0$, where $\hat{M}$ is a 12×12 matrix differential operator and $\delta\vec{f}$ is a vector consisting of all independent plasma and EM field perturbations, i.e., $\delta\vec{f} = (\delta\mu, \delta\mu_5, \delta T, \delta\mathbf{u}, \delta\mathbf{E}, \delta\mathbf{B})^T$. By making use of the ansatz in Eqs. (3.8)–(3.10) with the radial dependence in Eqs. (3.22)–(3.24), it is easy to check that all coordinate dependence factorizes and the problem reduces to a set of homogeneous linear equations, $M\delta\vec{f} = 0$, where M is a 12×12 algebraic matrix. For the system to have a nontrivial solution, the characteristic equation should be satisfied, i.e., $\det(M) = 0$. In essence, the latter is a polynomial equation for the frequencies of collective modes. The roots for k_0 define dispersion relations of hydrodynamic modes. In general, the corresponding frequencies (energies) are functions of the wave vectors $k_\parallel$ and $k_\perp$, as well as the eigenvalue m of the angular momentum operator. The associated nontrivial solutions for $\delta\vec{f}$ ("eigenvectors") specify the nature of the collective modes.

It is instructive to note that the above general procedure for obtaining the dispersion relations of hydrodynamic modes could easily be adjusted to take into account any boundary conditions consistent with the cylindrical symmetry. As we mentioned earlier, we will assume that the perturbations vanish at the cylindrical boundary of the system. Such boundary conditions are satisfied automatically when the values of the transverse wave vector are restricted to take only the following discrete values: $k_\perp^{(i)} = \alpha_{m,i}/R$, where $\alpha_{m,i}$ (with $i = 1, 2, ...$) is the ith zero of the Bessel function $J_m(z)$. By making use of the asymptotic form for the Bessel function, we can derive the following approximate expression for the large transverse wave vectors: $k_\perp^{(i)} \simeq (i + m/2 - 1/4)\pi/R$ for $i \gg m$. By imposing the periodic boundary conditions in the z direction (with period L), the longitudinal wave vector is discretized, i.e., $k_z^{(j)} = 2\pi j/L$, where j is an integer. When the system is large, the discretized wave vectors of both types are closely located and, thus, become almost indistinguishable

from a continuum. In such a case, the discretization plays little role and could be ignored.

3.2.2 The linearized equations at nonzero vorticity

In the general case of a rotating plasma, the self-consistent analysis of hydrodynamic modes becomes much more complicated. One of the primary reasons for this complication is the nontrivial radial dependence of the magnetic field and density in the unperturbed state of a uniformly rotating plasma; see Eqs. (3.6) and (3.7). In this case, the radial parts of local perturbations in Eqs. (3.22)–(3.24) can be written in the form of Fourier-Bessel series:

$$\delta s(r) = \sum_{i=1}^{\infty} \delta s^{(i)} J_m(k_\perp^{(i)} r), \quad \text{for} \quad s = \mu, \mu_5, T, \tag{3.25}$$

$$\delta v^3(r) = \sum_{i=1}^{\infty} \delta v^3 J_m(k_\perp^{(i)} r), \quad \text{for} \quad v^3 = u^3, B^3, E^3, \tag{3.26}$$

$$\delta v_\pm(r) = \sum_{i=1}^{\infty} \delta v_\pm^{(i)} J_{m\pm1}(k_\perp^{(i)} r), \quad \text{for} \quad v_\pm = u_\pm, B_\pm, E_\pm, \tag{3.27}$$

where $k_\perp^{(i)} = \alpha_{m,i}/R$ is the ith discretized value of the transverse wave vector, introduced in the previous subsection. The set of Bessel eigenfunctions used in the series above is complete and orthogonal (Boas and Pollard (1947); Watson (1995)). The orthogonality condition and other useful properties of the Bessel eigenfunctions are discussed in Appendix C.

By substituting perturbations (3.25)–(3.27) into the complete set of hydrodynamic equations (see Appendix D) and projecting the results onto the Bessel functions with different $k_\perp^{(i)}$, we arrive at an algebraic system of equations with the following block-

matrix form:

$$\begin{pmatrix} M^{(11)} & M^{(21)} & \dots \\ M^{(12)} & M^{(22)} & \dots \\ \vdots & \vdots & \ddots \end{pmatrix} \cdot \begin{pmatrix} \delta\vec{f}^{(1)} \\ \delta\vec{f}^{(2)} \\ \vdots \end{pmatrix} = \begin{pmatrix} \vec{0} \\ \vec{0} \\ \vdots \end{pmatrix}, \tag{3.28}$$

where $M^{(ij)}$ are 12×12 matrices made of the ith set of coefficient functions projected onto the jth Bessel eigenfunctions, and $\delta\vec{f}^{(i)} = (\delta\mu^{(i)}, \delta\mu_5^{(i)}, \delta T^{(i)}, \delta\mathbf{u}^{(i)}, \delta\mathbf{E}^{(i)}, \delta\mathbf{B}^{(i)})^T$. Formally, Eq. (3.28) is an infinite system of equations. By noting, however, that the hydrodynamic description is limited to a finite range of low energies and momenta, the system can be truncated in a self-consistent way. In general, it is sufficient to limit the sum in Eqs. (3.25)–(3.27) to values of the transverse wave vector $k_\perp^{(i)}$ that are less than $1/l_{\rm mfp}$, where $l_{\rm mfp}$ is the mean free path of particles. In practice, though, when focusing on the low-energy part of the spectrum and/or studying the limit of small vorticity, the truncation could be even more restrictive.

Before proceeding further with the analysis, it is instructive to discuss the dependence of the matrix blocks in Eq. (3.28) on the angular velocity Ω. As is clear from the discussion in the previous subsection, in the absence of vorticity (i.e., at $\Omega = 0$), all off-diagonal blocks in Eq. (3.28) vanish. Indeed, in such a limit, hydrodynamic modes are characterized by well-defined values of $k_\perp^{(i)}$. Also, the energies of the corresponding modes are determined by the roots of the characteristic equations $\det(M^{(ii)}) = 0$, where $M^{(ii)}$ are the diagonal blocks associated with specific values $k_\perp^{(i)}$.

At nonzero vorticity, the off-diagonal blocks in Eq. (3.28) do not vanish any more and, as a result, all hydrodynamic modes become nontrivial mixtures of partial waves with different values of $k_\perp^{(i)}$. In principle, the corresponding spectrum could be obtained by solving Eq. (3.28) using numerical methods. While such an approach is straightforward conceptually, it is rather tedious and is beyond the scope of this

study. Instead, in the rest of this paper, we will investigate the limit of small, but nonzero vorticity.

In order to determine the spectrum of collective modes at small Ω, we will solve the characteristic equations $\det(M) = 0$ to leading order in Ω. While this may seem to be a very strong limitation, it should be noted that even rather optimistic estimates of vorticity in heavy-ion collisions are not that large in relative terms (Becattini *et al.* (2015); Jiang *et al.* (2016, 2017); Deng and Huang (2016)). As is easy to check, in the limit of small Ω, nontrivial corrections to the off-diagonal blocks in Eq. (3.28) start from the *linear* order terms in Ω. In the calculation of $\det(M)$, therefore, such off-diagonal matrices contribute only starting at the *quadratic* order in Ω. This means, in particular, that all linear corrections to the dispersion relations of hydrodynamic modes are determined completely by the linear corrections to the diagonal blocks. The corresponding characteristic equations are given by $\det(M^{(ii)} + \Omega M_1^{(ii)}) = 0$, where $M_1^{(ii)} \equiv (\partial M^{(ii)}/\partial\Omega)|_{\Omega=0}$.

From the above general structure of the approximate characteristic equations, it should also be clear that, to linear order in Ω, the hydrodynamic modes can be unambiguously labeled by well-defined values of the transverse wave vector $k_\perp^{(i)}$. In other words, while the dispersion relations of the modes are modified by the vorticity, their classification remains the same as in the $\Omega = 0$ case. Of course, this is hardly surprising and should have been expected since, in essence, we used a perturbation theory with Ω playing the role of a small parameter. In this connection, we should add though that, starting already from the quadratic order in Ω, the off-diagonal blocks in Eq. (3.28) are non-negligible and a substantial mixing of partial waves with different $k_\perp^{(i)}$ will be unavoidable.

For a detailed discussion of this question, as well as a method of finding higher-order Ω corrections see appendix B.

3.3 Hydrodynamic modes in high temperature plasma

In this section, we study the spectrum of hydrodynamic modes in a chiral rotating plasma at high temperature, i.e., $T \gg \mu$, or, in other words, we assume that the fermion number chemical potential is small compared to the temperature. As is clear, such a regime is most suitable for describing hot plasmas in the early universe and in heavy-ion collisions. The opposite limit, i.e., $T \ll \mu$, will be addressed in the next section.

Before proceeding to the technical part of the study, it is instructive to discuss the general validity of the hydrodynamic approach and the hierarchy of various length scales in the problem at hand. The shortest length scale of relevance is the de Broglie wavelength for chiral particles $l_d \simeq \hbar/T$ (at high density, it will be replaced by $l_d \simeq \hbar/\mu$). Clearly, the hydrodynamic description cannot work on such short microscopic distances. In fact, it becomes relevant only on the scales much larger than the particle mean free path, i.e., $l_{\rm mfp} \simeq \tau$ (recall that $c = 1$ in the units used here), where the definition of local equilibrium could be meaningful. In a background magnetic field, there is an additional scale defined by the magnetic length $l_B = \sqrt{\hbar/eB}$. We will assume that the field is weak in the sense that $\sqrt{\hbar eB} \ll T$, which is usually the case in most applications. This implies that $l_d \ll l_B$. The magnetic length could, however, be comparable to the mean free path. In fact, the hierarchy between the two scales could be used to distinguish the regime of very weak fields, i.e., $l_B \gtrsim l_{\rm mfp}$, from that of moderately strong fields, i.e., $l_B \lesssim l_{\rm mfp}$.

When discussing hydrodynamic modes, we will have to deal with yet another window of length scales, defined by the wavelengths of the modes, i.e., $\lambda_k \simeq 1/k$, where k is the corresponding wave vector. Clearly, the hydrodynamic description for such modes makes sense only if $\lambda_k \gg l_{\rm mfp}$ (or, equivalently, $k \ll 1/l_{\rm mfp}$). In a

finite system, at the same time, the maximum wavelength is limited by the size of the system itself, $\lambda_k \lesssim R$. Finally, the size of a uniformly rotating relativistic plasma is limited by the scale of Ω^{-1}. Therefore, in the analysis of collective modes below, we will assume the following hierarchy of scales: $l_d \ll l_B \lesssim l_{\rm mfp} \ll \lambda_k \lesssim R \ll \Omega^{-1}$. This hierarchy will also be used in the derivation of analytical results. In order to simplify the task of keeping track of different scales, it will be convenient to use the following values and ranges of dimensionless parameters:

$$l_{\rm mfp}\Omega \simeq \xi^2, \qquad \xi^{3/2} \simeq \frac{l_{\rm mfp}}{R} \lesssim k l_{\rm mfp} \lesssim \xi^{1/2}, \qquad \frac{l_{\rm mfp}}{l_B} \simeq \xi^{-1/4}, \qquad \frac{l_{\rm mfp}}{l_d} \simeq \xi^{-1}, \tag{3.29}$$

where we introduced a small parameter $\xi \simeq 10^{-2}$ in order to easily separate all relevant scales in the problem. While concentrating on the high-temperature regime here, it might be interesting to see how the effects of a small chemical potential start showing up in the spectrum of collective modes. Therefore, we also include a nonzero μ, but assume that its value is very small, e.g., $|\mu| \simeq \xi^2 T$ (or, equivalently, $|\mu| l_d \simeq \xi^2 \hbar$).

3.3.1 Charged plasma at $\Omega = 0$

Before addressing hydrodynamic modes at nonzero vorticity, it is instructive to set up the stage by first discussing the benchmark results at $\Omega = 0$. As expected in the hydrodynamic regime, there are generically two very different types of modes: propagating and diffusive. The dispersion relations of the former ones have nonzero real parts and relatively small imaginary parts. The diffusive modes, on the other hand, have either no real parts at all, or the imaginary parts much larger than real ones.

By solving the linearized equations (3.16)–(3.21), we find that there are two kinds of propagating modes at $\Omega = 0$, namely, a sound wave with the dispersion relation

given by

$$k_0 = \frac{s_e k}{\sqrt{3}} - \frac{2}{15} i\tau k^2, \tag{3.30}$$

and an Alfvén wave with the dispersion relation approximately given by

$$k_0^{(\pm)} = s_e \frac{3\sqrt{5} B \hbar^{3/2} k_z}{\sqrt{7}\pi T^2} \left(1 \pm \frac{\sqrt{5} e\mu}{2\sqrt{7}\pi\hbar^{3/2} k} \right) - \frac{1}{10} i\tau k^2. \tag{3.31}$$

In both cases, $k = \sqrt{k_z^2 + k_\perp^2}$ and $s_e = \pm 1$. As is clear, both choices of s_e (i.e., the overall sign in front of the real part of the energy) correspond to the same mode. In most cases, the signs s_e could be associated simply with different directions of propagation. As is easy to check, in fact, this is the case for the Alfvén waves in Eq. (3.31).

The sound wave in Eq. (3.30) describes the propagation of longitudinal elastic deformations in plasma. The propagation of such a wave does not induce any local oscillations of the electric charge and, as a result, there are no dynamical electromagnetic fields induced. Also, as expected for the ultrarelativistic matter, the speed of sound c_s is determined by its compressibility, $c_s^2 = \partial P/\partial\rho = 1/3$. (As we mentioned earlier, in a more realistic case of a strongly interacting quark-gluon plasma, the value of c_s^2 is expected to be somewhat smaller than 1/3 (Bazavov *et al.* (2014)), but there is no reason to expect that the nature of the corresponding sound mode will change qualitatively.)

A few words are in order about the Alfvén waves with the dispersion relations given by Eq. (3.31). These are magnetohydrodynamic modes with two possible circular polarizations: the left-handed one with $\delta u_+ \ll \delta u_-$ and the right-handed one with $\delta u_+ \gg \delta u_-$. From the viewpoint of the fluid flow oscillations, these are transverse modes. The energies of the corresponding two branches of waves differ slightly because the term with the chemical potential μ comes with opposite signs. In the limit $\mu \to 0$, the speed of propagation of these waves is the same for both polarizations. As is easy

to check by neglecting the dissipative effects, the expression for the speed can also be written as $v_A = B/\sqrt{\epsilon_{\rm eq} + P_{\rm eq}}$, which is the standard expression for the Alfvén waves in a relativistic plasma (Harris (1957)). It might be appropriate to mention that the propagation of Alfvén waves is accompanied by the fluid flow oscillations with nonzero local dynamical vorticity.

Here it might be appropriate to note that the analytical expressions in Eq. (3.31) were obtained by using the expansion in small parameter ξ, which was introduced in Eq. (3.29) in order to separate different scales in the problem. Therefore, while the corresponding dispersion relations provide good analytical approximations, they cannot be extended to the regions of very small and very large values of the wave vector. In order to support the validity of the approximate results obtained analytically, we compare them in Fig. 3.2 with the dispersion relations found numerically. The panels in Fig. 3.2 show the results for the real (red lines and points) and imaginary (blue lines and points) parts of the energy at three different fixed values of the magnetic field, i.e., $\hbar eB/T^2 = 0.5\times10^{-3}$, $\hbar eB/T^2 = 1\times10^{-3}$, and $\hbar eB/T^2 = 1.5\times10^{-3}$, respectively. Note that, for the model parameters used, the hydrodynamic regime breaks down in the gray shaded regions at small and large values of k_z. As is clear from Fig. 3.2, the analytical relations approximate well the numerical results basically in the whole region where the real part of the energy remains larger than its imaginary part, i.e., $\mathrm{Re}(k_0) \gtrsim \mathrm{Im}(k_0)$.

In addition to the propagating modes, there are also two types of purely diffusive modes. The latter include the electric field decay mode with

$$k_0 = -\frac{e^2}{9\hbar^3} i\tau T^2 \tag{3.32}$$

and the chiral charge diffusive mode described by

$$k_0 = -\frac{1}{3} i\tau k^2 - i\frac{27e^2B^2\hbar^2}{4\pi^4\tau T^4}. \tag{3.33}$$

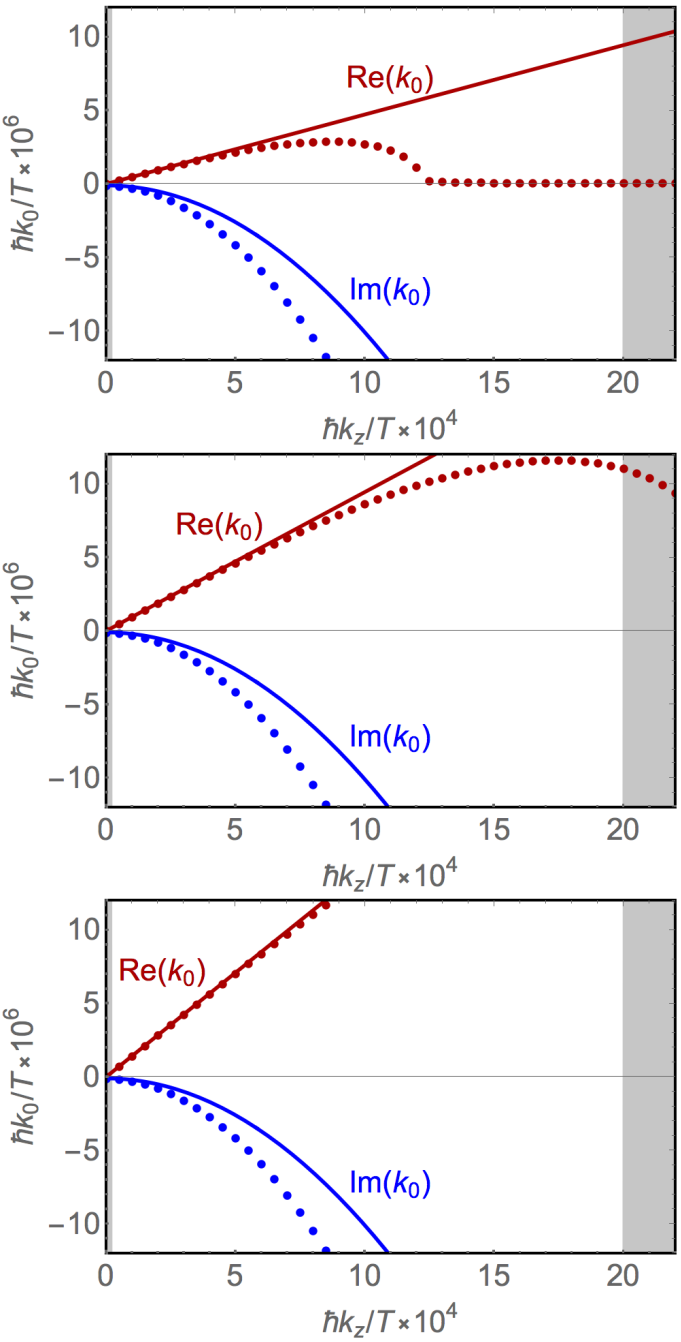

Figure 3.2: The comparison of the approximate analytical results (solid lines) for the real (red lines and points) and imaginary (blue lines and points) parts of the energy for the Alfvén waves with the corresponding numerical results (points) at $\Omega = 0$ for three fixed values of the magnetic field: $\hbar eB/T^2 = 0.5 \times 10^{-3}$ (top panel), $\hbar eB/T^2 = 10^{-3}$ (middle panel), and $\hbar eB/T^2 = 1.5 \times 10^{-3}$ (bottom panel). The real and imaginary parts of the energy are shown in red and blue, respectively. The other model parameters are $\tau T/\hbar = 10^2$, $\mu/T = 10^{-4}$, and $\hbar k_\perp/T = 10^{-4}$.

It should be noted that there are three degenerate modes with the dispersion relation in Eq. (3.32), which correspond to three different polarizations of the electric field. The origin of these modes can be traced back to Ampere's law that takes a particularly simple approximate form $\partial_t \mathbf{E} + \sigma_E \mathbf{E} \approx 0$. This is also reconfirmed by the fact that the imaginary part in Eq. (3.32) is completely determined by the electrical conductivity, $\mathrm{Im}(k_0) = -\sigma_E$.

Before concluding this section, we would like to emphasize that there is no propagating mode in the spectrum that could be identified with the chiral magnetic wave. It is natural to ask, therefore, what is the reason for its absence. As we will explain later in more detail, the chiral magnetic wave is overdamped because of a high conductivity of hot plasma, which causes a rapid screening of the electric charge fluctuations and, thus, prevents the wave from forming. While the situation is slightly more complicated in the strongly coupled quark-gluon plasma created in heavy-ion collisions, the chiral magnetic wave is still strongly overdamped due to the combined effects of electrical conductivity and charge diffusion (Shovkovy *et al.* (2018)).

3.3.2 Charged plasma at $\Omega \neq 0$

Let us now discuss the spectrum of hydrodynamic modes in the case of small, but nonzero vorticity. As mentioned earlier, in order to simplify the analysis, we will limit ourselves only to linear order corrections to the dispersion relations in powers of Ω. In such an approximation, the modes are classified by the same values of $k_\perp^{(i)}$ as at $\Omega = 0$. Since there is no mixing of partial waves with different values of $k_\perp^{(i)}$, we will utilize a simpler notation $k_\perp$ instead of $k_\perp^{(i)}$ in the rest of the paper.

Let us start by noting that the dispersion relation of the sound wave receives a

linear correction in vorticity, i.e.,

$$k_0 = \frac{s_e k}{\sqrt{3}} - \frac{2}{15} i\tau k^2 + m\Omega \left(\frac{2}{3} + \frac{5e^2\mu^2}{14\pi^2\hbar^3 k^2} \right). \tag{3.34}$$

As in the case of vanishing vorticity, it remains a longitudinal wave. Its propagation is sustained primarily by oscillations of temperature δT and velocity δu^μ. However, at nonzero μ, the wave could also excite small perturbations of the electromagnetic fields.

To the leading linear order in the angular velocity Ω, the dispersion relations of the Alfvén waves are given by the following approximate expression:

$$\begin{aligned} k_0^{(\pm)} = m\Omega + s_e k_z \sqrt{\frac{45\mathcal{B}_\pm^2\hbar^3}{7\pi^2 T^4} + \left(\frac{\Omega}{k} - \frac{15e\mathcal{B}_\pm\mu}{14\pi^2 T^2 k} \right)^2} \\ \pm k_z \left(\frac{\Omega}{k} - \frac{15e\mathcal{B}_\pm\mu}{14\pi^2 T^2 k} \right) - i\tau k^2 \left(\frac{1}{10} + \frac{9\hbar^3}{2e^2\tau^2 T^2} \right), \end{aligned} \tag{3.35}$$

where we introduced the following shorthand notation:

$$\mathcal{B}_\pm = B - \frac{e n_{\rm eq}\Omega}{6k_\perp^2} \left[2(m \pm 1)(m \pm 2) + k_\perp^2 R^2 \right]. \tag{3.36}$$

Note that we used $n_{\rm bg} = n_{\rm eq}$, which enforces the electric charge neutrality in the plasma at $\Omega = 0$, see Eq. (3.7). As we can see, there are four different branches of Alfvén waves. They are determined by two different circular polarizations, labeled by the $\pm$ signs in Eq. (3.35), and two directions of propagation with respect to the z axis. The latter are formally distinguished by $s_e = \pm 1$. (Recall that both the background magnetic field and the axis of rotation are parallel to the z axis.)

By comparing the result in Eq. (3.35) with the dispersion relation at $\Omega = 0$, given by Eq. (3.31), we see that the inclusion of vorticity lifts the degeneracy of modes propagating in opposite directions with respect to the background magnetic field (and/or vorticity). Moreover, we also find that the propagation of these types of waves is modified by the chiral vortical effect. This is most pronounced in the

case of small k_z (i.e., $k_z \lesssim k_\perp$). In such a case, therefore, it might be suitable to call these modes the Alfvén-vortical waves. The dispersion relations for several modes with different values of the angular momentum m are shown in Fig. 3.3. (The hydrodynamic regime breaks down in the gray shaded regions at small and large values of k_z.) Note that the approximate analytical expressions (represented by solid lines) are in good agreement with the numerical results (shown with dots) in the region of small momenta.

It is interesting to note that the energies of the circularly polarized Alfvén waves depend on the magnetic field only via the combinations $\mathcal{B}_\pm$, defined in Eq. (3.36). This means that one of the circularly polarized waves with a fixed angular momentum m could be fine-tuned (e.g., by adjusting the magnetic field so that $\mathcal{B}_- = 0$) into a pure chiral vortical wave with the dispersion relation given by $k_0 \approx m\Omega + (s_e - 1)\frac{k_z}{k}\Omega - \frac{1}{10}i\tau k^2$.

For completeness, let us now briefly discuss the diffusive modes. The electric field decay mode remains the same as in Eq. (3.32). As for the chiral charge diffusive mode, at nonzero Ω, it is given by

$$k_0 = m\Omega - i\frac{27(e\mathcal{B}_0)^2\hbar^2}{4\pi^4\tau T^4} - \frac{1}{3}i\tau k^2, \tag{3.37}$$

where we introduced the following shorthand notation:

$$\mathcal{B}_0 = B - \frac{en_{\rm eq}\Omega}{6k_\perp^2}\left[2(m-1)(m+1) + k_\perp^2 R^2\right]. \tag{3.38}$$

Note that the energy of the chiral charge diffusive mode has a nonzero real part proportional to Ω. One might speculate, therefore, that under certain conditions and beyond the leading order in Ω, it may even become a propagating mode. As is easy to check, the chiral charge diffusive mode is determined primarily by the corresponding continuity relation. At nonzero Ω, in particular, the latter can be approximately

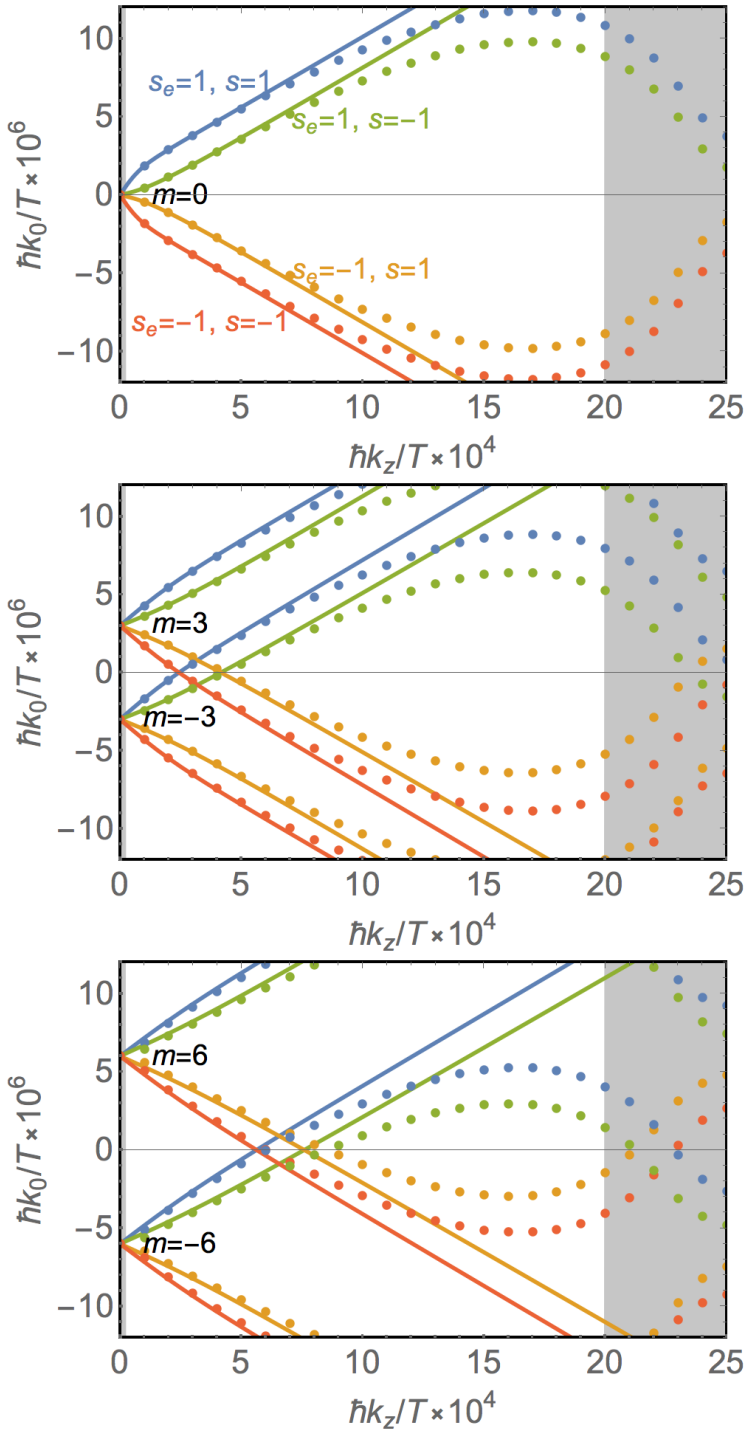

Figure 3.3: The real parts of the energies of the Alfvén waves with different values of the angular momentum: $m = 0$ (top panel), $m = \pm 3$ (middle panel), and $m = \pm 6$ (bottom panel). The other model parameters are $\tau T/\hbar = 10^2$, $\mu/T = 10^{-4}$, $\hbar\Omega/T = 10^{-6}$, $\hbar eB/T^2 = 10^{-3}$, $RT/\hbar = 10^4\alpha_{0,1} \approx 2.4 \times 10^4$, and $k_\perp = \alpha_{m,1}/R$.

given by

$$\partial_0 n_5 = -\frac{\tau}{3}\nabla^2 n_5 - (\boldsymbol{\Omega} \times \boldsymbol{\nabla} n_5) \cdot \boldsymbol{r}_\perp. \tag{3.39}$$

By solving this, we can indeed reproduce the first and the last terms in the dispersion relation (3.37). This reconfirms that, while other degrees of freedom may influence this diffusive mode in principle, their role is minor.

3.3.3 Charged plasma at $\Omega \neq 0$ without dynamical electromagnetic fields

As we argued in the chapter 2 by using rather general arguments, a self-consistent treatment of charged chiral plasma requires a proper inclusion of fully dynamical electromagnetic fields. In this subsection, we test the validity of such a claim by performing a comparative study without the inclusion of the dynamical fields. In order to achieve such a regime in the charged chiral plasma, we will assume that the matter is affected only by the static *background* magnetic field. No additional background electric fields can be allowed because those would drive dissipative Ohm currents. When neglecting dynamically induced electromagnetic fields, there will be no effect from such fields on the plasma modes. As we will see, many signature features of hydrodynamic modes will be lost in such an approximation. This finding, therefore, will reconfirm the importance of accounting for the dynamical fields.

When dynamical electromagnetic fields are neglected, the Maxwell equations play no role in determining the properties of hydrodynamic modes. This means that one is left with the system of only six continuity equations (2.31)–(2.34). To leading order in Ω, we can assume that the background values of the chemical potential and temperature are spatially uniform. In the absence of the background electric field, the chiral anomaly is effectively switched off. This means that both fermion number (electric) and chiral currents are conserved and affect collective modes in similar ways.

We find that there are three kinds of propagating hydrodynamic modes: a lon-

gitudinal sound wave, a transverse vortical wave, and a transverse chiral magnetic wave. (Note that the terms longitudinal and transverse refer to the direction of fluid flow oscillations with respect to the wave vector.) Their dispersion relations read

$$k_0 = \frac{s_e k}{\sqrt{3}} + \frac{2}{3} m\Omega - \frac{2}{15} i\tau k^2, \tag{3.40}$$

$$k_0 = m\Omega + s_e \frac{2k_z\Omega}{k} - \frac{1}{5} ik^2\tau, \tag{3.41}$$

$$k_0 = m\Omega + s_e \frac{3e\mathcal{B}_0\hbar k_z}{2\pi^2 T^2} - \frac{1}{3} ik^2\tau, \tag{3.42}$$

respectively. As expected, the sound mode is not affected much by omitting dynamical electromagnetic fields. However, it did become completely independent of the chemical potential. This should have been expected though since oscillations of local electric fields from charge density perturbations are artificially switched off now.

The modes in Eq. (3.41) are substitutes for the Alfvén waves (3.35) in the fully dynamical case. By comparing their dispersion relations, we clearly see that the modes are drastically different. This is further confirmed by reviewing the underlying nature of the two sets of modes. For example, the vortical wave (3.41) is driven almost exclusively by velocity perturbations δu^μ. A pair of the weakly damped chiral magnetic waves (3.42) is driven by oscillations of either left-handed ($s_e = -1$) or right-handed ($s_e = 1$) particles. As expected, they replace a pair of diffusive modes found in the dynamical regime in the previous subsection. At $\mathcal{B}_0 = 0$, they turn again into diffusive electric and chiral charge waves, driven by the perturbations of $\delta\mu$ and $\delta\mu_5$, respectively.

To summarize the results of this subsection, we find that neglecting dynamical electromagnetic fields has a profound effect on the spectrum of collective modes in the hydrodynamic regime. One of them is the appearance of propagating chiral magnetic waves, which are absent in the charged chiral plasma with dynamical electromagnetism. The other qualitative difference is the absence of the correct Alfvén waves,

which are replaced by the vortical wave with a rather different dispersion relation.

3.3.4 Plasma of neutral particles at $\Omega \neq 0$

For completeness, it might also be interesting to discuss the hydrodynamic modes in a chiral plasma made of neutral particles. Clearly, the Maxwell equations play no role in this case. The hydrodynamic description is governed by Eqs. (2.31)–(2.34) with the vanishing electromagnetic fields. To leading order in Ω, the values of the chemical potential μ and temperature T for the uniformly rotating neutral plasma can be assumed constant in the global equilibrium. Moreover, we can even include an arbitrary nonzero axial chemical potential μ_5.

Among the propagating modes in neutral plasma, we find the usual longitudinal sound wave with the dispersion relation given by

$$k_0 = \frac{s_e k}{\sqrt{3}} + \frac{2}{3} m\Omega - \frac{2}{15} i\tau k^2, \tag{3.43}$$

where $s_e = \pm 1$, and a single circularly polarized vortical wave with the dispersion relation

$$k_0 = m\Omega + s_e \frac{2k_z\Omega}{k} - \frac{1}{5} i\tau k^2. \tag{3.44}$$

It should be emphasized that the sign $s_e = \pm 1$ defines one of the two possible directions of propagation of the vortical wave with respect to the z axis. For each direction of the propagation, though, there is only one circularly polarized mode. This differs qualitatively from the Alfvén-vortical waves in charged plasmas which have two propagating circularly polarized modes for each direction.

The dispersions of diffusive modes associated with the fermion number charge and the chiral charge are degenerate and resemble the zero-field limit of that in Eq. (3.37). In particular, they are given by

$$k_0 = m\Omega - \frac{1}{3} i\tau k^2. \tag{3.45}$$

It is rather interesting to point out that, to leading order in Ω, the equilibrium values of the chemical potentials μ and μ_5 do not affect the energy spectrum of the modes in the neutral chiral plasma. The spectra also are not dependent on temperature.

3.4 Hydrodynamic modes in dense plasma

In this section, we study the spectrum of hydrodynamic modes in a chiral rotating plasma at high density, i.e., $\mu \gg T$. Such a regime could be realized in compact stars and, perhaps, also in Dirac and Weyl materials, in which low-energy electron quasiparticles behave as pseudorelativistic chiral fermions.

As in the case of hot plasma in the previous section, it is convenient to use a specific hierarchy of all relevant scales in the problem by relating them via a single small parameter $\xi \simeq 10^{-2}$. In the case of dense plasma, we will use

$$l_{\rm mfp}\Omega \simeq \xi^{5/2}, \qquad \xi^{3/2} \simeq \frac{l_{\rm mfp}}{R} \lesssim k l_{\rm mfp} \lesssim \xi^{1/2}, \qquad \frac{l_{\rm mfp}}{l_B} \simeq \xi^{-1/4}, \qquad \frac{l_{\rm mfp}}{l_d} \simeq \xi^{-1}. \tag{3.46}$$

It should be noted that here we consider even smaller vorticity in relative terms than in hot chiral plasma, see Eq. (3.29). This is motivated by the need to keep the vorticity corrections to the magnetic field (3.38) and (3.36) under control in the regime of a large fermion number density. While considering the high-density regime, it is instructive to see how the effects of a small temperature start showing up in the spectrum of collective modes. For this purpose, we include a nonzero temperature, but assume that its value is small, e.g., $T \simeq \xi\mu$ (or, equivalently, $T l_d \simeq \xi\hbar$, where $l_d = \hbar/\mu$).

3.4.1 Charged plasma at $\Omega = 0$

Before considering the case of nonzero vorticity, we review the spectrum of hydrodynamic modes in the case $\Omega = 0$ by solving the linearized system of equations

(3.16)–(3.21). As expected, we find that there are two kinds of propagating modes at $\Omega = 0$, namely, plasmons and helicons. Also, there are two diffusive modes with identical dispersions, $k_0 = -i\tau k^2/3$. Note that, in the regime of dense matter, there are no usual sound waves. They are replaced by plasmons. Similarly, the Alfvén waves are morphed into helicons.

Plasmons describe the propagation of charge oscillations sustained by dynamically induced electric fields. As is well known, their frequency for the ultrarelativistic plasma without background fields and rotation is given by $\omega_{\rm PL} = \frac{e\mu}{\sqrt{3}\pi\hbar^{3/2}}$. The plasmon can have three degenerate modes with different polarizations. We find that the degeneracy is lifted by the magnetic field. Indeed, from our linearized system of equations, we find that the dispersion relations of the plasmon modes are given by

$$k_0^{(s)} = s_e \frac{e\mu}{\sqrt{3}\pi\hbar^{3/2}} + s\frac{eB}{2\mu} - \frac{ie^2\tau T^2}{18\hbar^3} - \frac{1}{10}i\tau k^2, \tag{3.47}$$

where $s_e = \pm 1$ and $s = -1, 0, 1$. In terms of the hydrodynamic variables, plasmons are primarily driven by the oscillations of flow velocity $\delta u_\pm$ and electric field $\delta E_\pm$. For $s = \pm 1$, the modes have clockwise (with nonzero δu_+ and δE_+) and anticlockwise (with nonzero δu_- and δE_-) circular polarizations, respectively. The case of $s = 0$ corresponds to the mode with the linear polarization in the z direction.

The dispersion relations of the helicon mode are given by

$$k_0 = s_e \frac{3\pi^2 eBkk_z\hbar^3}{e^2\mu^3} - \frac{3\pi^2\hbar^3}{5e^2\mu^2}i\tau k^4, \tag{3.48}$$

where $s_e = \pm 1$. One of the signature features of such magnetohydrodynamic modes is their quadratic dispersion relations. They are circularly polarized with a given handedness, determined by the sign of s_e. In terms of the hydrodynamic variables, the propagation of helicons is driven primarily by oscillations of flow velocity $\delta u_\pm$, temperature δT, and magnetic field $\delta B_\pm$. It might be appropriate to mention that,

for a typical choice of the model parameters with the hierarchy of scales in Eq. (3.46), the helicons are well-defined propagating (rather than overdamped) modes in the whole region of momenta, $\xi^{3/2} \lesssim k l_{\rm mfp} \lesssim \xi^{1/2}$. This remains also marginally true even for a range of somewhat weaker magnetic fields, provided $l_{\rm mfp}/l_B \gtrsim 1$. However, in the case of very weak fields, the helicons will become overdamped already at some intermediate values of the wave vector (e.g., $k l_{\rm mfp} \simeq \xi^{3/4}$ when $l_{\rm mfp}/l_B \simeq \xi^{1/4}$).

3.4.2 Charged plasma at $\Omega \neq 0$

Let us now proceed to the case of a rotating chiral plasma. As in the case of hot plasma in the previous section, we will study the modifications of hydrodynamic modes up to linear order in Ω. In this case, the modes are classified by well-defined transverse wave vectors $k_\perp$. (Recall that the corresponding values are discretized $k_\perp^{(i)} = \alpha_{m,i}/R$, but we will omit the superscript in order to simplify the presentation.)

We start by noting that the $\Omega = 0$ plasmon dispersion relation given by Eq. (3.47) remains almost the same, but the magnetic field B in the subleading term is replaced by $\mathcal{B}_s$, i.e.,

$$k_0^{(s)} = s_e \frac{e\mu}{\sqrt{3}\pi\hbar^{3/2}} + s\frac{e\mathcal{B}_s}{2\mu} - \frac{ie^2\tau T^2}{18\hbar^3} - \frac{1}{10} i\tau k^2. \tag{3.49}$$

As for the helicon mode, its dispersion relation becomes

$$k_0 = m\Omega\left(\frac{1}{2} - \frac{k_z^2}{k_\perp^2}\right) + s_e\sqrt{\frac{m^2\Omega^2}{4} + \frac{9\pi^4(\mathcal{B}_+ + \mathcal{B}_-)^2 k^2 k_z^2 \hbar^5}{4\mu^6}} - \frac{3\pi^2\hbar^3}{5e^2\mu^2} i\tau k^4, \tag{3.50}$$

where $s_e = \pm 1$. As is easy to see, the positive branches of the real part of energy (i.e., $s_e = +1$) are gapped for $m > 0$ and gapless for $m \leq 0$. Concerning the case of $m > 0$, the values of the gaps are determined by the angular velocity, $m\Omega$. A typical spectrum is illustrated in Fig. 3.4, where the dispersion relations for several fixed values of the angular momentum ($m = -4, -2, 0, 2, 4$) are shown. Note that, in the figure, we zoomed into the region of very small energies. By taking into account

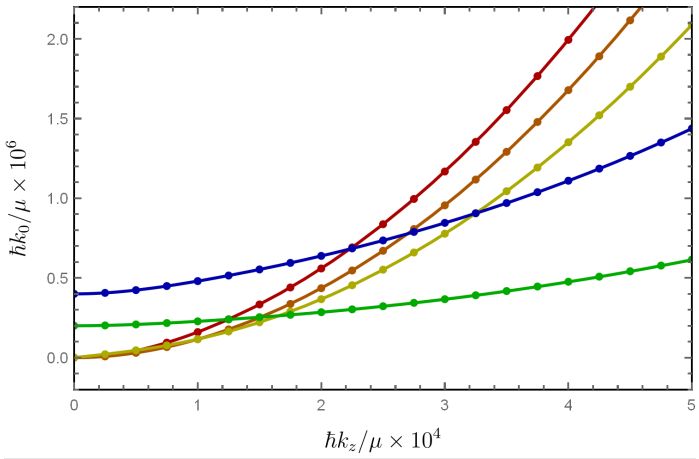

Figure 3.4: The positive branches of the real part of helicon energies for several values of the angular momentum, i.e., $m = -4$ (red line), $m = -2$ (orange line), $m = 0$ (olive line), $m = 2$ (green line), and $m = 4$ (blue line). The other model parameters are $\hbar eB/\mu^2 \approx 2 \times 10^{-3}$, $\tau\mu/\hbar = 100$, $\hbar\Omega/\mu = 10^{-7}$, and $k_\perp = \alpha_{m,1}/R$.

that Ω is very small, it should be clear that the complete spectrum contains a nearly continuous range of gaps.

It is interesting to note that for certain values of the angular momentum (when the magnetic field is fixed), the effective field $(\mathcal{B}_+ + \mathcal{B}_-)$ could become very small, or even zero. In this case, the first term in the dispersion relation (3.50) dominates and leads to a quadratic dependence on k_z with a negative overall coefficient. (Note that the energies for the branches with negative values of m have opposite signs.)

From a physics viewpoint, the negative curvature of the dispersion relation as a function of k_z implies that the group velocity of such modes v_z is negative. This is a rather interesting feature that, potentially, could be important in applications. By analyzing the analytical expression in Eq. (3.50), we find, however, that a negative group velocity can be realized only for rather large magnetic fields. Indeed, by making use of the properties of the Bessel functions, we find that the negative slope is possible only when the magnetic field lies in the following window: $en_{\rm eq}R^2\Omega/6 < B < en_{\rm eq}R^2\Omega/2$. This corresponds to the dimensionless ratio $l_{\rm mfp}/l_B \simeq \xi^{-7/4}(e/\sqrt{\hbar})$, which is substantially larger than 1 even for a rather small coupling constant, $e/\sqrt{\hbar} = 1/\sqrt{137}$. The

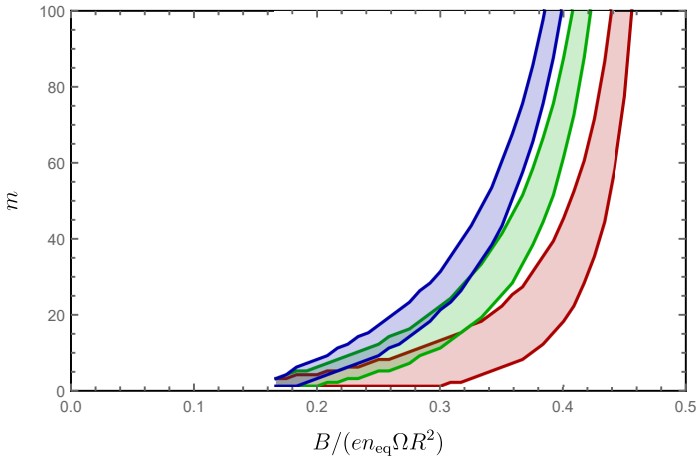

Figure 3.5: The ranges of angular momenta m for which helicon modes can have negative group velocity. The colored bands correspond to three smallest values of the transverse momenta $k_\perp^{(i)}$ with $i = 1, 2, 3$ (from red to blue, respectively).

ranges of angular momenta m of the modes with $v_z < 0$ are illustrated graphically in Fig. 3.5. There we show three colored bands that correspond to the three smallest values of the transverse momenta $k_\perp^{(i)}$ with $i = 1, 2, 3$. As we see, the ranges of bands in m rise very steeply as $B/(en_{\rm eq}R^2\Omega)$ approaches $1/2$. The bands also have a tendency to shift upwards with increasing $k_\perp^{(i)}$.

In addition to the propagating modes, there is also a pair of overdamped modes associated with the diffusion of chiral charge and energy, i.e.,

$$k_0 = m\Omega - \frac{1}{3}i\tau k^2, \tag{3.51}$$

$$k_0 = m\Omega\left(1 - \frac{e^2\mu^2\tau^2}{9\pi^2\hbar^3}\right) - \frac{1}{3}i\tau k^2, \tag{3.52}$$

respectively. In the hydrodynamic regime defined by the hierarchy of length scales in Eq. (3.46), neither of these modes has a chance of becoming a well-resolved propagating mode.

3.4.3 *Charged plasma at $\Omega \neq 0$ without dynamical electromagnetic fields*

As in the case of hot plasma in the previous section, here it is also instructive to verify that the description of hydrodynamic modes is substantially modified in the background-field approximation, i.e., when the dynamical electromagnetic fields are neglected.

Switching off the dynamical electromagnetic fields is equivalent to ignoring the Maxwell equations. Then the simplified system of the six linearized equations contains only continuity equations (2.31)–(2.34). Here we will concentrate on the propagating modes, which are particularly interesting. As for the diffusive modes, one can verify that there are two degenerate modes with the dispersion relation given by Eq. (3.51).

One of the immediate consequences of the approximation without dynamical electromagnetic fields is the absence of the plasmons in the spectrum. They are replaced by the sound waves with the energy given by

$$k_0 = \frac{s_e k}{\sqrt{3}} + \frac{2}{3} m\Omega - \frac{2}{15} i\tau k^2. \tag{3.53}$$

The underlying physics of such a dramatic change is clear. While neglecting the Gauss law, local oscillations of the electric charge density do not produce any electric field, resulting in a gapless sound wave exactly as in the case of plasma made of neutral particles.

While the helicon remains in the spectrum, its dispersion relation is substantially modified. In particular, its energy in the background-field approximation is given by

$$k_0 = m\Omega + \frac{s_e}{5\mu} e\mathcal{B}_s k k_z \tau^2 - \frac{1}{5} i\tau k^2, \tag{3.54}$$

where $s_e = \pm 1$. In essence, this is a purely hydrodynamic mode, which is driven by oscillations of the fluid velocity. Its propagation is accompanied by oscillations of temperature, as well as small oscillations of the electric and chiral chemical potentials.

3.4.4 *Chiral plasma of neutral particles at $\Omega \neq 0$*

For completeness, let us also discuss the case of chiral plasma made of neutral particles. Since the chiral anomaly is absent in this case, it is straightforward to include a nonzero chiral chemical potential μ_5 along with the fermion number chemical potential μ. Note, however, that none of the hydrodynamic modes in this regime will be modified by the values of μ_5 and μ. This situation is qualitatively the same as in the case of hot plasma made of neutral particles. Also, as in that case, the spectra do not depend on temperature.

The energies of the sound and vortical waves are given by the following expressions:

$$k_0 = \frac{s_e k}{\sqrt{3}} + \frac{2}{3} m\Omega - \frac{2}{15} i\tau k^2, \tag{3.55}$$

$$k_0 = m\Omega + s_e \frac{2k_z\Omega}{k} - \frac{1}{5} i\tau k^2, \tag{3.56}$$

respectively. While the former is a longitudinal wave, the latter is a transverse circularly polarized one. There is also a pair of degenerate diffusion modes with the dispersion relation given by Eq. (3.51).

3.5 The chiral magnetic wave

As was already mentioned in the first chapter the prediction of the chiral magnetic wave (CMW) in chiral theories (Kharzeev and Yee (2011)) started an intensive theoretical and experimental research on the subject. However, the analysis in the previous section showed that no such mode is realized, or at least it is heavily damped by dissipation processes. Let us therefore concentrate on this particular collective mode and explain using simple physical arguments why this mode cannot be realized under the most common conditions.

Since one of the most interesting applications of the CMW was proposed in the context of relativistic heavy-ion collisions (Gorbar *et al.* (2011); Burnier *et al.* (2011)),

it is instructive to start our analysis from the case of chiral plasma in the regime of high temperature. In order to sort out the key details of underlying physics, however, it will be illuminating to first consider the simplest case of a chiral plasma made of single flavor massless fermions. It will be also instructive to start from the case of a weakly interacting case (which is realized, for example, at sufficiently high temperatures). As we will see in Sec. 3.5.1, the key details of the analysis are similar also in the nonperturbative regime of the strongly-interacting quark-gluon plasma with several light flavors.

In order to model the conditions in the plasma produced by relativistic heavy-ion collisions, where the typical values of the chemical potentials are much smaller than the temperature, it is sufficient to set $\mu = \mu_5 = 0$ in our analysis. (The quantitative effects of a small nonzero chemical potential μ in the high-temperature regime were already considered in the previous section). This also means that we don't need a positive background charge $n_{\rm bg} = 0$ to overcome the Coulomb repulsion.

In order to further simplify the argument we choose the plasma without the background vorticity $\Omega = 0$ since its presence is not essential for the propagation of the predicted in Kharzeev and Yee (2011) chiral magnetic wave. Therefore, the background state of a one-component massless chiral plasma is characterized only by a uniform temperature T, local velocity, which in the fluid rest frame takes the form $u^\mu = (1, 0, 0, 0)$, and a background magnetic field pointing in the $\hat{z}$ direction $B^\mu \equiv \tilde{F}^{\mu\nu} u_\nu = (0, 0, 0, B)$. As is clear, there should be no electric field in equilibrium, i.e., $E^\mu \equiv F^{\mu\nu} u_\nu = 0$.

The propagation of collective modes through a chiral plasma is generically accompanied by the oscillations of all available dynamical parameters: the chemical potentials $\delta\mu$ and $\delta\mu_5$, the temperature δT, the flow velocity δu^μ, as well as the electric and magnetic fields δE^μ and δB^μ. In the linear approximation, it is justified to

take them all in the form of plain waves, i.e., $\delta X \propto e^{-ik\cdot x}$. Note, that using this ansatz we neglect the effect of the geometry on the collective modes. This, however, should not be critical in the bulk of the plasma far from the boundaries. A more rigorous cylindrical border and oscillation profile was considered in the previous section.

For simplicity, in this section we assume that all dissipative processes in the system are controlled by the same phenomenological relaxation-time parameter τ. In the case of electrical conductivity, for example, one can use $\sigma_E \simeq e^2\tau\chi/3$, where $\chi = \partial n/\partial\mu$ is the fermion number susceptibility Gorbar *et al.* (2016). Similarly, the chiral counterpart of conductivity σ_E^5 can be given as $\sigma_E^5 \simeq e^2\tau\chi'$, where $\chi' = \partial n_5/\partial\mu$ Gorbar *et al.* (2016).

As is easy to show, the time-components of all three vector quantities are nondynamical. In fact, they can be shown to vanish identically, i.e., $\delta u^0 = \delta B^0 = \delta E^0 = 0$, after taking into account the constraints $u^\mu B_\mu = u^\mu E_\mu = 0$ and $u^\mu u_\mu = 1$, as well as the explicit definition for the local (oscillating) electromagnetic field strength tensor in the laboratory frame, i.e.,

$$F^{\mu\nu} = \varepsilon^{\mu\nu\alpha\beta}\bar{u}_\alpha(\bar{B}_\beta + \delta B_\beta) + \delta E^\mu \bar{u}^\nu - \bar{u}^\mu \delta E^\nu. \tag{3.57}$$

After using the Maxwell equation (2.35), the linearized versions of the hydrodynamic equations (2.31)–(2.34) can be rewritten in the following explicit form:

$$k_0\delta n - (\mathbf{B}\cdot\mathbf{k})\delta\sigma_B + i\frac{\tau}{3}\mathbf{k}^2\delta n - \frac{1}{e}\sigma_E(\mathbf{k}\cdot\delta\mathbf{E}) - \frac{1}{e}\sigma_E(\mathbf{k}\cdot(\delta\mathbf{u}\times\mathbf{B})) = 0, \tag{3.58}$$

$$k_0\delta n_5 - (\mathbf{B}\cdot\mathbf{k})\delta\sigma_B^5 + i\frac{\tau}{3}\mathbf{k}^2\delta n_5 - i\frac{e^2}{2\pi^2}(\mathbf{B}\cdot\delta\mathbf{E}) = 0. \tag{3.59}$$

$$k_0\delta\epsilon - \frac{4}{3}\epsilon(\mathbf{k}\cdot\delta\mathbf{u}) = 0, \tag{3.60}$$

$$\frac{4}{3}\epsilon k_0\delta\mathbf{u} - \frac{1}{3}\mathbf{k}\delta\epsilon + i\frac{4\tau\epsilon}{15}\left(\mathbf{k}^2\delta\mathbf{u} + \frac{1}{3}\mathbf{k}(\mathbf{k}\cdot\delta\mathbf{u})\right)$$
$$-k_0(\mathbf{B}\times\delta\mathbf{E}) + (\mathbf{B}\cdot\mathbf{k})\delta\mathbf{B} - \mathbf{k}(\mathbf{B}\cdot\delta\mathbf{B}) = 0. \tag{3.61}$$

The linearized Maxwell equations take the form:

$$(\mathbf{k}\cdot\delta\mathbf{E}) + ie\delta n = 0, \tag{3.62}$$

$$(\mathbf{k}\times\delta\mathbf{B}) + k_0\delta\mathbf{E} + ie\mathbf{B}\delta\sigma_B + e\frac{\tau}{3}\mathbf{k}\delta n + i\sigma_E\left[\delta\mathbf{E} + (\delta\mathbf{u}\times\mathbf{B})\right] = 0, \tag{3.63}$$

$$-(\mathbf{k}\times\delta\mathbf{E}) + k_0\delta\mathbf{B} = 0, \tag{3.64}$$

$$(\mathbf{k}\cdot\delta\mathbf{B}) = 0. \tag{3.65}$$

As we see, after taking the Faraday's law (3.64) into account, the dynamical oscillations of the magnetic field $\delta\mathbf{B}$ can be expressed in terms of the electric field $\delta\mathbf{E}$, namely $\delta\mathbf{B} = (\mathbf{k}\times\delta\mathbf{E})/k_0$. In such a form, the latter also automatically satisfies Eq. (3.65), provided $k_0 \neq 0$.

After carefully examining the general structure of the above coupled set of equations and expressing $\delta\mathbf{B}$ through $\delta\mathbf{E}$ explicitly, we find that the system can be factorized into two blocks. In particular, the independent variables in one of the blocks can be chosen as follows: $\delta\mu$, $\delta\mu_5$, $(\mathbf{k}\cdot\delta\mathbf{E})$, $(\mathbf{B}\cdot\delta\mathbf{E})$, and $((\mathbf{k}\times\mathbf{B})\cdot\delta\mathbf{u})$. This is the block that describes the would-be CMW among other eigenmodes.

Because of the specific dependence of the CSE and CME currents on the magnetic field, i.e., $\mathbf{j}^5_{\rm CSE} = \mu e\mathbf{B}/(2\pi^2)$ and $\mathbf{j}_{\rm CME} = \mu_5 e\mathbf{B}/(2\pi^2)$, the propagation of the CMW is most prominent in the direction of the magnetic field. This is also clear from Eqs. (3.58) and (3.59), where the CSE and CME are captured by the terms proportional to $(\mathbf{B}\cdot\mathbf{k})$. For the purposes of our study, therefore, it is sufficient to concentrate only on the case with the wave vector $\mathbf{k}$ parallel to the background magnetic field $\mathbf{B}$. Then, the equations for the CMW greatly simplify, i.e.,

$$k_0\delta n - kB\delta\sigma_B + i\frac{\tau}{3}k^2\delta n - \frac{1}{e}\sigma_E k\delta E_z = 0, \tag{3.66}$$

$$k_0\delta n_5 - kB\delta\sigma^5_B + i\frac{\tau}{3}k^2\delta n_5 - i\frac{e^2}{2\pi^2}B\delta E_z = 0, \tag{3.67}$$

$$k\delta E_z + ie\delta n = 0. \tag{3.68}$$

It might be instructive to emphasize that these equations do not contain any dependence on the oscillations of the fluid velocity $\delta\mathbf{u}$. This is the consequence of assuming $\mathbf{k} \parallel \mathbf{B}$ and is not true in general for the CMW with an arbitrary direction of propagation.

After taking into account the explicit expressions for the number density and chiral charge density susceptibilities, $\chi = \partial n/\partial\mu$ and $\chi_5 = \partial n_5/\partial\mu_5$, in the high-temperature plasma we find

$$\frac{\delta\sigma_B}{\delta n_5} = \frac{e}{2\pi^2\chi_5} = \frac{3e}{2\pi^2T^2}, \tag{3.69}$$

$$\frac{\delta\sigma_B^5}{\delta n} = \frac{e}{2\pi^2\chi} = \frac{3e}{2\pi^2T^2}. \tag{3.70}$$

By making use of these relations, and eliminating the electric field δE_z with the help of Gauss's law (3.68), we then derive the following system of equations:

$$\left(k_0 + i\frac{\tau}{3}k^2 + i\sigma_E\right)\delta n - \frac{3eBk}{2\pi^2T^2}\delta n_5 = 0, \tag{3.71}$$

$$-\left(\frac{3eBk}{2\pi^2T^2} + \frac{e^3B}{2\pi^2k}\right)\delta n + \left(k_0 + i\frac{\tau}{3}k^2\right)\delta n_5 = 0. \tag{3.72}$$

By solving the corresponding characteristic equation, we finally obtain the spectrum of collective modes

$$k_0^{(\pm)} = -i\frac{\sigma_E}{2} \pm i\frac{\sigma_E}{2}\sqrt{1 - \left(\frac{3eB}{\pi^2T^2\sigma_E}\right)^2\left(k^2 + \frac{e^2T^2}{3}\right)} - i\frac{\tau}{3}k^2. \tag{3.73}$$

It might be appropriate to mention here that a similar dependence of the CMW energy on the electrical conductivity was also obtained by Abbasi *et al.* (2017). As is clear, the collective modes are diffusive when the expression under the square root is positive, i.e., when the following condition is satisfied:

$$\frac{eB}{\pi^2\sigma_E\sqrt{\chi\chi_5}}\sqrt{k^2 + e^2\chi} = \frac{3eB}{\pi^2T^2\sigma_E}\sqrt{k^2 + \frac{e^2T^2}{3}} < 1. \tag{3.74}$$

For the long wavelength modes with $k \lesssim eT$, this inequality is easily satisfied in sufficiently hot plasmas and/or for sufficiently weak background magnetic fields.

In fact, in the case of weakly coupled plasmas, Eq. (3.74) always holds true when the hydrodynamic limit is realized. Indeed, at weak coupling, the validity of hydrodynamics implies the following hierarchy of scales: $l_d \ll l_B \lesssim l_{\rm mfp} \ll \lambda_k$, where $l_d \simeq 1/T$ is de Broglie wavelength, $l_B = 1/\sqrt{eB}$ is the magnetic length, $l_{\rm mfp} \simeq \tau \sim l_d/e^2$ is the particle mean free path, and $\lambda_k \simeq 2\pi/k$ is the characteristic wavelength of the hydrodynamic modes. Note also that the electrical conductivity scales as $\sigma_E \sim T/(e^2 \ln e^{-1})$ at weak coupling (Arnold *et al.* (2000)).

The situation in the near-critical regime of the quark-gluon plasma created in the relativistic heavy-ion collisions is not as simple, however. First of all, because of strong coupling, there is no clear separation between the relevant length scales, $l_d \simeq l_{\rm mfp}$. Additional complications arise from the fact that the plasma is created in a rather small region of space. Nevertheless, the hydrodynamic description is expected to be suitable for such finite-size fireballs of quark-gluon plasma. The quantitative analysis of the corresponding case will be presented in Sec. 3.5.1.

It is instructive to study the physical reasons for the diffusive nature of the collective modes in Eq. (3.73) in the case of chiral plasmas at sufficiently high temperature and/or sufficiently weak background magnetic fields, i.e., when the expression on the left-hand side of Eq. (3.74) is much smaller than 1. Out of the two modes in Eq. (3.73), the first one has a smaller imaginary part, i.e.,

$$k_0^{(+)} \simeq -\frac{i}{\sigma_E}\left(\frac{3eB}{2\pi^2 T^2}\right)^2 \left(k^2 + \frac{e^2T^2}{3}\right) - i\frac{\tau}{3}k^2, \tag{3.75}$$

and describes the chiral charge diffusion, with a small admixture of an induced electric charge,

$$\delta n^{(+)} \simeq -i\frac{3eB}{2\pi^2 T^2 \sigma_E} k \delta n_5^{(+)}. \tag{3.76}$$

The other mode has a larger imaginary part, which is determined almost completely

by the electrical conductivity, i.e.,

$$k_0^{(-)} \simeq -i\sigma_E + \frac{i}{\sigma_E}\left(\frac{3eB}{2\pi^2T^2}\right)^2\left(k^2+\frac{e^2T^2}{3}\right) - i\frac{\tau}{3}k^2, \tag{3.77}$$

and describes the electric charge diffusion, with a small admixture of an induced chiral charge,

$$\delta n_5^{(-)} \simeq i\frac{3eB}{2\pi^2T^2\sigma_E}\left(k+\frac{e^2T^2}{3k}\right)\delta n^{(-)}. \tag{3.78}$$

Clearly, neither of the two modes resembles the conventional CMW with the expected dispersion relation $k_0^{(\mathrm{CMW})} = \pm v_{\mathrm{CMW}}k$, where $v_{\mathrm{CMW}} = 3eB/(2\pi^2T^2)$ obtained in the background-field approximation by Kharzeev and Yee (2011). The dramatic difference is the result of carefully taking dynamical electromagnetism into account. In fact, it is the high electrical conductivity of the plasma that plays the most important role. This can be explicitly verified by considering the limit $\sigma_E \to 0$ in Eqs. (3.66) and (3.67). In such a formal limit, the dispersion relations become

$$k_0^{(\pm)} = \pm\frac{3eB}{2\pi^2T^2}\sqrt{k^2+\frac{e^2T^2}{3}} - i\frac{\tau}{3}k^2, \quad \text{when} \quad \sigma_E \to 0. \tag{3.79}$$

These describe a pair of propagating CMW modes, although they are not the conventional ones because of a nonzero energy gap in the spectrum. The origin of the gap can be traced to the last term on the left-hand side of Eq. (3.67), which is the usual chiral anomaly term proportional to $B\delta E_z$. It gives a nontrivial contribution after the Gauss law (3.68) is taken into account. So, strictly speaking, the gap is the result of dynamical electromagnetism as well. Note that the gap in the energy spectrum of the CMW was also found in the context of Weyl semimetals (Sukhachov *et al.* (2018)).

From a physics viewpoint, the detrimental role of electrical conductivity on the propagation of the CMW can be relatively easily understood. The fundamental time scale for the CMW is set by the CSE and CME, which convert the oscillating electric and chiral charge densities into each other. The corresponding time is

$t_{\rm CMW} \simeq 2\pi^2 T^2/(3eBk)$. However, at sufficiently high temperatures and/or low magnetic fields, this is much longer than the time scale for screening of the electric charge fluctuations due to the electrical conductivity, $t_{\rm scr} \simeq \sigma_E^{-1}$. As a result, any local charge perturbation dissipates much quicker than the time it takes to produce a substantial chiral charge imbalance to sustain the CMW.

3.5.1 The chiral magnetic wave in heavy-ion collisions

As we mentioned earlier, in the case of strongly coupled quark-gluon plasma created in the relativistic heavy-ion collisions, the analysis is not so simple because there is no clear separation between the relevant length scales in the problem. One also has to take into account the effects associated with a small size of the system, its finite life-time, and to use realistic values for the transport coefficients. Here we perform the corresponding study in the nonperturbative regime of the quark-gluon plasma by using the transport coefficients obtained in lattice calculations (Aarts *et al.* (2007); Amato *et al.* (2013); Aarts *et al.* (2015)).

Let us start by writing down the complete set of chiral hydrodynamic equations for the plasma made of two light quark flavors,

$$\partial_\mu j_f^\mu = 0, \tag{3.80}$$

$$\partial_\mu j_{f,5}^\mu = -\frac{e^2 q_f^2}{8\pi^2} F^{\mu\nu}\tilde{F}_{\mu\nu}, \tag{3.81}$$

$$\partial_\nu T^{\mu\nu} = eF^{\mu\nu}\sum_f q_f j_{f,\nu}, \tag{3.82}$$

where $f = u, d$, and the quark charges are $q_u = 2/3$ and $q_d = -1/3$. Note that the total electric current is given in terms of the individual flavor number density currents as follows: $j_{\rm el}^\mu = e\sum_f q_f j_f^\mu$. For simplicity, we ignore the effects of the strange quark, which is considerably more massive than the two light quarks. It can be checked, however, that the results do not change much even if the strange quarks are included

either as (i) an additional massless flavor that contributes to both sets of continuity relations (3.80) and (3.81), or (ii) as a sufficiently massive flavor that contributes to Eq. (3.80), but not to Eq. (3.81).

The complete set of linearized equations that describes the longitudinal CMW in the multi-flavor quark-gluon plasma reads

$$k_0\delta n_f - \frac{eq_fBk}{2\pi^2\chi_{f,5}}\delta n_{f,5} + iD_fk^2\delta n_f - \frac{1}{eq_f}\sigma_{E,f}k\delta E_z = 0, \tag{3.83}$$

$$k_0\delta n_{f,5} - \frac{eq_fBk}{2\pi^2\chi_f}\delta n_f + iD_fk^2\delta n_{f,5} - i\frac{e^2q_f^2}{2\pi^2}B\delta E_z = 0, \tag{3.84}$$

$$k\delta E_z + ie\sum_f q_f\delta n_f = 0, \tag{3.85}$$

where we used the following relations:

$$\delta\sigma_{B,f} \equiv \frac{eq_f}{2\pi^2}\delta\mu_{f,5} = \frac{eq_f}{2\pi^2\chi_{f,5}}\delta n_{f,5}, \tag{3.86}$$

$$\delta\sigma^5_{B,f} \equiv \frac{eq_f}{2\pi^2}\delta\mu_f = \frac{eq_f}{2\pi^2\chi_f}\delta n_f, \tag{3.87}$$

which are given in terms of the fermion number and chiral charge susceptibilities $\chi_f \equiv \partial n_f/\partial\mu_f$ and $\chi_{f,5} \equiv \partial n_{f,5}/\partial\mu_{f,5}$.

In the continuity relations for the flavor number charge, we also used the partial flavor contributions to the electrical conductivity, i.e., $\sigma_{E,f} = c_\sigma e^2 q_f^2 T$. Note that the total conductivity σ_E takes the form

$$\sigma_E = \sum_f \sigma_{E,f} = c_\sigma C^\ell_{\rm em} T, \tag{3.88}$$

where $C^\ell_{\rm em} = e^2\sum_f q_f^2 = 5e^2/9 \approx 5.1\times10^{-2}$, where we took into account the definition of the fine structure constant, $e^2/(4\pi) = 1/137$. In the case of deconfined quark-gluon plasma, the numerical coefficient c_σ was obtained in lattice calculations by Aarts *et al.* (2007); Amato *et al.* (2013); Aarts *et al.* (2015). According to the most recent calculation of Aarts *et al.* (2015), its value ranges from about $c_\sigma \approx 0.111$ at

$T = 200$ MeV to about $c_\sigma \approx 0.316$ at $T = 350$ MeV, see Table 3.1. In the study of collective modes below, we will use these lattice values for the transport coefficients.

T	c_σ	c_χ	c_D
200 MeV	0.111	0.804	0.758
235 MeV	0.214	0.885	1.394
350 MeV	0.316	0.871	1.826

Table 3.1: Numerical values of coefficients c_σ, c_χ, and c_D at three fixed temperatures obtained from lattice calculations by Aarts *et al.* (2015).

We will also use the lattice results for the light-flavor number density susceptibilities χ_f and the diffusion coefficients D_f (Aarts *et al.* (2007); Amato *et al.* (2013); Aarts *et al.* (2015)), i.e.,

$$\chi_f = c_\chi \chi_f^{(SB)}, \tag{3.89}$$

$$D_f = \frac{c_D}{2\pi T}, \tag{3.90}$$

where the values of numerical coefficients are flavor independent (for the light u- and d-quarks) and are given in Table 3.1. Note that the Stefan-Boltzmann expression for the susceptibility is $\chi_f^{(SB)} \equiv T^2/3$. We will assume that the chiral charge susceptibility is the same as the fermion number one, i.e., $\chi_{f,5} = \chi_f$.

While the structure of Eqs. (3.83)–(3.85) is very similar to Eqs. (3.66)–(3.68), one should note that the total number of coupled equations is larger because the fermion number and chiral charges for each flavor satisfy independent continuity relations. With a larger number of equations, unfortunately, the characteristic equation becomes more complicated and no simple analytical solutions can be presented. Nevertheless, by making use of the intuition gained in the simpler model in the previous section, it is straightforward to check numerically that the underlying physics remains essentially the same.

In application to quark-gluon plasma created in heavy-ion collisions, it is important to take into account a relatively small size of the system. Such a size plays an important role as it sets an upper bound for the wavelengths of collective modes that could be realized, i.e., $\lambda_k \lesssim R$, where R is the system size. This implies, in turn, that there is an unavoidable lower bound for the values of wave vectors, $k \gtrsim 2\pi/R$. In the numerical analysis below, we will assume that the size of the system lies between about 12 fm and 24 fm. This would translate into an infrared cutoff for the possible wave vectors of about 100 MeV at $R \simeq 12$ fm and 50 MeV at $R \simeq 24$ fm.

Of course, there is also an upper bound for the values of wave vectors of collective modes. It is set by the inverse mean free part of the system. In the case of the deconfined quark-gluon plasma in the near-critical region, the latter is likely to be of the order of 1 fm or so. For our purposes, however, it will be sufficient to consider the wavelength $\lambda_k \gtrsim 2$ fm, which translates into the upper limit for the wave vectors $k \lesssim 600$ MeV.

The numerical analysis reveals that there are two pairs of overdamped collective modes. The dispersion relations for both modes take the following general form:

$$k_{0,n}^{(\pm)} = \pm E_n(k) - i\Gamma_n(k), \quad \text{with} \quad n = 1, 2, \tag{3.91}$$

where $E_n(k)$ and $\Gamma_n(k)$ are real and imaginary parts of the energies of collective modes. It is interesting to note that, in the long wavelength regime, one of the modes is the usual CMW, while the other corresponds to electrically neutral oscillations with $n_d \approx 2n_u$. The numerical results for the corresponding dispersion relations are summarized in Fig. 3.6, where we show the dependence of the real parts of the energies, as well as the ratios of the real to imaginary parts, on the wave vector k for three fixed values of temperature $T = 200$ MeV, 235 MeV, and 350 MeV, and for three fixed values of the background magnetic field, i.e., $eB = (50 \text{ MeV})^2$,

$(100\ \text{MeV})^2$, and $(200\ \text{MeV})^2$. The numerical data is presented for the wave vectors in the range $50\ \text{MeV} \lesssim k \lesssim 620\ \text{MeV}$, which corresponds to a rather wide window of the wavelengths, $2\ \text{fm} \lesssim \lambda_k \lesssim 24\ \text{fm}$. For the data in the gray shaded regions at small values of k, the values of the wavelengths lie between $\lambda_k \approx 24$ fm and $\lambda_k \approx 12$ fm. Most likely, these are already unrealistically large, but we decided to presented the corresponding results for completeness.

In order to obtain the numerical results in Fig. 3.6, we used the lattice data for the transport coefficients from Aarts *et al.* (2015). In this connection, it should be noted that the three selected choices of the temperature, $T = 200$ MeV, 235 MeV, and 350 MeV, correspond to $1.09T_c$, $1.27T_c$, and $1.9T_c$ in the notation of Aarts *et al.* (2015), where $T_c \approx 185$ MeV is the deconfinement critical temperature obtained from the position of the peak in the Polyakov loop susceptibility.

As is clear from the results in Fig. 3.6, all CMW-type modes are overdamped, although not always completely diffusive. This differs somewhat from the case of the very high temperature and/or weak magnetic field considered before. In fact, we find that this is largely due to the combination of the following two effects: (i) a relatively small electrical conductivity of the quark-gluon plasma in the near-critical region of temperatures and (ii) substantial charge diffusion effects for all wave vectors allowed by the small size of the system, i.e., $k \gtrsim 50$ MeV.

Because of a nonzero electrical conductivity, we find that one of the CMW modes becomes diffusive when the magnetic fields are not very strong and the wave vectors are not too large. Note that this is qualitatively consistent with the condition in Eq. (3.74). Indeed, as we see from the top row of panels in Fig. 3.6, one of the modes is diffusive (i.e., its real part of the energy is zero) in the whole range of wave vectors shown, when the field is not very strong, $eB = (50\ \text{MeV})^2$, but the temperature is high, $T = 350$ MeV. Even with decreasing the temperature, one of the modes still

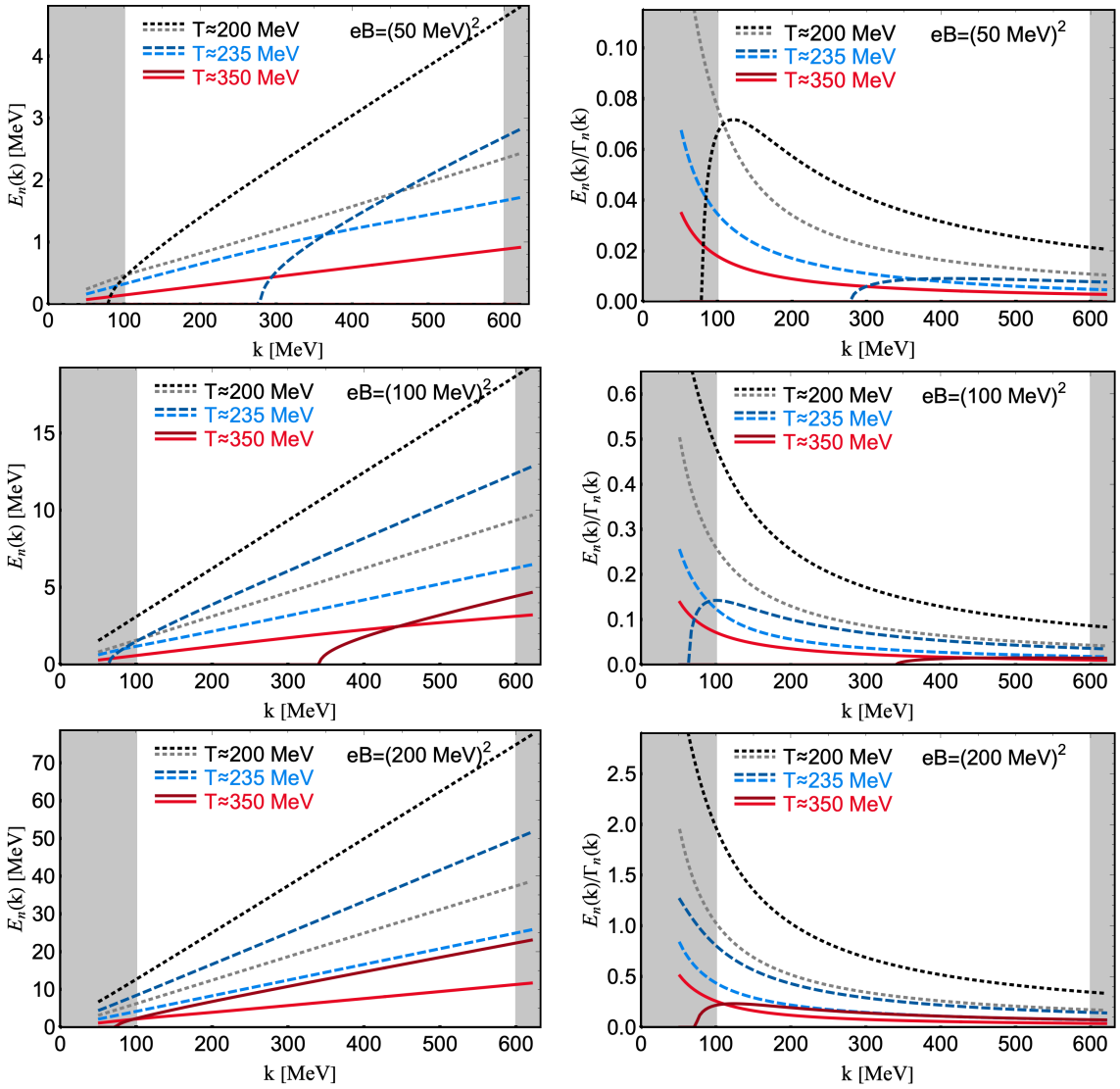

Figure 3.6: The real parts of the energies (left panels) and the ratios of the real to imaginary parts of the energies (right panels) of the CMW-type collective modes at three fixed values of temperature. The three rows of panels show the results for three choices of the magnetic field, i.e., $eB = (50\ \text{MeV})^2$, $(100\ \text{MeV})^2$, and $(200\ \text{MeV})^2$, respectively. In the gray shaded regions, the wavelengths lie outside the range 2 fm $\lesssim \lambda_k \lesssim$ 12 fm. The actual results are plotted down to the wave vectors as small as $k \approx 50$ MeV, which corresponds to $\lambda_k \lesssim 24$ fm.

remains diffusive at sufficiently small wave vectors, namely below $k \simeq 279$ MeV at $T = 235$ MeV and below $k \simeq 79$ MeV at $T = 200$ MeV. With increasing the magnetic field, as we see from the second and third rows of panels in Fig. 3.6, the range with one diffusive mode is pushed to smaller values of the wave vectors. For example,

at $eB = (100\ \text{MeV})^2$, the CMW is diffusive below $k \simeq 341$ MeV at $T = 350$ MeV and below $k \simeq 64$ MeV at $T = 235$ MeV. In fact, only at the smallest value of temperature, $T = 200$ MeV, the real part of the energy is nonzero in the whole range of allowed wave vectors. Nevertheless, the corresponding value of the real part remains considerably smaller than the imaginary part. In fact, as we see from the third row of panels in Fig. 3.6, the diffusive regime of the CMW is not completely avoided even in a rather strong magnetic field if the temperature stays sufficiently high. Indeed, at $eB = (200\ \text{MeV})^2$, one of the modes is still diffusive below $k \simeq 73$ MeV at $T = 350$ MeV. Only at sufficiently low temperatures, the CMW gradually revives and becomes a propagating mode at such an extremely strong field.

The existence/absence of a completely diffusive mode in the spectrum can be easily investigated in the whole range of relevant model parameters. In the plane of wave vectors and magnetic field, the corresponding regions are presented graphically in Fig. 3.7 for the three different values of temperatures. In the shaded regions (below the "critical" lines), the spectrum contains a diffusive mode. It should be pointed out that the corresponding regions agree qualitatively with the validity of the condition in Eq. (3.74).

As we see from the numerical results in Fig. 3.6, the collective modes are overdamped for all magnetic fields with the values of up to $eB \simeq (100\ \text{MeV})^2$, i.e., even if they are not completely diffusive. Indeed, the ratios of the real to imaginary parts of the energies $E_n(k)/\Gamma_n(k)$ are less than 1 in the whole range of the wave vectors down to the smallest values allowed by the system size, i.e., $k \simeq 50$ MeV, which corresponds to $\lambda_k \simeq 24$ fm. It easy to figure out that such strong damping cannot be explained by the effects of the electrical conductivity alone.

As it turns out, the charge diffusion also contributes substantially to the strong damping of the collective modes in a wide range of wave vectors. This is despite the

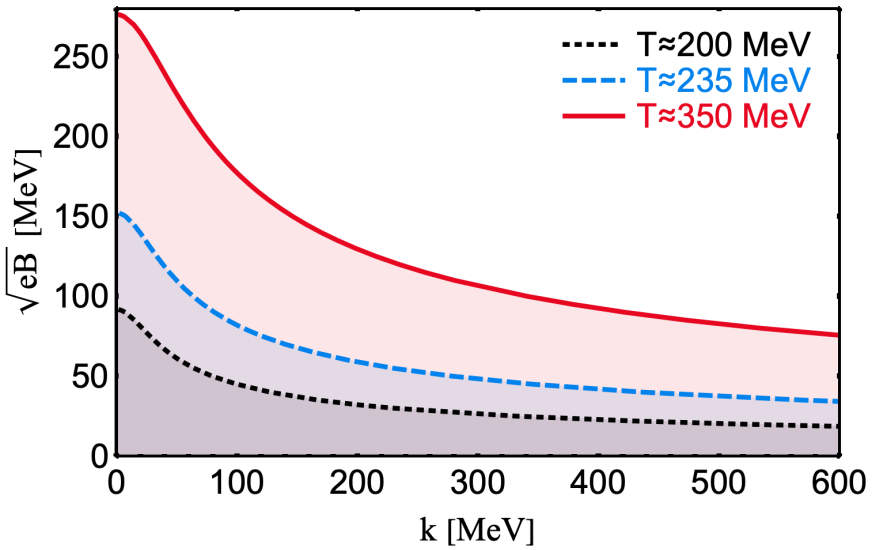

Figure 3.7: The graphical representation of the parameter space regions (shaded) where one of the modes becomes completely diffusive. Different colors (and line types) represent the results for three fixed values of temperature.

fact that, in the strongly coupled quark-gluon plasma in the near-critical regime, the diffusion coefficient takes a rather small value, $D_f \simeq 1/(2\pi T)$, see Eq. (3.90) and Table 3.1. By taking into account that the wave vector is bound from below by the inverse system size, however, one can easily see that the relevant modes are subject to a sizable damping.

3.6 The chiral vortical wave

The results of the previous sections show that there are substantial problems with realization of the non-damped chiral magnetic wave in electrically charged one-component chiral plasmas due to Ohmic dissipation. Indeed, in all but the strongest magnetic fields dissipation damps the wave into a purely dissipative mode with no oscillations. This poses a serious challenge for the experimental efforts to detect it (note, however, that situation may be different for multi-component plasmas, which may allow electrically neutral chiral modes). Because of these problems it may there-

fore be promising to consider closely the chiral vortical wave, which may exist in neutral plasmas without Ohmic dissipation.

The governing set of equations for the neutral chiral plasma is Eqs. (2.31)–(2.34) with the right-hand sides set to zero. The system is obviously decoupled from the Maxwell equations and so we will ignore them in this section. For simplicity we will concentrate only on the collective modes in the bulk far from the boundary and neglect the effects of geometry. In order to compare the results we choose the equilibrium analogous to the one we used in the previous sections, albeit without the background magnetic field, which does not influence the neutral system. In particular, we consider a chiral neutral plasma with a constant temperature T, chemical potential μ, chiral chemical potential μ_5, and velocity profile u^μ describing a uniform rotation with an angular velocity Ω along the $\hat{z}$ axis given in Eq. 3.1 (here and later we omit the bars above the equilibrium parameters). Note, that in the case of a neutral plasma we do not require any background charges to ensure stability against Coulomb repulsion. Analogously, the plasma may possess a non-zero vector current in the equilibrium, as it does not lead to a magnetic field production. Therefore, we may take a non-zero (but uniform) chiral chemical potential $\mu_5 \neq 0$ without breaking the equilibrium. As usual, we limit our analysis up to the linear order in Ω. In short, most of the arguments of the section 3.1 still apply to the neutral case with the only two exceptions being that the electromagnetic field has no influence on the system and the chiral chemical potential may be non-zero.

Having defined the equilibrium the next step is to impose a small perturbation on top of it and search for the collective modes. We deliberately disregard the geometry of the problem and so it makes sense to take the perturbations in the form of a plane-wave. We then solve for the collective modes near the axis of rotation far from the boundary. In the most general case all the chemical potentials, temperature, and

fluid velocity will oscillate around their average values, i.e.,

$$\delta\mu(x) = e^{-ikx}\delta\mu, \qquad \delta\mu_5(x) = e^{-ikx}\delta\mu_5, \tag{3.92}$$

$$\delta T(x) = e^{-ikx}\delta T, \qquad \delta u^\mu(x) = e^{-ikx}\delta u^\mu, \tag{3.93}$$

where k^μ is the wave vector, and $\delta\mu$, $\delta\mu_5$, δT, and δu^μ are the amplitudes of oscillations of the corresponding quantities. Note, that similar to the previous section we used a plane-wave perturbation profile, which is justified close to the axis of rotation and far from the boundaries. The velocity normalization $u^\mu u_\mu = 1$ constrains the corresponding oscillation to be orthogonal to the background velocity, $u_\mu \delta u^\mu = 0$. This is automatically satisfied for the waves with the fluid velocity oscillations along the direction of the vorticity, i.e., $\delta u^\mu \parallel \omega^\mu \parallel \hat{z}$. Using the fact that the chiral vortical wave propagates along the direction of vorticity (Jiang *et al.* (2015)) for simplicity we also take the wave vector to be parallel to it, i.e., $k^\mu = (k_0, 0, 0, k_z)$.

By substituting the perturbed hydrodynamic variables into the continuity equations (2.31)–(2.34) and using (2.26)–(2.28), we derive the following system of coupled

equations:

$$\sum_{\zeta_i}\left(k_0\frac{\partial n}{\partial\zeta_i}-i\frac{\tau}{3}k_\perp^2\frac{\partial n}{\partial z_i}+k_\mu\omega^\mu\frac{\partial\sigma_\omega}{\partial\zeta_i}\right)\delta\zeta_i+n\left(1+i\tau k_0\right)(k\cdot\delta u)-2k_0\sigma_\omega(\omega^\mu\cdot\delta u)=0, \tag{3.94}$$

$$\sum_{\zeta_i}\left(k_0\frac{\partial n_5}{\partial\zeta_i}-i\frac{\tau}{3}k_\perp^2\frac{\partial n_5}{\partial\zeta_i}+k_\mu\omega^\mu\frac{\partial\sigma_\omega^5}{\partial\zeta_i}\right)\delta\zeta_i+n_5\left(1+i\tau k_0\right)(k\cdot\delta u)-2k_0\sigma_\omega^5(\omega\cdot\delta u)=0, \tag{3.95}$$

$$\sum_{\zeta_i}\left(k_0\frac{\partial\epsilon}{\partial\zeta_i}+k_\mu\omega^\mu\frac{\partial\xi_\omega}{\partial\zeta_i}\right)\delta\zeta_i+\frac{4}{3}\epsilon(k\cdot\delta u)-3k_0\xi_\omega(\omega\cdot\delta u)=0, \tag{3.96}$$

$$\sum_{\zeta_i}\left(\omega^\mu k_0\frac{\partial\xi_\omega}{\partial\zeta_i}-k_\perp^\mu\frac{1}{3}\frac{\partial\epsilon}{\partial\zeta_i}\right)\delta\zeta_i+\left(\frac{4}{3}\epsilon k_0+\frac{3}{4}\xi_\omega(k\cdot\omega)\right)\delta u^\mu+\xi_\omega\omega^\mu(k\cdot\delta u)$$
$$+\frac{1}{4}\xi_\omega(\omega\cdot\delta u)k_\perp^\mu-\frac{i}{2}\xi_\omega k_0\varepsilon^{\mu\nu\alpha\beta}u_\nu k_\alpha\delta u_\beta-i\frac{8\tau\epsilon}{15}\Delta_{\alpha\beta}^{\mu\nu}k_\nu k^\alpha\delta u^\beta=0. \tag{3.97}$$

Here $\omega^\mu=(0,0,0,\Omega)$ is the vorticity four-vector in accordance with Eq. (3.2) up to the linear order in Ω, and we used a short-hand notation $k_\perp^\mu=k^\mu-u^\mu(k\cdot u)$, and the summation index $\zeta_i=(\mu,\mu_5,T)$.

The obtained system of homogeneous linear equations has nontrivial solutions only when the determinant of the corresponding matrix of coefficients vanishes. Thus, by solving the characteristic equation, we obtain dispersion relations for two different types of waves: the sound wave and the two modes that resemble the chiral vortical wave. As we will see, the latter differs from the simplified solutions of the chiral vortical wave in Jiang *et al.* (2015) because its propagation is profoundly affected by the hydrodynamic flow of the fluid itself.

For the sake of completeness let us first consider the sound wave. To the linear order in Ω and τ, the resulting dispersion relation is given by

$$k_0=\frac{s_e k_z}{\sqrt{3}}+\frac{3}{8}\Omega\frac{n_5}{\epsilon}\hbar k_z-\frac{2}{15}i\tau k_z^2, \tag{3.98}$$

where $s_e = \pm 1$. Comparing this result to (3.43) it is readily seen that they differ in the vorticity correction term, which in this case vanishes for $\mu_5 = 0$.

The dispersion relations of the chiral vortical wave reads:

$$k_0 = \hbar\Omega v_1 k_z - \frac{1}{3} i\tau k_z^2, \qquad k_0 = \hbar\Omega v_2 k_z - \frac{1}{3} i\tau k_z^2, \tag{3.99}$$

where $v_{1,2}$ are the roots of a quadratic equation $av^2 + bv + c = 0$ with the following coefficients:

$$\begin{aligned} a = \epsilon\Big[&7\pi^6 T^6 + 3\pi^2 T^2 \left(11\mu^4 + 18\mu^2\mu_5^2 + 11\mu_5^4\right) \\ &+ 27\pi^4 T^4 \left(\mu^2 + \mu_5^2\right) + 45\left(\mu^2 - \mu_5^2\right)^2 \left(\mu^2 + \mu_5^2\right)\Big], \end{aligned} \tag{3.100}$$

$$\begin{aligned} b = -\frac{\mu_5}{10\pi^2}\Big[&14\pi^8 T^8 - 15\pi^2 T^2 \left(30\mu^6 + 5\mu^4\mu_5^2 - 72\mu^2\mu_5^4 - 43\mu_5^6\right) \\ &+ \pi^6 T^6 \left(78\mu^2 + 127\mu_5^2\right) + 45\pi^4 T^4 \mu_5^2 \left(11\mu^2 + 9\mu_5^2\right) \\ &- 225\left(\mu^2 - \mu_5^2\right)\left(2\mu^6 + 5\mu^4\mu_5^2 + 8\mu^2\mu_5^4 + \mu_5^6\right)\Big], \end{aligned} \tag{3.101}$$

$$\begin{aligned} c = -\frac{3}{20\pi^2}\Big[&\pi^6 T^6 \left(4\mu^2 + 21\mu_5^2\right) + 5\pi^4 T^4 \left(8\mu^4 + 45\mu^2\mu_5^2 - 13\mu_5^4\right) \\ &+ 25\pi^2 T^2 \left(4\mu^6 + 27\mu^4\mu_5^2 - 6\mu^2\mu_5^4 - 9\mu_5^6\right) \\ &+ 75\mu_5^2 \left(\mu^2 - \mu_5^2\right)\left(5\mu^4 + 10\mu^2\mu_5^2 + \mu_5^4\right)\Big]. \end{aligned} \tag{3.102}$$

This result seems to qualitatively agree with the dispersion relations obtained by Abbasi *et al.* (2016, 2017). From a physical point of view, the two velocities $\hbar\Omega v_{1,2}$ correspond to the two opposite directions of propagation with respect to the vorticity and in general may be different. It is interesting to note that the two velocities are nonzero even at $\mu = 0$, which appears to contradict the prediction of Kalaydzhyan and Murchikova (2017), where similar waves were analyzed. We may suggest that this is the result of using a more general scheme in this study, in which both the fermion-number and axial-charge conservations are enforced (see also Abbasi *et al.* (2016, 2017)).

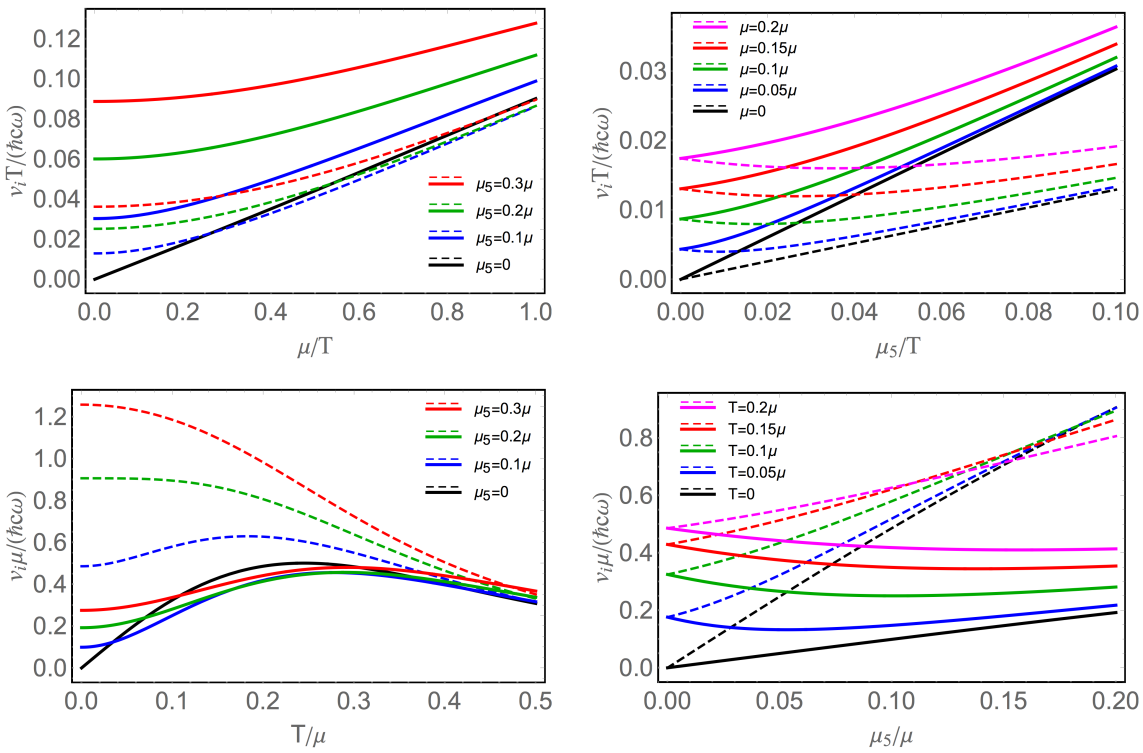

Figure 3.8: The two parameters $v_{1,2}$ that control the speed of the chiral vortical wave in the case of high temperature (top row) and high density (bottom row). The graph clearly shows the essential role of μ_5 in splitting the speeds of the CVW when it propagates along or against the direction of vorticity (the two coincide for $\mu_5 = 0$). This is also in agreement with the symmetry argument that the chiral chemical potential breaks parity.

The two parameters $v_{1,2} = (\hbar\Omega)^{-1}\partial k_0/\partial k_z$ from Eq. (3.99) of the chiral vortical wave propagating along and against the vorticity are shown on Fig. 3.8 for the cases of large temperature and chemical potential and different values of μ_5. As can be seen from the plots the chiral chemical potential plays an essential role in the splitting of the two velocities, which become equal at $\mu_5 = 0$. This inequality in its turn may produce an imbalance in the system evolution along the axis of vorticity. This observation is in agreement with the fact that the chiral chemical potential breaks the parity of the system.

In order to compare results with previous sections let us consider a special case of a plasma with vanishing chiral chemical potential $\mu_5 = 0$. In this case, the dispersion

relation for the sound wave is similar to that in Eq. (3.43), but has no correction due to vorticity. This should not be surprising for we chose $\mathbf{k}||\hat{z}$ in this section. As for the dispersion relation of the chiral vortical wave, it is given by the following explicit expression:

$$k_0 = s_e \frac{\Omega\hbar T\mu(\pi^2T^2 + 5\mu^2)k_z}{2\pi\sqrt{5\epsilon(5\epsilon - 2T^2\mu^2)(\pi^2T^2 + 3\mu^2)}} - \frac{1}{3}i\tau k_z^2. \tag{3.103}$$

Comparing this with Eq. (3.44) one can see the general resemblance ($\Re k_0 \propto \Omega k_z$), although there are significant differences in the coefficients. This may be attributed to the fact that this result was obtained without regard to the geometry by using a plane-wave perturbation ansatz. It may be suggested, therefore, that a proper account of boundary effects may play a crucial part in the analysis of chiral collective modes.

Chapter 4

CONCLUSIONS

As we mentioned in the introduction chiral symmetry plays an important role in the evolution of many physical systems ranging from the primordial plasma in the early Universe, to modern solid-state systems called Dirac and Weyl materials with relativistic-like quasi-particles, to quark-gluon plasma produced in high-energy heavy-ion collisions at the LHC and RHIC. From the theoretical point of view the properties of such systems are affected by the chiral anomaly, i.e., anomalous symmetry breaking. In this dissertation we concentrated on the influence of the chiral symmetry and its breaking on the collective modes of chiral plasmas.

In chapter 1 we examined the rapidly developing field of chiral plasmas, their examples and applications in different branches of physics, phenomenology, and theoretical approaches. This research is actively pursued in computer simulations of astrophysical phenomena, design of chiral condensed matter systems, and development of new observables in heavy-ion collisions. We reviewed the two main methods used in studies of chiral forms of matter, i.e., chiral kinetic theory and chiral hydrodynamics and discussed their range of validity. In passing, we also mentioned other methods proposed in the literature.

In chapter 2 we used covariant relativist chiral kinetic theory to derive a closed system of first order chiral hydrodynamic equations for a charged chiral plasma in electromagnetic fields. In the second part of the chapter we also derived a causal and stable second-order chiral hydrodynamics for a neutral plasma. It is interesting to note that hydrodynamical description of chiral systems has a number of peculiar features. For example, there may exist non-zero non-dissipative currents in a system

even in equilibrium due to the chiral magnetic and the chiral vortical effects. An interesting point in using the relaxation time approximation is the need for the so-called no-drag reference frame (in contrast to the more commonly used Landau and Eckart frames) unique for chiral systems. This is the same well-known artifact of the relaxation time approximation as in the conventional relativistic hydrodynamics, which is only slightly modified by the chiral effects.

In chapter 3 we started from identifying the range of validity of magnetohydrodynamics and established the hierarchy of the relevant scales in the problem. Then we found an equilibrium state of a uniformly rotating chiral plasma in cylindrical geometry in a magnetic field, which models a situation common in high-energy heavy-ion collisions. Using this equilibrium we then analytically found the full spectrum of long-wavelength collective modes. It was found that in the high-temperature (low-density) case the system carries a sound wave, an Alfvén-vortical wave and a few diffusive modes. In the high-density (low-temperature) case the system carries a plasmon mode, a helicon mode, and a number of overdamped diffusive modes. It is important to emphasize here that we found no "purely" chiral modes, such as the chiral magnetic and the chiral vortical waves predicted in chiral plasmas using less rigorous approaches (Kharzeev and Yee (2011); Jiang *et al.* (2015)). We stress the importance of the inclusion of dynamical electromagnetism and dissipation in the analysis of chiral effects as we showed the qualitative difference in the results without them.

We then investigated the reasons for the absence of both the CMW and CVW in detail. We found that in charged plasmas under all but most extreme conditions the electric conductivity overpowers any chiral propagation mechanism and damps a local charge imbalance before it has a chance to propagate. Therefore, all theoretical proposals for the detection of the CMW must be carefully reevaluated and, most-

likely, substantially modified in order to find robust physical observables pointing to the chiral nature and anomalous features of the quark-gluon plasma. In neutral plasmas the situation is similar and the chiral modes are strongly damped by the ordinary kinetic diffusion. The only conditions for the chiral modes to survive are extreme magnetic fields or vorticity. Under such conditions, however, the kinetic and hydrodynamic descriptions of the plasma break down. It is worth mentioning that we found a significant difference in velocities of the chiral vortical waves traveling in opposing directions (see Fig. 3.8) if even a small chiral imbalance μ_5 is initially present in the system. We argue that this may lead to physical observables even for damped modes. It must be noted also that the analysis of the chiral vortical wave showed that a proper account of boundary effects and geometry of the problem may play a role in the analysis of chiral collective modes.

Despite the considerable progress there is still a lot of questions that need further research regarding the anomalous effects in chiral plasmas. We could start by mentioning the effects of small non-zero masses in chiral kinetic and hydrodynamic theories. Since most (if not all) elementary particles have non-zero masses, it must be important in some physical scenarios and can even lead to new qualitative effects. The relevant questions also include the quantitative estimates for the range of validity of CKT and chiral hydrodynamics and the effects of mass-induced chirality flipping on signature anomalous phenomena. A limited progress in this direction was recently made in recent papers by Hattori *et al.* (2019) and Wang *et al.* (2019). However, it is fair to say that the problem has not been completely solved.

By continuing the research program started in this dissertation it would be interesting to derive the second-order chiral hydrodynamics for a charged plasma. One could use the same technique as the one used in chapter 2 for the neutral case. The initial investigation in this direction suggests that there will be many more terms in

constituent relations, including new qualitative features.

Having a closed set of kinetic and hydrodynamic equations begs for a direct solver or particle-in-cell computer simulation algorithm that fully accounts for dynamical electromagnetism and all dissipative effects. Even something basic as a gradual subsiding of chiral charge can be useful to model the stability and lifetime of local inhomogeneities in plasma. It will be even more important for reexamining the conversion of plasma chirality to magnetic field helicity in the early Universe (inverse magnetic cascade) (Brandenburg *et al.* (2017); Schober *et al.* (2018)). In particular, one truly needs to establish whether finite conductivity plasma would not kill the primordial magnetic field generation in the early Universe.

In the context of chiral effects in heavy-ion collisions it is interesting to establish what kind of new observables can be predicted from the type and spectrum of collective modes obtained in this dissertation. Since the Alfvén waves are slightly modified by the anomalous physics, it is plausible that some multi-particle correlators could be sufficiently sensitive to their details and could be extracted from the observable data. The corresponding research program is likely to be very difficult due to complications from finite-size a short lifetime effects, non-uniform vorticity and background fields profiles, etc..

Aarts, G., C. Allton, A. Amato, P. Giudice, S. Hands and J.-I. Skullerud, "Electrical conductivity and charge diffusion in thermal QCD from the lattice", J. High Energy Phys. **2**, 186 (2015).

Aarts, G., C. Allton, J. Foley, S. Hands and S. Kim, "Spectral Functions at Small Energies and the Electrical Conductivity in Hot Quenched Lattice QCD", Phys. Rev. Lett. **99**, 2, 022002 (2007).

Abbasi, N., D. Allahbakhshi, A. Davody and S. F. Taghavi, "Hydrodynamic excitations in hot QCD plasma", Phys. Rev. D **96**, 12, 126002 (2017).

Abbasi, N., A. Davody, K. Hejazi and Z. Rezaei, "Hydrodynamic waves in an anomalous charged fluid", Phys. Rev. B **762**, 23–32 (2016).

Adams, J., M. M. Aggarwal, Z. Ahammed, J. Amonett, B. D. Anderson, D. Arkhipkin, G. S. Averichev, S. K. Badyal, Y. Bai, J. Balewski and et al., "Experimental and theoretical challenges in the search for the quark-gluon plasma: The STAR Collaboration's critical assessment of the evidence from RHIC collisions", Nucl. Phys. A **757**, 102–183 (2005).

Adcox, K., S. S. Adler, S. Afanasiev, C. Aidala, N. N. Ajitanand, Y. Akiba, A. Al-Jamel, J. Alexander, R. Amirikas, K. Aoki and et al., "Formation of dense partonic matter in relativistic nucleus-nucleus collisions at RHIC: Experimental evaluation by the PHENIX Collaboration", Nucl. Phys. A **757**, 184–283 (2005).

Adler, S. L., "Axial-Vector Vertex in Spinor Electrodynamics", Phys. Rev. **177**, 2426–2438 (1969).

Amato, A., G. Aarts, C. Allton, P. Giudice, S. Hands and J.-I. Skullerud, "Electrical Conductivity of the Quark-Gluon Plasma Across the Deconfinement Transition", Phys. Rev. Lett. **111**, 17, 172001 (2013).

Anderson, J. L. and H. R. Witting, "A relativistic relaxation-time model for the Boltzmann equation", Physica **74**, 466–488 (1974).

Armitage, N. P., E. J. Mele and A. Vishwanath, "Weyl and Dirac semimetals in three-dimensional solids", Reviews of Modern Physics **90**, 1, 015001 (2018).

Arnold, P., G. D. Moore and L. G. Yaffe, "Transport coefficients in high temperature gauge theories (I): leading-log results", J. High Energy Phys. **11**, 001 (2000).

Banerjee, N., J. Bhattacharya, S. Bhattacharyya, S. Dutta, R. Loganayagam and P. Surówka, "Hydrodynamics from charged black branes", J. High Energy Phys. **1**, 94 (2011).

Bazavov, A., T. Bhattacharya, C. DeTar, H.-T. Ding, S. Gottlieb, R. Gupta, P. Hegde, U. M. Heller, F. Karsch, E. Laermann, L. Levkova, S. Mukherjee, P. Petreczky, C. Schmidt, C. Schroeder, R. A. Soltz, W. Soeldner, R. Sugar, M. Wagner, P. Vranas and HotQCD Collaboration, "Equation of state in (2 +1)-flavor QCD", Phys. Rev. D **90**, 9, 094503 (2014).

Becattini, F., W. Florkowski and E. Speranza, "Spin tensor and its role in non-equilibrium thermodynamics", Phys. Lett. B **789**, 419–425 (2019).

Becattini, F., G. Inghirami, V. Rolando, A. Beraudo, L. Del Zanna, A. De Pace, M. Nardi, G. Pagliara and V. Chandra, "A study of vorticity formation in high energy nuclear collisions", Eur. Phys. J. C **75**, 406 (2015).

Becattini, F. and L. Tinti, "The ideal relativistic rotating gas as a perfect fluid with spin", Annals Phys. **325**, 1566–1594 (2010).

Bell, J. S. and R. Jackiw, "A PCAC puzzle: $\pi^0 \to \gamma\gamma$ in the σ-model", Nuovo Cimento A Serie **60**, 47–61 (1969).

Boas, R. P. and H. Pollard, "Complete sets of bessel and legendre functions", Ann. Math. **48**, 2, 366–384, URL `http://www.jstor.org/stable/1969177` (1947).

Brandenburg, A., J. Schober, I. Rogachevskii, T. Kahniashvili, A. Boyarsky, J. Fröhlich, O. Ruchayskiy and N. Kleeorin, "The Turbulent Chiral Magnetic Cascade in the Early Universe", Astrophys. J. **845**, L21 (2017).

Burnier, Y., D. E. Kharzeev, J. Liao and H.-U. Yee, "Chiral Magnetic Wave at Finite Baryon Density and the Electric Quadrupole Moment of the Quark-Gluon Plasma", Phys. Rev. Lett. **107**, 5, 052303 (2011).

Buzzegoli, M. and F. Becattini, "General thermodynamic equilibrium with axial chemical potential for the free Dirac field", J. High Energy Phys. **12**, 2 (2018).

Carignano, S., C. Manuel and J. M. Torres-Rincon, "Consistent relativistic chiral kinetic theory: A derivation from on-shell effective field theory", Phys. Rev. D **98**, 7, 076005 (2018).

Chapman, S. and T. G. Cowling, *The mathematical theory of non-uniform gases. an account of the kinetic theory of viscosity, thermal conduction and diffusion in gases* (1970).

Chen, J.-W., S. Pu, Q. Wang and X.-N. Wang, "Berry Curvature and Four-Dimensional Monopoles in the Relativistic Chiral Kinetic Equation", Phys. Rev. Lett. **110**, 26, 262301 (2013).

Chen, J.-Y., D. T. Son, M. A. Stephanov, H.-U. Yee and Y. Yin, "Lorentz Invariance in Chiral Kinetic Theory", Phys. Rev. Lett. **113**, 18, 182302 (2014).

Chernodub, M. N., "Chiral heat wave and mixing of magnetic, vortical and heat waves in chiral media", J. High Energy Phys. **1**, 100 (2016).

Christensson, M., M. Hindmarsh and A. Brandenburg, "Inverse cascade in decaying three-dimensional magnetohydrodynamic turbulence", Phys. Rev. E **64**, 5, 056405 (2001).

Del Zanna, L. and N. Bucciantini, "Covariant and 3 + 1 equations for dynamo-chiral general relativistic magnetohydrodynamics", Mon. Not. Roy. Astron. Soc. **479**, 657–666 (2018).

Deng, W.-T. and X.-G. Huang, "Vorticity in heavy-ion collisions", Phys. Rev. C **93**, 6, 064907 (2016).

Denicol, G. S., T. Kodama, T. Koide and P. Mota, "Stability and causality in relativistic dissipative hydrodynamics", J. Phys. G **35**, 11, 115102 (2008).

Denicol, G. S., T. Koide and D. H. Rischke, "Dissipative Relativistic Fluid Dynamics: A New Way to Derive the Equations of Motion from Kinetic Theory", Phys. Rev. Lett. **105**, 16, 162501 (2010).

Denicol, G. S., E. Molnár, H. Niemi and D. H. Rischke, "Derivation of fluid dynamics from kinetic theory with the 14-moment approximation", Eur. Phys. J. A **48**, 170 (2012).

Dubovsky, S., L. Hui, A. Nicolis and D. T. Son, "Effective field theory for hydrodynamics: Thermodynamics, and the derivative expansion", Phys. Rev. D **85**, 8, 085029 (2012).

Erdmenger, J., M. Haack, M. Kaminski and A. Yarom, "Fluid dynamics of R-charged black holes", J. High Energy Phys. **1**, 055 (2009).

Florkowski, W., M. P. Heller and M. Spaliński, "New theories of relativistic hydrodynamics in the LHC era", Reports on Progress in Physics **81**, 4, 046001 (2018a).

Florkowski, W., A. Kumar and R. Ryblewski, "Vortex-like solutions and internal structures of covariant ideal magnetohydrodynamics", Eur. Phys. J. A **54**, 184 (2018b).

Fukushima, K., D. E. Kharzeev and H. J. Warringa, "Chiral magnetic effect", Phys. Rev. D **78**, 7, 074033 (2008).

Gao, J.-H., Z.-T. Liang, S. Pu, Q. Wang and X.-N. Wang, "Chiral Anomaly and Local Polarization Effect from the Quantum Kinetic Approach", Phys. Rev. Lett. **109**, 23, 232301 (2012).

Gorbar, E. V., V. A. Miransky and I. A. Shovkovy, "Normal ground state of dense relativistic matter in a magnetic field", Phys. Rev. D **83**, 8, 085003 (2011).

Gorbar, E. V., V. A. Miransky and I. A. Shovkovy, "Chiral anomaly, dimensional reduction, and magnetoresistivity of Weyl and Dirac semimetals", Phys. Rev. B **89**, 8, 085126 (2014).

Gorbar, E. V., D. O. Rybalka and I. A. Shovkovy, "Second-order dissipative hydrodynamics for plasma with chiral asymmetry and vorticity", Phys. Rev. D **95**, 9, 096010 (2017).

Gorbar, E. V., I. A. Shovkovy, S. Vilchinskii, I. Rudenok, A. Boyarsky and O. Ruchayskiy, "Anomalous Maxwell equations for inhomogeneous chiral plasma", Phys. Rev. D **93**, 10, 105028 (2016).

Gradshteyn, I. S. and I. M. Ryzhik, *Table of integrals, series, and products* (Academic press, 2014).

Gyulassy, M. and L. McLerran, "New forms of QCD matter discovered at RHIC", Nucl. Phys. A **750**, 30–63 (2005).

Haehl, F. M., R. Loganayagam and M. Rangamani, "Effective action for relativistic hydrodynamics: fluctuations, dissipation, and entropy inflow", J. High Energy Phys. **10**, 194 (2018).

Harris, E. G., "Relativistic Magnetohydrodynamics", Phys. Rev. **108**, 1357–1360 (1957).

Hattori, K., Y. Hidaka and D.-L. Yang, "Axial Kinetic Theory for Massive Fermions", arXiv e-prints (2019).

Heinz, U. and R. Snellings, "Collective Flow and Viscosity in Relativistic Heavy-Ion Collisions", Ann. Rev. Nucl. Part. Sci. **63**, 123–151 (2013).

Hidaka, Y., S. Pu and D.-L. Yang, "Relativistic chiral kinetic theory from quantum field theories", Phys. Rev. D **95**, 9, 091901 (2017).

Hidaka, Y., S. Pu and D.-L. Yang, "Nonlinear responses of chiral fluids from kinetic theory", Phys. Rev. D **97**, 1, 016004 (2018).

Hidaka, Y. and D.-L. Yang, "Nonequilibrium chiral magnetic/vortical effects in viscous fluids", Phys. Rev. D **98**, 1, 016012 (2018).

Hiscock, W. A. and L. Lindblom, "Stability and causality in dissipative relativistic fluids.", Annals Phys. **151**, 466–496 (1983).

Hosur, P. and X. Qi, "Recent developments in transport phenomena in Weyl semimetals", Comptes Rendus Physique **14**, 857–870 (2013).

Huang, X., L. Zhao, Y. Long, P. Wang, D. Chen, Z. Yang, H. Liang, M. Xue, H. Weng, Z. Fang, X. Dai and G. Chen, "Observation of the Chiral-Anomaly-Induced Negative Magnetoresistance in 3D Weyl Semimetal TaAs", Phys. Rev. X **5**, 3, 031023 (2015).

Huang, X.-G., A. Sedrakian and D. H. Rischke, "Kubo formulas for relativistic fluids in strong magnetic fields", Annals Phys. **326**, 3075–3094 (2011).

Isachenkov, M. V. and A. V. Sadofyev, "The chiral magnetic effect in hydrodynamical approach", Phys. Lett. B **697**, 404–406 (2011).

Israel, W., "Nonstationary irreversible thermodynamics: A causal relativistic theory", Annals Phys. **100**, 310–331 (1976).

Israel, W. and J. M. Stewart, "Transient relativistic thermodynamics and kinetic theory", Annals Phys. **118**, 341–372 (1979).

Jaiswal, A., "Relativistic dissipative hydrodynamics from kinetic theory with relaxation-time approximation", Phys. Rev. C **87**, 5, 051901 (2013a).

Jaiswal, A., "Relativistic third-order dissipative fluid dynamics from kinetic theory", Phys. Rev. C **88**, 2, 021903 (2013b).

Jaiswal, A., B. Friman and K. Redlich, "Relativistic second-order dissipative hydrodynamics at finite chemical potential", Phys. Rev. B **751**, 548–552 (2015).

Jiang, Y., X.-G. Huang and J. Liao, "Chiral vortical wave and induced flavor charge transport in a rotating quark-gluon plasma", Phys. Rev. D **92**, 7, 071501 (2015).

Jiang, Y., Z.-W. Lin and J. Liao, "Rotating quark-gluon plasma in relativistic heavy-ion collisions", Phys. Rev. C **94**, 4, 044910 (2016).

Jiang, Y., Z.-W. Lin and J. Liao, "Erratum: Rotating quark-gluon plasma in relativistic heavy-ion collisions [Phys. Rev. C 94, 044910 (2016)]", Phys. Rev. C **95**, 4, 049904 (2017).

Kalaydzhyan, T. and E. Murchikova, "Thermal chiral vortical and magnetic waves: New excitation modes in chiral fluids", Nucl. Phys. B **919**, 173–181 (2017).

Kaushik, S., D. E. Kharzeev and E. J. Philip, "Chiral Magnetic Photocurrent in Dirac and Weyl Materials", arXiv e-prints (2018).

Kharzeev, D., "Parity violation in hot QCD: Why it can happen, and how to look for it", Phys. Rev. B **633**, 260–264 (2006).

Kharzeev, D., K. Landsteiner, A. Schmitt and H.-U. Yee, eds., *Strongly Interacting Matter in Magnetic Fields*, vol. 871 of *Lecture Notes in Physics, Berlin Springer Verlag* (2013).

Kharzeev, D. E., "The Chiral Magnetic Effect and anomaly-induced transport", Progress in Particle and Nuclear Physics **75**, 133–151 (2014).

Kharzeev, D. E., J. Liao, S. A. Voloshin and G. Wang, "Chiral magnetic and vortical effects in high-energy nuclear collisions - A status report", Prog. Part. Nucl. Phys. **88**, 1–28 (2016).

Kharzeev, D. E., L. D. McLerran and H. J. Warringa, "The effects of topological charge change in heavy ion collisions: 'Event by event P and CP violation'", Nucl. Phys. A **803**, 227–253 (2008).

Kharzeev, D. E. and H.-U. Yee, "Chiral magnetic wave", Phys. Rev. D **83**, 8, 085007 (2011).

Landsteiner, K., E. Megías and F. Pena-Benitez, "Gravitational Anomaly and Transport Phenomena", Phys. Rev. Lett. **107**, 2, 021601 (2011).

Lappi, T. and L. McLerran, "Some features of the glasma", Nucl. Phys. A **772**, 200–212 (2006).

Li, Q., D. E. Kharzeev, C. Zhang, Y. Huang, I. Pletikosić, A. V. Fedorov, R. D. Zhong, J. A. Schneeloch, G. D. Gu and T. Valla, "Chiral magnetic effect in $ZrTe_5$", Nature Physics **12**, 550–554 (2016).

Loizides, C., "Experimental overview on small collision systems at the LHC", Nucl. Phys. A **956**, 200–207 (2016).

Lv, B. Q., H. M. Weng, B. B. Fu, X. P. Wang, H. Miao, J. Ma, P. Richard, X. C. Huang, L. X. Zhao, G. F. Chen, Z. Fang, X. Dai, T. Qian and H. Ding, "Experimental Discovery of Weyl Semimetal TaAs", Phys. Rev. X **5**, 3, 031013 (2015).

Masada, Y., K. Kotake, T. Takiwaki and N. Yamamoto, "Chiral magnetohydrodynamic turbulence in core-collapse supernovae", Phys. Rev. D **98**, 8, 083018 (2018).

Metlitski, M. A. and A. R. Zhitnitsky, "Anomalous axion interactions and topological currents in dense matter", Phys. Rev. D **72**, 4, 045011 (2005).

Miransky, V. A. and I. A. Shovkovy, "Quantum field theory in a magnetic field: From quantum chromodynamics to graphene and Dirac semimetals", Phys. Rept. **576**, 1–209 (2015).

Monnai, A., "Off-equilibrium corrections to energy and conserved charge densities in the relativistic fluid in heavy-ion collisions", Phys. Rev. C **98**, 3, 034902 (2018).

Nagle, J. L. and W. A. Zajc, "Small System Collectivity in Relativistic Hadronic and Nuclear Collisions", Annual Review of Nuclear and Particle Science **68**, 211–235 (2018).

Neiman, Y. and Y. Oz, "Relativistic hydrodynamics with general anomalous charges", J. High Energy Phys. **3**, 23 (2011).

Obergaulinger, M., O. Just and M. A. Aloy, "Core collapse with magnetic fields and rotation", J. Phys. G **45**, 8, 084001 (2018).

Peskin, M. E. and D. V. Schroeder, *An Introduction to Quantum Field Theory* (Westview Press, 1995).

Pu, S., T. Koide and D. H. Rischke, "Does stability of relativistic dissipative fluid dynamics imply causality?", Phys. Rev. D **81**, 11, 114039 (2010).

Rajagopal, K. and A. V. Sadofyev, "Chiral drag force", J. High Energy Phys. **10**, 18 (2015).

Rybalka, D. O., E. V. Gorbar and I. A. Shovkovy, "Hydrodynamic modes in a magnetized chiral plasma with vorticity", Phys. Rev. D **99**, 016017, URL `https://link.aps.org/doi/10.1103/PhysRevD.99.016017` (2019).

Sadofyev, A. V. and Y. Yin, "Drag suppression in anomalous chiral media", Phys. Rev. D **93**, 12, 125026 (2016).

Schober, J., I. Rogachevskii, A. Brandenburg, A. Boyarsky, J. Fröhlich, O. Ruchayskiy and N. Kleeorin, "Laminar and Turbulent Dynamos in Chiral Magnetohydrodynamics. II. Simulations", Astrophys. J. **858**, 124 (2018).

Shovkovy, I. A., D. O. Rybalka and E. V. Gorbar, "The overdamped chiral magnetic wave", (2018).

Son, D. T. and B. Z. Spivak, "Chiral anomaly and classical negative magnetoresistance of Weyl metals", Phys. Rev. B **88**, 10, 104412 (2013).

Son, D. T. and P. Surówka, "Hydrodynamics with Triangle Anomalies", Phys. Rev. Lett. **103**, 19, 191601 (2009).

Son, D. T. and N. Yamamoto, "Berry Curvature, Triangle Anomalies, and the Chiral Magnetic Effect in Fermi Liquids", Phys. Rev. Lett. **109**, 18, 181602 (2012).

Son, D. T. and N. Yamamoto, "Kinetic theory with Berry curvature from quantum field theories", Phys. Rev. D **87**, 8, 085016 (2013).

Stephanov, M. A. and H.-U. Yee, "No-Drag Frame for Anomalous Chiral Fluid", Phys. Rev. Lett. **116**, 12, 122302 (2016).

Stephanov, M. A. and Y. Yin, "Chiral Kinetic Theory", Phys. Rev. Lett. **109**, 16, 162001 (2012).

Sukhachov, P. O., E. V. Gorbar, I. A. Shovkovy and V. A. Miransky, "Collective excitations in Weyl semimetals in the hydrodynamic regime", J. Phys. Condens. Matter **30**, 27, 275601 (2018).

't Hooft, G., "Magnetic monopoles in unified gauge theories", Nucl. Phys. B **79**, 276–284 (1974).

Tanabashi, M., K. Hagiwara, K. Hikasa, K. Nakamura, Y. Sumino, F. Takahashi, J. Tanaka, K. Agashe, G. Aielli, C. Amsler and et al., "Review of Particle Physics", Phys. Rev. D **98**, 3, 030001 (2018).

Tashiro, H., T. Vachaspati and A. Vilenkin, "Chiral effects and cosmic magnetic fields", Phys. Rev. D **86**, 10, 105033 (2012).

Vasak, D., M. Gyulassy and H.-T. Elze, "Quantum transport theory for abelian plasmas", Annals Phys. **173**, 462–492 (1987).

Vilenkin, A., "Parity violating currents in thermal radiation", Phys. Lett. B **80**, 150–152 (1978).

Vilenkin, A., "Macroscopic parity-violating effects: Neutrino fluxes from rotating black holes and in rotating thermal radiation", Phys. Rev. D **20**, 1807–1812 (1979).

Vilenkin, A., "Equilibrium parity-violating current in a magnetic field", Phys. Rev. D **22**, 3080–3084 (1980a).

Vilenkin, A., "Quantum field theory at finite temperature in a rotating system", Phys. Rev. D **21**, 2260–2269 (1980b).

Wang, Z., X. Guo, S. Shi and P. Zhuang, "Mass Correction to Chiral Kinetic Equations", arXiv e-prints (2019).

Wang, Z., Y. Sun, X.-Q. Chen, C. Franchini, G. Xu, H. Weng, X. Dai and Z. Fang, "Dirac semimetal and topological phase transitions in A_3Bi (A=Na, K, Rb)", Phys. Rev. B **85**, 19, 195320 (2012).

Wang, Z., H. Weng, Q. Wu, X. Dai and Z. Fang, "Three-dimensional Dirac semimetal and quantum transport in Cd_3As_2", Phys. Rev. B **88**, 12, 125427 (2013).

Watson, G., *A Treatise on the Theory of Bessel Functions*, Cambridge Mathematical Library (Cambridge University Press, 1995), URL `https://books.google.com/books?id=Mlk3FrNoEVoC`.

Xu, S.-Y., I. Belopolski, N. Alidoust, M. Neupane, G. Bian, C. Zhang, R. Sankar, G. Chang, Z. Yuan, C.-C. Lee, S.-M. Huang, H. Zheng, J. Ma, D. S. Sanchez, B. Wang, A. Bansil, F. Chou, P. P. Shibayev, H. Lin, S. Jia and M. Z. Hasan, "Discovery of a Weyl fermion semimetal and topological Fermi arcs", Science **349**, 613–617 (2015).

Zhao, J., "Search for the chiral magnetic effect in relativistic heavy-ion collisions", Int. J. Mod. Phys. A **33**, 1830010 (2018).

Zhelyazkov, I. and R. Chandra, "High mode magnetohydrodynamic waves propagation in a twisted rotating jet emerging from a filament eruption", Mon. Not. Roy. Astron. Soc. **478**, 5505–5513 (2018).

APPENDIX A

TABLE INTEGRALS AND THERMODYNAMIC FUNCTIONS IN EQUILIBRIUM

In the calculation of moments of the distribution function, the following integrals are useful:

$$\int \frac{d^4p}{(2\pi\hbar)^3}\delta(p^2)(p\cdot u)^n f_0 = -\frac{\Gamma(n+2)}{4\pi^2}T^{n+2}\sum_{\chi=\pm1}\chi^{n+2}\mathrm{Li}_{n+2}\left(-e^{\frac{\chi\mu_\lambda}{T}}\right) \equiv I_{n+2}, \quad \text{(A.1)}$$

$$\int \frac{d^4p}{(2\pi\hbar)^3}\delta(p^2)(p\cdot u)^n p^\alpha f_0 = u^\alpha I_{n+3}, \quad \text{(A.2)}$$

$$\int \frac{d^4p}{(2\pi\hbar)^3}\delta(p^2)(p\cdot u)^n p^\alpha p^\beta f_0 = \left(-\frac{1}{3}g^{\alpha\beta}+\frac{4}{3}u^\alpha u^\beta\right) I_{n+4}, \quad \text{(A.3)}$$

$$\int \frac{d^4p}{(2\pi\hbar)^3}\delta(p^2)(p\cdot u)^n p^\alpha p^\beta p^\gamma f_0 = \left(-g^{(\alpha\beta}u^{\gamma)}+2u^\alpha u^\beta u^\gamma\right) I_{n+5}, \quad \text{(A.4)}$$

$$\int \frac{d^4p}{(2\pi\hbar)^3}\delta(p^2)(p\cdot u)^n p^\alpha p^\beta p^\gamma p^\delta f_0 = \left(\frac{1}{5}g^{(\alpha\beta}g^{\gamma\delta)}-\frac{12}{5}g^{(\alpha\beta}u^\gamma u^{\delta)}+\frac{16}{5}u^\alpha u^\beta u^\gamma u^\delta\right) I_{n+6}, \quad \text{(A.5)}$$

where f_0 is the equilibrium function at vanishing vorticity, i.e.,

$$f_0 = \frac{1}{1+e^{\mathrm{sign}(p_0)(\varepsilon_{p,0}-\mu_\lambda)/T}}, \quad \text{(A.6)}$$

with $\varepsilon_{p,0} = p\cdot u$, and the round brackets in superscripts denote the symmetrization over all possible permutations of indices, e.g., $A^{(\alpha}B^\beta C^{\gamma)} \equiv (A^\alpha B^\beta C^\gamma + A^\alpha B^\gamma C^\beta + A^\beta B^\alpha C^\gamma + A^\beta B^\gamma C^\alpha + A^\gamma B^\beta C^\alpha + A^\gamma B^\alpha C^\beta)/3!$.

It is easy to check that the lower moments can be obtained from the higher ones multiplying the latter by the four-velocity u^μ. As is easy to check, the explicit results for several lowest-order moments read

$$I_1 = \frac{\mu_\lambda}{4\pi^2\hbar^3}, \quad \text{(A.7)}$$

$$I_2 = \frac{\mu_\lambda^2}{8\pi^2\hbar^3}+\frac{T^2}{24\hbar^3}, \quad \text{(A.8)}$$

$$I_3 = \frac{\mu_\lambda^3}{12\pi^2\hbar^3}+\frac{\mu_\lambda T^2}{12\hbar^3}, \quad \text{(A.9)}$$

$$I_4 = \frac{\mu_\lambda^4}{16\pi^2\hbar^3}+\frac{\mu_\lambda^2 T^2}{8\hbar^3}+\frac{7\pi^2T^4}{240\hbar^3}. \quad \text{(A.10)}$$

Note that these moments satisfy the following recurrent relation: $\partial I_{n+1}/\partial\mu_\lambda = nI_n$. Using this relation it is easy to obtain similar chains of integrals with the first derivative of the distribution function $f_0' = \partial f_0/\partial\varepsilon_{p,0} = -\partial f_0/\partial\mu_\lambda$ if one makes a substitution $I_n \to -(n-1)I_{n-1}$. For f_0'', the substitution is $I_n \to (n-1)(n-2)I_{n-2}$ and so on.

APPENDIX B

SEARCH FOR THE COLLECTIVE MODES IN THE PRESENCE OF VORTICITY

In this appendix, we present a method of finding the linear and higher order corrections in vorticity Ω to the dispersion of the collective modes used in chapter 3.

Let us start by recalling the general formulation of the problem. The general system of hydrodynamic equations (presented in appendix D) contains 12 differential equations on 12 perturbations $\delta X(r)$, where $X = \mu, \mu_5, T, u^\mu, B^\mu, E^\mu$. Next we expand all perturbations into the Fourier-Bessel series: $\delta X(r) = \sum_i \delta X_i \, J_m(k_\perp^i r)$, and substitute them into the system. The equations themselves are the functions of r and so they can be integrated with the weight $rJ_m(k_\perp^j r)$ using the Bessel functions orthogonality condition. In the case of zero vorticity after simplifications only the pure Bessel functions are present in the system and so after the integration we get an algebraic system on 12 amplitudes δX_j. This system can be solved for each $k_\perp^j$ separately, i.e., different $k_\perp^j$ are independent.

Next we turn on a "small" vorticity Ω so that the spectrum and the eigenfuctions of the general system of differential equations do not change "much". Therefore, we again substitute the same Fourier-Bessel series instead of the unknown amplitude functions $\delta X(r)$. After simplifications the system contains only a few different functions of the radius: $J_m(k_\perp^i r)$, $rJ_m(k_\perp^i r)$ and $r^2 J_m(k_\perp^i r)$. Here the straightforward Bessel orthogonality condition fails and so different $k_\perp^j$ are no longer independent. But the question is "how far from being independent are they"? To answer that we find the expansions:

$$\begin{aligned} rJ_m(k_\perp^j r) &= a_j J_m(k_\perp^j r) + \sum_{i\neq j} a_i J_m(k_\perp^i r), \\ r^2 J_m(k_\perp^j r) &= b_j J_m(k_\perp^j r) + \sum_{i\neq j} b_i J_m(k_\perp^i r). \end{aligned} \tag{B.1}$$

Several sets of coeffcients a_i and b_i are given as a bar chart in Fig. B.1. The charts show that both coefficients subside quite rapidly for large $|i-j|$. Hence, as an approximation, we can neglect the sum in Eq. (B.1) and set $rJ_m(k_\perp^j r) \approx a_j J_m(k_\perp^j r)$ and $r^2 J_m(k_\perp^j r) \approx b_j J_m(k_\perp^j r)$. This effectively makes different $k_\perp^j$ independent again and so we can apply the Bessel orthogonality to get a closed algebraic system on amplitudes with the inclusion of vorticity.

If we leave the sum in the expansion Eq. (B.1) and integrate the system with the weight $rJ(k_\perp^j r)$ we end up with an algebraic system made up of $n \times n$ blocks of the size 12×12, each of which corresponds to the amplitudes δX_i for a given $k_\perp^i$, and n is defined from the UV cutoff $k_\perp^i < k_{\rm UV}$ or may even be infinite. The system of equations can be divided into the vorticity-less and vortical parts: $\mathcal{M} = A + \Omega B$, where in the matrix A only diagonal blocks are nonzero. Let us also introduce a combined index (i, α) to numerate the entries in the matrix, where $i = 1, ..$ numerates the wave vector and $\alpha = 1, .., 12$ numerates the amplitude.

The system of equations $\mathcal{M}$ has nontrivial solutions if its determinant is zero. Using the textbook definition of the determinant we can write:

$$\det \mathcal{M} = \varepsilon^{a_{(1,1)} a_{(1,2)} \cdots a_{(1,12)} \cdots\cdots a_{(n,12)}} \mathcal{M}_{(1,1),a_{(1,1)}} \mathcal{M}_{(1,2),a_{(1,2)}} \ldots \mathcal{M}_{(1,12),a_{(1,12)}} \cdots\cdots \mathcal{M}_{(n,12),a_{(n,12)}}, \tag{B.2}$$

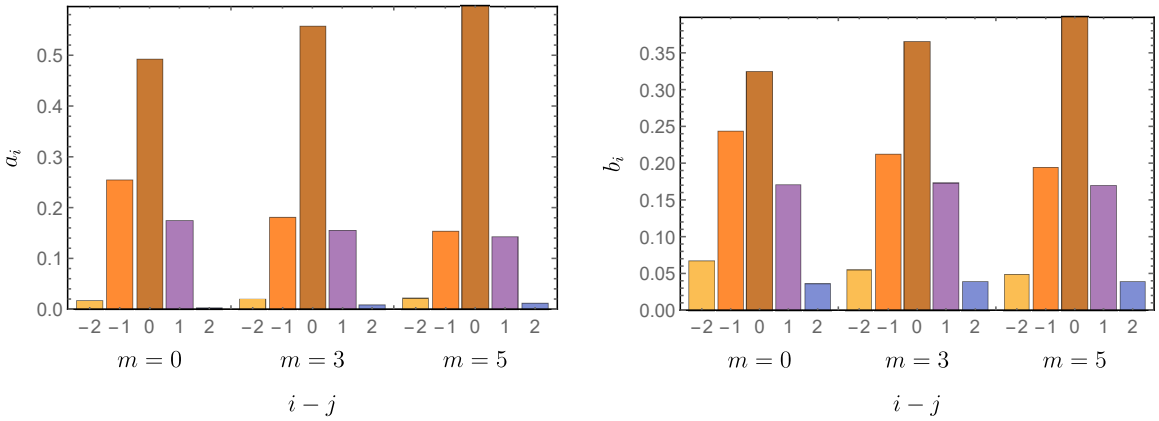

Figure B.1: Coefficients a_i and b_i from the expansions in Eq. (B.1) for the few indexes i around $j = 3$ at $m = 0, 3, 5$. As can be seen from the graph both coefficients subside quickly for large $|i - j|$.

where $a_{(i,\alpha)}$ enumerates all indexes and ε is a Levi-Civita tensor of an appropriate size. Substituting $\mathcal{M} = A + \Omega B$ into the formula the zeroth order in Ω can be evaluated:

$$\det \mathcal{M}_{\Omega^0} = \varepsilon^{a_{(1,1)}\ldots a_{(1,12)}\ldots\ldots a_{(n,12)}} A_{(1,1),a_{(1,1)}} \ldots A_{(1,12),a_{(1,12)}} \ldots\ldots A_{(n,12),a_{(n,12)}} \tag{B.3}$$

The matrix A is block diagonal and so only the indexes from the same block survive: $a_{(i,\alpha)} = (i, a^i_\alpha)$ and $A_{(i,\alpha),a_{(i,\alpha)}} = A^i_{\alpha,a^i_\alpha}$, where $a^i_\alpha = 1, \ldots, 12$ and A^i is the i-th 12×12 block matrix on the diagonal. The determinant is then:

$$\det \mathcal{M}_{\Omega^0} = \varepsilon^{(1,a^1_1)\ldots(1,a^1_{12})\ldots\ldots(n,a^n_{12})} A^1_{1,a^1_1} \ldots A^1_{12,a^1_{12}} \ldots\ldots A^n_{12,a^n_{12}} \tag{B.4}$$

$$= \left(\varepsilon^{a^1_1\ldots a^1_{12}} A^1_{1,a^1_1} \ldots A^1_{12,a^1_{12}}\right) \ldots \left(\varepsilon^{a^n_1\ldots a^n_{12}} A^n_{1,a^n_1} \ldots A^n_{12,a^n_{12}}\right) = \det A^1 \ldots \det A^n. \tag{B.5}$$

In other words the determinant of the block-diagonal matrix is a product of the block determinants. In the first order we change one of the A to B:

$$\det \mathcal{M}_{\Omega^1} = \sum_i \sum_\alpha \varepsilon^{a_{(1,1)}\ldots a_{(1,12)}\ldots\ldots a_{(n,12)}} A_{(1,1),a_{(1,1)}} \ldots B_{(i,\alpha),a_{(i,\alpha)}} \ldots A_{(n,12),a_{(n,12)}}. \tag{B.6}$$

Using the block-diagonality of the matrix A we get:

$$\det \mathcal{M}_{\Omega^1} = \sum_{i=1}^{n} \sum_{\alpha=1}^{12} \det A^1 \ldots \left(\varepsilon^{a^i_1\ldots a^i_{12}} A^i_{1,a^i_1} \ldots B^i_{\alpha,a^i_\alpha} \ldots A^i_{12,a^i_{12}}\right) \ldots \det A^n \tag{B.7}$$

$$= \sum_{i=1}^{n} \det A^1 \ldots \det\left(A^i + \Omega B^i\right) \ldots \det A^n + O(\Omega^2) \tag{B.8}$$

$$= \det\left(A^1 + \Omega B^1\right) \ldots \det\left(A^n + \Omega B^n\right) + O(\Omega^2), \tag{B.9}$$

where B^i is the i-th diagonal block of the matrix B similar to the notation A^i. Therefore, the spectrum of the system in the linear order is found by solving each diagonal

block separately: $\det(A^i + \Omega B^i) = 0$. However, there are several complications with this method. First of all, the trick of the determinant factorization is ambiguous. Second, the generalization to the quadratic order is not so straightforward and may require the summation of a large (if not infinite) number of blocks.

There is, however, another method that allows a generalization to the higher orders. It is based on the QM perturbation theory. The idea is the following: if we knew the eigenvalues λ_i of the matrix $\mathcal{M}$, then the determinant could be factorized as $\det \mathcal{M} = \prod_i \lambda_i$ and the spectrum found from the equations $\lambda_i(k_0) = 0$. Moreover, if we knew just the eigenvalues and the eigenvectors of the matrix A we could use the perturbation theory and find the first and higher corrections to the eigenvalues in the systematic way. In this way we could get the first and higher order vorticity corrections to the dispersion in the systematic way from the equation $\lambda_i(k_0) = 0$.

The problem is that even in the vorticity-less case we do not know the eigenvalues. However, we can make a trick to overcome this problem in the first order in Ω. Let us consider the block-eigenvalue problem $\mathcal{M}|n\rangle = |n\rangle\langle\Lambda_n\rangle$, where the block-eigenvector $|n\rangle$ is a $12n \times 12$ matrix and the block-eigenvalue $\langle\Lambda_n\rangle$ is a 12×12 matrix. Such a problem is useful because the set of all eigenvalues of the matrices $\langle\Lambda_n\rangle$ coincide with the set of eigenvalues of $\mathcal{M}$ (this can be proven analogous to the usual eigendecomposition by showing that $\mathcal{M}$ is similar to $\mathrm{diag}(\langle\Lambda_n\rangle)$). Note, that unlike the usual case where the eigenvector can have variable length and the eigenvalue is fixed in this case the block-eigenvalue is defined up to the similarity transformation $|n'\rangle = |n\rangle P$, $\langle\Lambda'_n\rangle = P\langle\Lambda_n\rangle P^{-1}$.

In the case without vorticity the simplest eigenvector contains only one block of the identity matrix $|n^0\rangle = (0, 0, .., I, ..0)$ and the corresponding eigenvalue is one of diagonal blocks of A, i.e., $\langle\Lambda^0_n\rangle = A^n$. Following the perturbation theory we assume that the eigenvalues and the eigenvectors can be decomposed into a series in the powers of Ω:

$$|n\rangle = |n^0\rangle + \Omega|n^1\rangle + ..., \qquad \langle\Lambda_n\rangle = \langle\Lambda^0_n\rangle + \Omega\langle\Lambda^1_n\rangle + ... \tag{B.10}$$

Substituting this into the equation $(A + \Omega B)|n\rangle = |n\rangle\langle\Lambda_n\rangle$ we get in the first order:

$$A|n^1\rangle + B|n^0\rangle = |n^0\rangle\langle\Lambda^1_n\rangle + |n^1\rangle\langle\Lambda^0_n\rangle. \tag{B.11}$$

Assuming that the vector $|n\rangle$ is normalized to 1 similar to $|n^0\rangle$ we get in the first order $\langle n^0|n^1\rangle = 0$. Multiplying the equation above by the co-vector $\langle n^0|$ we get the first block-eigenvalue correction:

$$\langle\Lambda^1_n\rangle = \langle n^0|B|n^0\rangle = B^n, \tag{B.12}$$

which is the n-th block on the diagonal of B. Therefore, up to the first order in the vorticity the eigenvalues and spectrum of $\mathcal{M}$ can be found from the eigenvalues of the diagonal blocks $(A^n + \Omega B^n)$.

The second order correction is much more complicated. In order to find it we first need to find the first-order correction to the eigenvector. It can be decomposed as $|n^1\rangle = \sum_{k\neq n} |k^0\rangle\langle\alpha^n_k\rangle$, where $\langle\alpha^n_k\rangle$ is some unknown 12×12 matrix. Substituting this into the first-order equation we get:

$$\langle\Lambda^0_k\rangle\langle\alpha^n_k\rangle - \langle\alpha^n_k\rangle\langle\Lambda^0_n\rangle + \langle k^0|B|n^0\rangle = 0. \tag{B.13}$$

This is a so-called Sylvester equation for the matrix $\langle \alpha_k^n \rangle$. It has a unique solution if the matrix A is non-degenerate, which is indeed the case in this problem. However, it is very non-trivial and, probably, is much more involving than the eigenvalue problem for A^i. Anyway, if we are able to find the solution $\langle \alpha_k^n \rangle$, then we can easily find the second-order correction to the block-eigenvalue and, therefore, the spectrum. Proceeding in the similar fashion one can find the higher-order corrections to the spectrum in the systematic way. Another advantage of this method is that we avoid calculating determinants of infinite matrices and only deal with 12×12 blocks.

APPENDIX C

BESSEL FUNCTIONS

In this appendix, we present some useful relations for the Bessel functions that are needed for the analysis in the main text of the dissertation.

Let us remember that the Bessel functions $J_m(z)$ have an infinite number of positive real zeros at $z = \alpha_{m,i}$, where $i = 1, 2, ...$ (Note that we use a nonstandard notation $\alpha_{m,i}$ instead of the usual $j_{m,i}$.)

By making use of the table integrals Gradshteyn and Ryzhik (2014)

$$\begin{aligned}\int_0^1 dx\; rJ_\nu(ax)J_\nu(bx) &= \frac{bJ_{\nu-1}(b)J_\nu(a) - aJ_{\nu-1}(a)J_\nu(b)}{a^2-b^2} \\ &= \frac{aJ_{\nu+1}(a)J_\nu(b) - bJ_{\nu+1}(b)J_\nu(a)}{a^2-b^2}, \qquad \text{(C.1)}\\ \int_0^1 dx\; xJ_\nu^2(ax) &= \frac{1}{2}\left(J_\nu^2(a) - \frac{2\nu}{a}J_\nu(a)J_{\nu-1}(a) + J_{\nu-1}^2(a)\right) \\ &= \frac{1}{2}\left(J_\nu^2(a) - \frac{2\nu}{a}J_\nu(a)J_{\nu+1}(a) + J_{\nu+1}^2(a)\right), \qquad \text{(C.2)}\end{aligned}$$

one can easily derive the following orthogonality relation:

$$\int_0^1 dx\; xJ_{\tilde{m}}(\alpha_{m,i}x)J_{\tilde{m}}(\alpha_{m,j}x) = \delta_{ij}\frac{1}{2}J_{m\pm1}^2(\alpha_{m,i}), \qquad \text{(C.3)}$$

which is valid for any $\tilde{m} = m-1, m, m+1$. In this connection, it is useful to note that $J_{m-1}(\alpha_{m,i}) = -J_{m+1}(\alpha_{m,i})$. As is easy to check, the latter follows from the well-known recurrence relation Gradshteyn and Ryzhik (2014),

$$xJ_{\nu-1}(x) + xJ_{\nu+1}(x) = 2\nu J_\nu(x). \qquad \text{(C.4)}$$

After integrating Eq. (C.3) by parts and taking into account the property of the Bessel functions Gradshteyn and Ryzhik (2014),

$$J_{\nu-1}(x) - J_{\nu+1}(x) = 2J_\nu'(x). \qquad \text{(C.5)}$$

we easily derive the following two integral relations:

$$\left(\frac{1}{2}J_{m\pm1}^2(\alpha_{m,i})\right)^{-1}\int_0^1 dx\; x^2J_m(\alpha_{m,i}x)J_{m\pm1}(\alpha_{m,i}x) = \frac{m\pm1}{\alpha_{m,i}}, \qquad \text{(C.6)}$$

$$\left(\frac{1}{2}J_{m\pm1}^2(\alpha_{m,i})\right)^{-1}\int_0^1 dx\; x^3J_{\tilde{m}}(\alpha_{m,i}x)J_{\tilde{m}}(\alpha_{m,i}x) = \frac{1}{3\alpha_{m,i}^2}\left(\frac{2\tilde{m}(\tilde{m}^2-1)}{m} + \alpha_{m,i}^2\right), \qquad \text{(C.7)}$$

where again $\tilde{m} = m-1, m, m+1$.

APPENDIX D

EXPLICIT FORM OF LINEARIZED EQUATIONS

In this appendix, we present the explicit form of the linearized equations for the perturbations around the unperturbed equilibrium state of a uniformly rotating charged chiral plasma.

By making use of Eqs. (2.31)–(2.35) and the ansatz in Eqs. (3.8)–(3.10) for the perturbations of the plasma parameters, we can derive the coupled system of linearized equations. The electric charge conservation relation leads to

$$\begin{aligned}
&\sum_i \Bigg[-i(k_0 - m\Omega)\frac{\partial n}{\partial \zeta_i} - ik_\mu \omega^\mu \frac{\partial \sigma_\omega}{\partial \zeta_i} - ik_\mu \left(B^\mu - \frac{1}{2} en \omega^\mu r^2 \right) \frac{\partial \sigma_B}{\partial \zeta_i} \\
&\qquad + \frac{\tau}{3}\frac{\partial n}{\partial \zeta_i}\left((k_0 - m\Omega)^2 - k_\mu k^\mu - \partial_r^2 - \frac{1}{r}\partial_r + \frac{m^2}{r^2} \right) \Bigg] \delta\zeta_i \\
&+ n\left[1 + i\tau(k_0 - m\Omega)\right]\left(-ik_\mu \delta u^\mu + D_1[\delta u]\right) - 2i\Omega\tau n D_2[\delta u] \\
&\qquad + \frac{1}{e}\sigma_E \left(-ik_\mu \delta E^\mu + D_1[\delta E]\right) = 0. \quad \text{(D.1)}
\end{aligned}$$

Similarly, the chiral charge conservation is given by

$$\begin{aligned}
&\sum_i \Bigg[-i(k_0 - m\Omega)\frac{\partial n_5}{\partial \zeta_i} - ik_\mu \omega^\mu \frac{\partial \sigma_\omega^5}{\partial \zeta_i} - ik_\mu \left(B^\mu - \frac{1}{2} en \omega^\mu r^2 \right) \frac{\partial \sigma_B^5}{\partial \zeta_i} \\
&\qquad + \frac{\tau}{3}\frac{\partial n_5}{\partial \zeta_i}\left((k_0 - m\Omega)^2 - k_\mu k^\mu - \partial_r^2 - \frac{1}{r}\partial_r + \frac{m^2}{r^2} \right) \Bigg] \delta\zeta_i \\
&+ 2i\sigma_\omega^5 k_0 \omega^\mu \delta u_\mu + \sigma_B^5 \left(-ik_\mu \delta B^\mu + D_1[\delta B]\right) = -\frac{e^2}{2\pi^2\hbar^2}\delta E^\mu \left(B_\mu - \frac{1}{2} en \omega_\mu r^2 \right), \quad \text{(D.2)}
\end{aligned}$$

The energy-momentum conservation relations read

$$\begin{aligned}
&\sum_i \left[-i(k_0 - \frac{4}{3}m\Omega)\frac{\partial \epsilon}{\partial \zeta_i} - ik^\mu \omega_\mu \frac{\partial \xi_\omega}{\partial \zeta_i} - ik^\mu \left(B_\mu - \frac{1}{2} en \omega_\mu r^2 \right) \frac{\partial \xi_B}{\partial \zeta_i} \right] \delta\zeta_i \\
&+ \frac{4}{3}\epsilon \left[-ik^\mu \delta u_\mu + D_1[\delta u] - k_0 \Omega r \left(\delta u^+ - \delta u^- \right) \right] - \frac{4\tau\epsilon}{45} im\Omega \left(ik_z \delta u^3 + D_1[\delta u] \right) \\
&- \frac{4\tau\epsilon}{15} i\Omega r \left[k_z^2 - \partial_r^2 - \frac{1}{r}\partial_r \right] \left(\delta u^+ - \delta u^- \right) - \frac{4\tau\epsilon}{15} i\Omega r \left[\frac{(m+1)^2}{r^2}\delta u^+ - \frac{(m-1)^2}{r^2}\delta u^- \right] \\
&= \sum_i \left[e\frac{\tau}{3}\frac{\partial n}{\partial \zeta_i} B\Omega r \partial_r \right] \delta\zeta_i - ik_0 e\tau n B\Omega r \left(\delta u^+ + \delta u^- \right) \\
&\qquad - \sigma_E B\Omega r \left(\delta E^+ + \delta E^- \right) - ien\Omega r \left(\delta E^+ - \delta E^- \right), \quad \text{(D.3)}
\end{aligned}$$

$$
\begin{aligned}
&\sum_i \left[\frac{1}{6}\frac{\partial\epsilon}{\partial\zeta_i}\left(\partial_r - s\frac{m}{r} + 4sk_0\Omega r\right) - \frac{1}{2}sk_zB\Omega r\frac{\partial\xi_B}{\partial\zeta_i}\right]\delta\zeta_i + \frac{2}{3}is\epsilon\Omega r\left(-ik^\mu\delta u_\mu + D_1[\delta u]\right)\\
&\quad - \frac{4}{3}i\epsilon\left[k_0 - (m+2s)\Omega\right]\delta u^s - \frac{2\tau\epsilon}{45}\left[\partial_r - s\frac{m}{r} + sk_0\Omega r\right]\left(ik_z\delta u^3 + D_1[\delta u]\right)\\
&\quad + \frac{2\tau\epsilon}{45}k_0\Omega r\left[\partial_r - s\frac{m-s}{r}\right]\left(\delta u^+ - \delta u^-\right) + \frac{4\tau\epsilon}{15}\left[k_z^2 - \partial_r^2 - \frac{1}{r}\partial_r + \frac{(m+s)^2}{r^2}\right]\delta u^s\\
&\quad - \frac{8\tau\epsilon}{15}k_0(m+2s)\Omega\delta u^s\\
&= \sum_i \left[e\frac{\tau}{6}is\left(B - \frac{1}{2}en\Omega r^2\right)\frac{\partial n}{\partial\zeta_i}\left(\partial_r - s\frac{m}{r}\right) + e\frac{\tau}{6}ik_0B\Omega r\frac{\partial n}{\partial\zeta_i}\right]\delta\zeta_i\\
&\quad + es\left(B - \frac{1}{2}en\Omega r^2\right)\left[\tau k_0 n\delta u^s - \frac{i}{e}\sigma_E\delta E^s\right] + en\delta E^s,
\end{aligned}
\tag{D.4}
$$

$$
\begin{aligned}
&\sum_i \left[\frac{1}{3}ik_z\frac{\partial\epsilon}{\partial\zeta_i} - ik_0\Omega\frac{\partial\xi_\omega}{\partial\zeta_i} - ik_0\left(B - \frac{1}{2}en\Omega r^2\right)\frac{\partial\xi_B}{\partial\zeta_i} + im\Omega B\frac{\partial\xi_B}{\partial\zeta_i}\right]\delta\zeta_i\\
&\quad - \frac{4}{3}i\epsilon(k_0 - m\Omega)\delta u^3 - \frac{8\tau\epsilon}{15}k_0m\Omega\delta u^3 + \frac{4\tau\epsilon}{15}\left[k_z^2 - \partial_r^2 - \frac{1}{r}\partial_r + \frac{m^2}{r^2}\right]\delta u^3\\
&\quad + \frac{4\tau\epsilon}{45}\left(k_z^2\delta u^3 - ik_zD_1[\delta u] + ik_zk_0\Omega r\left(\delta u^+ - \delta u^-\right)\right) = en\delta E^3.
\end{aligned}
\tag{D.5}
$$

Finally, the Maxwell equations take the form

$$
\begin{aligned}
&-2\Omega\delta E^3 + ik\Omega r\left(\delta E^+ + \delta E^-\right)\\
&\quad - \Omega r\partial_r\delta E^3 - i(k_0 - m\Omega)\delta B^0 + ik^\mu\delta B_\mu - D_1[\delta B] - ik_zB\delta u^0 = 0,
\end{aligned}
\tag{D.6}
$$

$$
\begin{aligned}
&-k_zs\delta E^s - \frac{1}{2}is\left[\partial_r - s\frac{m}{r}\right]\delta E^3 - \frac{1}{2}ik_0\Omega r\delta E^3 - i\left(k_0 - m\Omega\right)\delta B^s\\
&\quad - \frac{1}{2}is\Omega r\left(-ik^\mu\delta B_\mu + D_1[\delta B]\right) - ik_z\left(B - \frac{1}{2}en\Omega r^2\right)\delta B^s = 0,
\end{aligned}
\tag{D.7}
$$

$$
\begin{aligned}
&-iD_2[\delta E] + ik_0\Omega r\left(\delta E^+ + \delta E^-\right) - i(k_0 - m\Omega)\delta B^3\\
&\quad + \left(B - \frac{1}{2}en\Omega r^2\right)\left(-ik_0\delta u^0 + D_1[\delta u]\right) - en\Omega r\left(\delta u^+ + \delta u^-\right) = 0,
\end{aligned}
\tag{D.8}
$$

and

$$
\begin{aligned}
&-i\left(B - \frac{1}{2}en\Omega r^2\right)D_2[\delta u] + 2\Omega\delta B^3 + ien\Omega r\left(\delta u^+ - \delta u^-\right)\\
&\quad - ik_z\Omega r\left(\delta B^+ + \delta B^-\right) + \Omega r\partial_r\delta B^3 - ik_3\delta E^3 - D_1[\delta E]\\
&= e\sum_i\left[\left(1 - i\frac{\tau}{3}\Omega m\right)\frac{\partial n}{\partial\zeta_i}\right]\delta\zeta_i + en(1 + i\tau k_0)\delta u^0 + \sigma_E\delta E^0,
\end{aligned}
\tag{D.9}
$$

$$
\begin{aligned}
&sk_0\left(B-\frac{1}{2}en\Omega r^2\right)\delta u^s+\frac{1}{2}sB\Omega r\left[\partial_r-s\frac{m-s}{r}\right]\left(\delta u^+-\delta u^-\right)\\
&\quad-\frac{1}{2}iBk_z\Omega r\delta u^3+sk_z\delta B^s+\frac{1}{2}is\left[\partial_r-s\frac{m}{r}\right]\delta B^3\\
&\quad+\frac{1}{2}ik_0\Omega r\delta B^3-i\left(k_0-m\Omega\right)\delta E^s-is\Omega r\left(-ik_\mu\delta E^\mu+D_1[\delta E]\right)\\
&=en\delta u^s+ie\tau n\left[k_0-(m+2s)\Omega\right]\delta u^s\\
&\quad+e\sum_i\left[\frac{1}{2}is\Omega r\frac{\partial n}{\partial\zeta_i}-\frac{\tau}{6}\frac{\partial n}{\partial\zeta_i}\left(\partial_r-s\frac{m}{r}+sk_0\Omega r\right)\right]\delta\zeta_i+\sigma_E\delta E^s, \qquad \text{(D.10)}
\end{aligned}
$$

$$
\begin{aligned}
&iD_2[\delta B]-ik_0\Omega r\left(\delta B^+-\delta B^-\right)+B\Omega r\left[\partial_r+\frac{2}{r}\right]\delta u^3-i(k_0-m\Omega)\delta E^3\\
&=e\sum_i\left[-\frac{\tau}{3}ik_z\frac{\partial n}{\partial\zeta_i}+\Omega\frac{\partial\sigma_\omega}{\partial\zeta_i}+\left(B-\frac{1}{2}en\Omega r^2\right)\frac{\delta\sigma_B}{\partial\zeta_i}\right]\delta\zeta_i\\
&\quad+en\delta u^3+ie(k_0-m\Omega)\tau n\delta u^3+\sigma_E\delta E^3. \qquad \text{(D.11)}
\end{aligned}
$$

In these equations, the index $s=\pm1$ labels circular polarizations and the sums over $i=1,2,3$ account for the variations of the three physical parameters, $\delta\zeta_i=\delta\mu,\delta\mu_5,\delta T$. Note that the variations of all quantities are assumed to have a radial dependence, i.e., $\delta\mu=\delta\mu(r),\delta T=\delta T(r)$, etc., although it is not shown explicitly. In the linearized equations, we used the following differential operators:

$$
\begin{aligned}
D_1[\delta v] &= \partial_r(\delta v^+ + \delta v^-)+\frac{m+1}{r}\delta v^+-\frac{m-1}{r}\delta v^-, \qquad \text{(D.12)}\\
D_2[\delta v] &= \partial_r(\delta v^+ - \delta v^-)+\frac{m+1}{r}\delta v^++\frac{m-1}{r}\delta v^-. \qquad \text{(D.13)}
\end{aligned}
$$

Last but not least, let us remind the reader that the zeroth components of the vector quantities are not independent. They are expressed in terms of the spatial component; see Eqs. (3.11)–(3.13).